昭和６０－６２年度　文部省科学研究費補助金　（一般研究　Ｂ）

研究成果　報告書　（課題番号　６０４６００４５）

中部・近畿地方の３次元速度・減衰構造とテクトニクスの研究

昭和６３年３月

昭和６０－６２年度　科学研究費補助金　（一般研究　Ｂ）

研究成果報告書

１・課題番号　　６０４６００４５

２・研究課題　　中部・近畿地方の３次元速度・減衰構造と
テクトニクスの研究

３・研究代表者　京都大学　防災研究所　教授　三雲　健

４・研究分担者　京都大学　防災研究所　助手　平原　和朗

名古屋大学　理学部　助手　伊神　輝　（60･61年度）

東京大学　地震研究所　助教授　佃　為成
（前京都大学　防災研究所　助手　）

京都大学　防災研究所　助手　安藤　雅孝

京都大学　防災研究所　助手　竹内　文朗　（62年度）

京都大学　理学部　助手　伊藤　潔　（62年度）

５・研究経費

昭和６０年度	１、７００千円
昭和６１年度	１、６００千円
昭和６２年度	１、５００千円
計	４、８００千円

研究成果発表論文

1. K. Hirahara, A. Ikami, M. Ishida, T. Mikumo, 1986,
Three-dimensional P-wave velocity structure beneath central Japan
- Low velocity bodies in the wedge portion of the upper mantle above high-velocity subducting plates - ,
submitted to Tectonophysics.

2. K.Hirahara, 1988, Detection of three-dimensional velocity anisotropy Phys.Earth & Planet Intr. 49 (in press).

3. T. Mikumo, H. Wada and M. Koizumi, 1988, Seismotectonics of the Hida region, central Honshu, Japan, Tectonophysics 146 (in press).

4. 三雲 健、平原和朗、竹内文朗、佃為成、和田博夫、藤井巌、西上欽也
1988, 飛騨地方の３次元上部地殻構造と活断層および地震活動
(English version, to be submitted to Tectonophysics)

5. 平原和朗、竹内文朗、1988,
北陸地方の３次元上部地殻構造
(English version, to be submitted to J.Phys.Earth)

6. 伊藤 潔、平原和朗、1988,
近畿北部のＰ波３次元速度構造と震源分布
(English version, to be submitted to J.Phys.Earth)

まえがき

この研究は、西南日本内陸部のうち、地殻活動が特に活発な中部・近畿地方下の地殻・上部マントルの詳細な３次元速度・減衰（Q）構造を明らかにし、これによってこの地域の複雑なテクトニクスおよび地震発生との関連性を解明しようとしたものである。

このうちわれわれが特に重要な課題と考えたのは、（a）中部地方の飛騨・木曽・赤石山脈など第四紀以来急速に隆起を続けてきた高山地帯下の深部（１５０kmまで）の速度・減衰構造が現在どのような状態にあるのか、（b）中部地方を走る火山フロント下や、活火山を含む飛騨山脈下の火成活動の原因と思われるマグマ溜やマントル・ダイアピルが検出できるか、（c）最近提唱されている北米プレートとユーラシア・プレートの境界とされるフオツサ・マグナが速度構造の境界として検出できるか、（d）これらの問題と関連して、中部日本下の上部マントルに異方性構造が存在するのか、（e）中部地方北西部（飛騨－北陸地方）から近畿地方中部の第四紀活断層が密に分布している地域下の上部地殻構造がどのようになっているのか、また糸魚川－静岡構造線や中央構造線などの大規模な活構造境界がどの程度の深さまで達しているか、（f）上部地殻構造と活断層や地震の震源分布との関連性などがどのような状態にあるのか、などの問題であった。

これらの課題解明の手段としては、中部・近畿地方に密に分布する各大学及び国立防災科学技術センターの高感度地震観測点で多数の地震の際に得られたＰ波走時を主として用い、インバージョン法を適用して３次元速度構造すなわち不均質性や異方性を推定した。

得られた研究結果はここに収録した６編の論文に詳しく述べられている。各論文の主要な結果を要約すれば次の通りである。

（１）論文１）は課題（a）、（b）、（c）に関係するものである。

ここでは 120 個の浅発及び中深発地震時に近畿・中部地方の 129 個所の高感度地震観測点で観測された 7,490 のＰ波走時を用い、Aki & Lee (1976) の方法を適用し、インバージョンによって深さ500 km迄のＰ波３次元速度異常を計算した。

この結果、中部日本下では沈み込む高速度層（high-V）のフィリピン海プレート及び太平洋プレートの真上のいわゆるマントル・ウェッジの部分に顕著な低速度体（low-V）が存在するという、複雑な３次元構造が明らかになった。この低速度体は活火山、特に飛騨山脈下や富士山周辺に存在し、100-150 kmの深さ迄存在することが見いだされた。この低速度体は、震度分布の解析から求められた減衰の大きい地帯（low Q）と一致し、またＳ波解析から推定されている飛騨地方下の異方性構造の場所とも一致する。

このドーム状の形をした低速度体はおそらく、この地方下に存在するマントル・ダイアピルの存在を示すものと考えられる。一方、中部地方を南北に縦断するフォッサマグナ両側では、プレート境界を示唆するような著しい速度構造の差は見いだされなかった。

（２）論文２）は課題（a）、（d）に関するものである。

この論文では、地球内部特に上部マントル内の等方性の不均質構造とともに、Ｐ波の３次元速度異方性の存在を検出する新しい方法が詳細に述べられている。第１のステップは３次元等方性構造に基づく走時残差をＡＲＴ法と呼ばれる方法により検出する。走時残差補正ダイアグラムが方向による速度変化を示す場合には次のステップとして、orthorhombic 対称の異方性媒質を表わす速度楕円体を用いて３次元異方性インバージョンを適用する。

この方法を前述の論文１）のデータに適用して、日本列島下の上部マントル中に異方性構造が存在するか否かを検討した。著者らの別の研究(1984)では、太平洋プレートとフィリピン海プレート中で、Ｐ波速度構造が海底の地磁気縞模様と直交する方向に速いことが見いだされている。今回の研究からは、Ｓ波の異方性が見いだされている中部地方の上部マントル中には、対応する僅かな異方性は存在するものの、明瞭なＰ波の異方性は検出されなかった。

（３）論文３）は課題（a）、（e）、（f）に関係する。

この論文は、主として地震活動と地震メカニズムに関する 1980年4月 - 1986年6月迄の最近約６年間の観測データに基づき、地形・地質学的データも参考にして飛騨地方北部の地震テクトニクスを詳しく論じたものである。

これから、この地方の主要な第四紀活断層である跡津川断層に沿い、長さ約70kmにわたって地震活動が極めて活発であることが見いだされた。しかしこの活動は東部及び西部で活発で中央部では比較的低い。このような

一様でない地震発生パターンは、ここで起こった1858年安政飛騨地震（M＝7.0）の後の応力集中と、断層強度の不均質性によるものと考えられる。また飛騨山脈下でも南北方向に帯状に延びる地震活動が活発である。これらの地震の最深度は前者の断層下で約15km、後者の山脈下では約8kmであるが、この著しい差は地震活動が脆性／延性へ転換する深さの差を示すものと思われ、活火山を含む飛騨山脈下のかなり浅い部分まで高温状態にあることが考えられる。一方、地震メカニズムから推定したこの地方の最大主応力の方向は平均してＥＳＥ－ＷＮＷ方向に近く、この方向は北米－ユーラシア両プレートの相対運動の方向より太平洋－ユーラシア両プレートの相対運動の方向に近い。最大剪断応力の大きさは700barを越えないものと考えられている。

（４）論文４）は課題（e）、（f）に関係する。

この論文は、飛騨地方及びその周辺部で発生した 240 個の中小地震（M≧３）を利用し、16 点の高感度微小地震観測点で観測された約 2,500 個のＰ波走時から Thurber（1983）の方法によるインバージョンを行なうことによって、この地方の上部地殻の３次元構造を推定し、さらに活断層や地震分布、重力分布との関係を論じたものである。

飛騨地方中北部の跡津川断層と飛騨山脈西縁で囲まれる三角地帯には地殻最上部より12kmの深さ迄、6.0-6.4 km/sec の高速度層が存在し、ここは固い地殻と考えられ、地震活動は極めて低い。しかし跡津川・茂住・牛首断層群の西半部では高速度層が深く迄貫入しており、地震活動は活発である。一方、飛騨山脈中軸部では 5.4-5.8 km/sec のかなり速度の遅い層が相当の深さ迄連続して存在する。この低速度層は上部では活火山の立山及び北西方の跡津川断層東部迄、南西方には活火山下の乗鞍岳、御岳、阿寺断層東側迄拡がり、地殻中部では西方の三角帯の東部迄拡がっているようである。また御母衣断層西側から両白山地の中部には 5.6-5.8 km/sec 層が拡がり、この低速度層は白山付近では深さ12km迄達している。飛騨山脈及び白山下の低速度層は火成活動に関係している可能性も考えられる。以上の３次元速度構造はこの地方の重力のブーゲー異常分布のパターンと大局的には調和しているように見える。

（５）論文５）は課題（e）、（f）に関するものである。

この論文は、1978年6月から1985年4月の間に北陸地方で発生した 278 個の地震を用い、この地域内の微小地震観測網の７観測点で観測されたＰ波走時残差をデータとして、３次元速度構造と震源の同時決定インバージョンプログラム SIMUL3 (Thurber,1983)によって、地殻上層部のＰ波３次元構造を求め、震源分布・活断層分・重力異常分布との関係を議論したものである。

表層では（深さ 0 km）、北陸の海岸線沿い（特に福井平野の西）に顕著

な低速度領域が存在する。また、この層と第２層（深さ 3 km)では、北東一南西の走行を持つ高速度領域が顕著である。さらに、高速度領域によって、福井断層はその南の断層系とに遮られているように見えることが分かった。また、福井断層の西の高速度領域では、地震活動が低い。さらに琵琶湖では、深いところ（12km）でかなりの低速度になっていて、負の重力異常と調和的であることが分かった。

（６）論文６）は課題（e）、（f）に関するものである。

この論文は、近畿地方中北部に発生した95個の地震を用い、この地域内の微小地震観測網の12観測点で観測したＰ波走時から SIMUL3（Thurber, 1983）により地殻上層部のＰ波３次元速度構造と震源を同時にインバージョンし、速度構造と震源分布、特に深さ分布を議論したものである。

データ依存性を調べるため、独立の２つのデータセットについてインバージョンを試みた結果、速度のゆらぎの絶対値は変化するが、そのパターンは変わらないことが分かった。また、この地域での地震の発生が、5-20 kmの深さに限られるため、最上層部の構造は十分に求めることができないが、地震の多い深さ付近ではよく決まり、この付近では速度のゆらぎは最大±８％でほとんどの地域が±４％の範囲である。速度の大きい地域では地震が少ないようにみえることも分かった。この地域で震源の下限が南西から北東にかけて深くなっているのが、３次元構造を考慮したこのインバージョンにより確かめられた。

以上に述べた通り、中部・近畿地方の３次元速度構造に関しては当初の目標に近いかなりの成果を挙げられたと考えているが、減衰（Q）構造の解明の研究は現在未だ進行中であり、今後の研究の進展に待ちたいと思う。

最後にこの研究に対して、多くの御援助を頂いた各位に厚く感謝を申し上げる次第である。

昭和63年2月

研究代表者　　三雲　健

Three-dimensional P-wave Velocity Structure beneath Central Japan - Low-Velocity Bodies in the Wedge Portion of the Upper Mantle above High-Velocity Subducting Plates -

Kazuro HIRAHARA*, Akira IKAMI**, Mizuho ISHIDA***
and Takeshi MIKUMO*

* Disaster Prevention Research Institute, Kyoto University
Uji, Kyoto 611, Japan
**Regional Center for Earthquake Prediction Observation,
Nagoya University, Chikusa, Nagoya 464, Japan
*** National Research Center for Disaster Prevention
Ibaraki 305, Japan

Submitted to Tectonophysics, Special Issue of IASPEI, 1985
on March, 1986
Re-submitted to Tectonophysics on November, 1987.

ABSTRACT

Three-dimensional(3-D) P-wave velocity structure beneath Central Japan has been investigated in detail by applying an inversion method. 7490 P-wave arrival times observed at 129 high-sensitive seismic stations from 120 shallow and intermediate depth earthquakes that occurred in this region are used to estimate velocity anomalies in 3-D subdivided blocks and hypocentral perturbations, simultaneously.

The results of our analysis clearly reveal complex 3-D structures with low velocity zones in the wedge portion of the upper mantle above the high-velocity Philippine Sea and Pacific plates subducting beneath this region. It was found that prominent low velocity bodies exist just beneath active volcanoes particularly in the Hida mountain range. There are remarkable spatial correlations of these low velocity bodies with the low-Q zones found by the recent analysis of seismic intensity data. One of these low velocity bodies well corresponds to the region where an anisotropic body was detected from the study of shear-wave splitting. These dome-shaped low velocity masses seem to represent partially melted mantle diapirs located at depth beneath this region. No clear evidence on velocity contrast has been identified across the Fossa Magna which is a tectonic boundary between Northeast and Southwest Japan.

1. INTRODUCTION

In Northeast Japan, the Pacific plate is subducting beneath the Eurasian plate from the east, while in Southwest Japan the Philippine Sea plate is subducting from the southeast. In Central Japan from the Kanto to Kinki regions shown in Fig.1, both of the two plates are subducting and produce remarkable lateral heterogeneities in the upper mantle. Beneath this region, the distribution of subcrustal earthquakes shows that the Philippine Sea plate subducts northwestwards from the Sagami and Suruga trouhgs to a depth of about 60 km in the Kanto and Tokai regions (e.g.,Ishida,1984; Yamazaki and Ooida, 1985), and the Pacific plate westwards from the Japan trench down to a depth of 400 km beneath the Kinki region. There is also a major tectonic belt called the Fossa Magna running north-south through Central Japan (Fig.1). It has been recently postulated (Kobayashi,1983; Nakamura,1983) that the northeastern Honshu arc, which might be a part of the North American plate, should be subducting beneath or colliding against the southwestern Honshu arc across the Fossa Magna.

Three-dimensional velocity analyses using an inversion technique of Aki and Lee (1976) have also successfully been applied to reveal the structure of these high-velocity plates (Hirahara,1981; Horie and Aki,1982; Ishida and Hasemi,1986). In the Tohoku region, Northeast Japan, on the other hand, the existence of low velocity structure in the wedge portion of the upper mantle, as well as the structure of the Pacific plate, has been revealed (Hasemi et al.,1984; Ohara et al.,1985). In the

Chubu region, Central Japan, moreover, Ando et al.(1983) found the existence of anisotropic bodies at depth from the study of shear-wave splitting. However, the corresponding low velocity structure in the wedge mantle has not yet been resolved in detail.

Our main purpose in this study is to elucidate more detailed velocity structures above the subducting Philippine Sea and Pacific plates in Central Japan, using the P-wave arrival time data observed at a dense network of high-sensitive seismic stations, which are deployed over this region for micro-earthquake observations. Further, we will discuss the obtained results in relation to the distribution of active volcanoes beneath Central Japan, the tectonic boundary across the Fossa Magna and to the structures of attenuation and anisotropy detected from other seismological studies. There are many organizations operating seismic networks in Central Japan, and the extensive use of the seismic data accumulated over several networks has just started. This study may be the first attempt to make use of an increasing volume of these data set.

2. DATA AND METHODS OF ANALYSIS

Data

We used the P-wave arrival times observed at high-sensitive seismic stations from earthquakes occuring in this region. Figure 2 shows the distribution of these 129 stations belonging to several institutes and universities, which form a high-density

seismic network. It is to be remarked that four OBS stations (JMA) off the Tokai region are included. We selected 120 earthquakes that took place in Central Japan below the crust to a depth of about 450 km during the period from August, 1979 to December, 1981. These epicenters are indicated in Fig. 3, where each symbol represents the depth range of the earthquakes, which is described in Section 3.

The initial velocity model adopted here is a spherically symmetric velocity model with the J-B mantle structure underlying the crustal model of Ukawa and Fukao (1981). Based on this model, we determined the initial hypocenters with station elevation and ellipticity corrections (Dziewonski and Gilbert,1976). The data employed here are only arrival times with absolute travel-time residuals less than 5.0 sec, which finally amount to 7490 data with a standard deviation of 0.48 sec.

Method of Analysis

The method of analysis used here is the same as that described in Hirahara(1981). The travel time residual data were inverted to determine the velocity anomalies in a number of subdivided 3-D blocks within a modeling space and the source corrections simultaneously, by applying the method of Aki and Lee(1976). We divided the shallower part of the modeling space above a depth of 200 km into five layers with a thickness of 33 km or 50 km and the deeper space at depths between 200 km and 500 km into three layers with a thickness of 100 km. Further, the upper layers were subdivided horizontally into 15 x 9 blocks with a smaller size of 0.5° x 0.5° and the lower layers

into 8 x 5 blocks with a larger size of 1.0° x 1.0°. As remarked in Hirahara(1981), our initial velocity model has smoothly varying velocities even within each layer, where down-going seismic waves from shallower earthquakes can readily be incorporated into the analysis.

Using a damped least squares method, we solved a total of 927 unknown parameters including 120 x 4 source corrections and 447 observed blocks. In order to obtain the solutions, we used the following a priori information on the estimated errors of parameters :

σ_d=0.3 sec (for data), σ_i=3.0 % (for velocity perturbation), $\sigma_\varphi = \sigma_\lambda$ =0.03° (for latitude and longitude corrections), σ_h=3.0 km (for depth correction), and σ_T=0.3 sec (for origin time correction).

Accordingly, the damping factors used in this analysis are:

θ_i=0.01(sec/%)^2, $\theta_\varphi = \theta_\lambda$=0.01(sec/0.01°)^2,

θ_h=0.01(sec/km)^2, and θ_T=10.

The use of different damping factors slightly changes the absolute values of velocity anomalies and source corrections. It has been confirmed, however, that as long as we use physically reasonable a priori information the patterns of velocity anomalies are not seriously affected.

With these damping factors, the initial data variance of 0.229 sec^2 was reduced to the residual variance of 0.139 sec^2 after inversion, which gives the resultant variance improvement of 40 %. The source corrections calculated for the latitudes, longitudes, depths and origin times were -0.02°~0.04°, -5~4 km

and -0.3 ~ 0.4 sec, respectively. The obtained velocity perturbations will be given in a later section. Their estimated errors resulting from the data errors had a maximum of about 1.5 % for their diagonal elements of resolution matrix around 0.5. On the other hand, a slightly different method of estimating errors has recently been proposed. Total variances of the obtained solutions $\sigma_{\hat{m}}$, which result not only from the random noise in the data but also from the probable errors of initial models, are given (e.g. Jackson and Matsu'ura,1985) by

$$\sigma_{\hat{m}}^2 = \sigma_{\hat{m}o}^2 \ (1 - R)$$

where σ_{mo}^2 and R are initial assumed variances of solutions and their resultant diagonal elements of resolution matrix, respectively. Accordingly, for example, the estimated errors for their diagonal elements of resolution matrix of 0.5, 0.7 and 0.9 are 2.12, 1.64 and 0.94 %, respectively, in this study. The calculated results shown in Fig.4 has a resolution around 0.7 or more in the major part of the region under consideration. From the above estimates, the standard errors involved in our results discussed in the following section are less than about 1.5 %.

3. RESULTS AND DISCUSSION

Figures 4(a)-(e) represent the obtained velocity anomalies ineach divided layer, together with the distribution of earthquakes located by ISC within the corresponding layer during the period from 1964 to 1975. Two solutions have been calculated for different block configurations, one of which is shifted southwestwards by a half-block length, to remove possible effects

of particular block configurations on the solutions. In the upper figures, both of these two solutions are plotted in per mill. In the lower figures, contours are drawn at every 1.5 % interval, where solid and broken lines indicate high and low velocity anomalies, respectively. The extent of regions with diagonal elements of resolution greater than 0.5 is enclosed by thin lines. Taking into consideration the resolution and block size, we will show and discuss only the results for Layers-1 to -5 down to a depth of 200 km.

Figure 4(a) shows the results for Layer-1 (0-33 km). This layer consists mainly of the crust. Low velocity anomalies can be recognized around the Chubu high mountain region and around the Tokyo Bay in the Kanto region, which well correspond to the observed negative Bouguer anomalies there (e.g. Tomoda and Fujimoto,1982). The former suggests a larger scale crustal thickning beneath the central part of the Chubu region, which is consistent with the results from explosion seismic observations (Aokiet al.,1972), and also with the existence of thick sedimentary layers in the northwestern part of the region. The low velocities in the Kanto region reflect the existence of thick sedimental layers (e.g. Tada,1982). Similar low velocity anomalies with a small scale can also be found off the Tokai region, which increase toward the ocean, although they do not have good resolutions. The off-Tokai results are derived exclusively from the OBS observations and seem to reflect ocean-bottom sedimental layers and also a transitional structure from the continental to oceanic crust, which are again consistent with

the results from explosion seismic observations (Research Group for Crustal Structure in the Tokai Region,1982). It can also be recognized that remarkable high velocities exist in the Izu Peninsula and the northern Kanto region. The high velocity anomalies in the Izu Peninsula indicate crustal thinning here (Ikami,1978). Towards the Kinki region and the Kii Peninsula, there appear small high velocities. However, in view of our data set employed in this study lacking suitable earthquakes and good coverage of stations over these regions, we do not discuss any more the results for these regions in this paper.

In Layer-2 (33-66 km), low velocity anomalies can be identified to extend northwards from the Izu Peninsula along the volcanic front (see Fig.1). Also in the Chubu and its northern regions, small low velocities appear just beneath the active volcanoes there. Comparing Figs. 4(b) and (c) with Fig. 5, which displays the distribution of active Quaternary volcanoes in this region, we immediately notice a remarkable correlation between the locations of low velocity anomalies and of active Quaternary volcanoes. On the other hand, high velocity anomalies appear in the eastern and western sides of the Izu Peninsula. These high velocities can be interpreted to represent the Philippine Sea plate subducting eastwards beneath the Kanto region and westwards beneath the Tokai region, respectively. In the Kanto region, another high velocity anomalies with high seismic activities can also be seen near the eastern coastal region, which correspond to the subducting Pacific plate. These results are consistent with those of Horie and Aki(1981) and Ishida and Hasemi,1986). Although our block size assigned in

this study is larger than those of theirs, considerably fine structures have been well retrieved. For example, within the high velocity region, a local low velocity zone appears in the eastern Kanto region, which was also found in Horie and Aki (1982). This small low velocity zone roughly coincides with the low-Q region detected from spectral studies of shear waves (Tsujiura,1973, Aki,1980). Horie and Aki (1982) postulated that downward bending of the Pacific plate may cause this low-V and low-Q region. The high velocities in the Tokai region correspond to seismic activities within the Philippine Sea plate, and appear to extend further northwards to regions without high seismicity. In Layers 1 and 2, on the other hand, no sharp velocity contrast can be identified across the northern to southern Fossa Magna which would correspond to a plate boundary. In the region west of the northern extension of the Fossa Magna to Japan Sea coast, however, there appears to be a high velocity zone in the crust and the upper mantle beneath the Toyama Bay. This makes a velocity contrast across the 138°-longitudinal line (see Figs.4(a) and (b)).

In Layer-3(66-100 km), a noticeable low velocity zone still exists just beneath a volcano, Mt. Fuji, north of the Izu Peninsula. The low velocity zone appears to extend north- and south-westwards, respectively. The existence of low velocities beneath the Hida region is convincing in view of good resolutions, which continues down from the upper layers, and extends northwards. However, the southward extended low velocity zone beneath the off-Tokai region is not so well

resolved. On the other hand, the high velocities that appear in the Kanto region correspond to high seismic activities, indicating the Pacific plate subducting around here. There are also high velocities in the Chubu region, but these do not correspond to seismic activities.

In Layer-4(100-150 km), low velocities appear to spread over the north of the Hida region and over the Tokai region. In Layer-5(150-200 km), there are no prominent velocity anomalies.

Next, we show vertical cross sections of the obtained velocity structure along three profiles indicated in Fig.5 to see more detailed features of the low velocity bodies mentioned above. Figures 6(a) and (b) display the west-east (A-A') and south-north (B-B') vertical profiles across and through the Hida high mountain region. From the two figures, the low velocity body can be clearly identified just beneath active volcanoes in the upper mantle above the subducting high velocity Pacific plate. It is noticed in Fig.6(b) that this low velocity body beneath the active volcanoes appears to incline towards the north and reach a depth of about 150 km. We can also see the Philippine Sea plate subducting beneath the Tokai region, which appears to extend down to a depth of 150 km but is not accompanied by any seismic activities. There are a few studies which have suggested a possible aseismic extension of the subducting Philippine Sea plate beneath Southwest Japan (Nakanishi,1979; Hirahara,1981) Figure 6(c) shows the vertical section (C-C') through the Izu Peninsula. Under the Izu Peninsula, there is a low velocity body sandwiched between the subducting Philippine Sea and Pacific plates, both of which are

learly identified by high velocities with seismic activities.

Our results indicate that there exist significant lateral heterogeneities even within low velocity zones in the wedge portion of the upper mantle, that is, the low velocity bodies are not uniformly embedded along the region west of the volcanic front, but appear to lie only beneath active volcanoes. Also in the Tohoku region, Northeast Japan, the similar features of low velocity structure have been detected (Hasemi et al.,1984; Ohara et al.,1985). On the other hand, a three-dimensional attenuation structure over the Japan Islands derived from the analysis of seismic intensity data (Hashida,1985) shows that highly attenuative areas are well correlated with the distribution of volcanoes. It was also pointed out that the areas have better correlations with active volcanoes than other Quaternary volcanoes. Our low velocity bodies extending northwards from the Izu Peninsula identified in Layers-2 and -3 coincide remarkably with the high attenuation zones detected by Hashida and Shimazaki(1985). On the other hand, Ando et al.(1983) found the existence of an anisotropic body beneath the Hida mountain region from the study of shear-wave splitting. There is a remarkable spatial consistency between our low velocity body and the ray paths of their observed split shear-waves in this region. Ando et al.(1985) also suggested that the low velocity and the shear-wave anisotropy may be caused by aligned melt-filled cracks in the upper mantle.

Thus, our dome-shaped low-velocity bodies found just beneath active volcanoes down to a depth of 100 or 150 km seem to be

accompanied with low-Q and anisotropic properties. It may be said that we are now viewing the deep structure of mantle diapirs beneath active volcanoes in this region.

4. CONCLUSION

We have investigated the three-dimensional P-wave velocity structure beneath Central Japan by applying an inversion technique developed by Aki and Lee (1976). In particular, the present analysis clearly reveals the existence of considerable lateral heterogeneities including remarkable low velocity zones in the wedge portion of the upper mantle right above the high velocity Pacific plate subducting beneath this region. The low velocity bodies, which originate at a depth of 100 or 150 km, have been detected just beneath active volcanoes. These bodies seem to have highly attenuative and anisotropic properties, which were evidenced from other geophysical investigations (Hashida and Shimazaki,1985; Ando et al.,1983). These dome-shaped low velocity bodies may represent partially melted diapirs in the wedge portion of the upper mantle, and may be closely related to island-arc volcanism. The present analysis does not provide any clear evidence on a possible plate boundary across the Fossa Magna.

ACKNOWLEDGEMENTS

This study has been carried out originally by the Research Group for 3-D Seismic Structure beneath Central Japan. For discussions and providing the observed data, we would like to thank other members of this group; K.Tsumura (J.M.A.), T.Tsukuda, T.Miyatake (E.R.I.), and H.Wada, F.Takeuchi, K.Ito (Kyoto Univ.). Our thanks are also due to M.Ando for his helpful discussions.

Computations were made at the Data Processing Center of Kyoto University. This study was partly supported by a Grant-in-Aid of the Ministry of Education, Science and Culture of Japan (B60460045).

REFERENCES

Aki, K., 1980. Attenuation of shear-waves in the lithosphere for frequencies from 0.05 to 25 Hz. Phys.Earth Planet.Inter., 21:50-60.

Aki, K. and Lee, W.H.K., 1976. Determination of three-dimensional velocity anomalies under a seismic array using first P arrival times from local earthquakes. 1. A homogeneous initial model. J.Geophys.Res., 81:4381-4399.

Aoki, H., Tada, T., Sasaki, Y, Ooida, T., Muramatu, I., Shimamura, H. and Furuya, I., 1972. Crustal structure in the profile across central Japan as derived from explosion seismic observations. J.Phys.Earth, 20:197-223.

Ando, M., Ishikawa, I. and Yamazaki, F., 1983. Shear wave polarization anisotropy in the upper mantle beneath Honshu, Japan. J.Geophys.Res., 10:5850-5864.

Ando, M., Hirahara, K., Ishikawa, U. and Ishida, M., 1985. Observations of shear-wave polarization anisotropy and low P-wave bodies: partially melted diapirs in the upper mantle. Abstr. 23rd Gereral Assembly IASPEI, 2:591.

Dziewonski, A.M.and Gilbert, F., 1976. The effect of small, aspherical perturbation on travel times and a re-examination of the correction for ellipticity. Geophys.J.R.Astron.Soc., 44:7-17.

Hirahara, K., 1981. Three-dimensional seismic structure beneath southwest Japan : the subducting Philippine Sea plate. Tectonophysics, 79:1-44.

Hasemi, A.H., Ishii, H. and Takagi, A., 1984. Fine structure beneath the Tohoku district, northeastern Japan arc, as

derived by an inversion of P-wave arrival times from local earthquakes. Tectonophysics, 101:245-265.

Hashida, T., 1985. Three-dimensional seismic attenuation structure beneath the Japanese Islands as determined from seismic intensity data. Ph.D. Thesis, Tokyo Univ. pp. 1-234.

Hashida, T. and Shimazaki, K., 1985. Seismic tomography: 3-D image of upper mantle attenuation beneath the Kanto district, Japan. Earth Planet.Sci.Lett., 75:403-409

Horie, A. and Aki, K., 1982. Three-dimensional velocity structure beneath the Kanto district, Japan. J.Phys.Earth, 30:255-281.

Ishida, M., 1984. The spatial distribution of earthquake hypocenters and the three-dimensional velocity structure in the Kanto-Tokai district, Japan. J.Phys.Earth, 32:399-422.

Ishida, M. and Hasemi, A.H., 1986. Three-dimensional fine velocity structure and hypocentral distribution of earthquakes beneath the Kanto-Tokai district, Japan. Submitted to J.Geophys.Res..

Ikami, A., 1978. Crustal structure in the Shizuoka district, central Japan as derived from explosion seismic observations. J.Phys.Earth, 26:299-331.

Jackson, D.D., and Matsu'ura, M., 1985. A bayesian approach to nonlinear inversion. J.Geophys.Res., 90:581-591.

J.M.A., 1975. National catlogue of the active volcanoes in Japan (in Japanese). 1-119.

Kobayashi, Y., 1983. Incipient subduction of a lithospheric plate under the eastern margin of the Japan Sea. The Earth Monthly, 5:510-514 (in Japanese).

Nakamura, K., 1983. Possible nascent trench along the eastern Japan Sea as the convergent boundary between Eurasian and North American plates, Bull.Earthq.Res.Inst., 58:711-722 (in Japanese with English Abstract).

Nakanishi, I., 1980. Precursors to ScS phases and dipping interface in the upper mantle beneath southwestern Japan. Tectonophysics, 69:1-35.

Ohara, K., Hasegawa, A. and Takagi, A., 1985. Three-dimensional velocity structure in the crust and the upper mantle beneath the northeastern Japan Arc. Prog.Abstr.Seismol.Soc.Jpn., 1:82 (in Japanese).

Research Group for Crustal Structure in the Tokai Region, 1982. Crustal structure revealed by the explosion seismic observation along the line between Kawakami and off-Tokai region. Prog.Abstr.Seismol.Soc.Jpn., 2:112 (in Japanese).

Tada, T., 1982. Structure of the basement and gravity anomaly in the Kanto plain (1). Depth distribution of the basement, Zisin, 35:607-617 (in Japanese).

Tomoda, Y. and Fujimoto, H., 1982. Maps of gravity anomalies and bottom topography in the western Pacific. Bull.Ocean Res.Inst.,Univ.Tokyo, 14.

Tsujiura, K., 1973. Regional variation of micro-earthquake spectrum - Kanto district. Zisin, 26:370-375 (in Japanese).

Ukawa, M. and Fukao, Y., 1981. Poisson's ratio of the upper and lower crust and the sub-Moho mantle beneath central Honshu, Japan. Tectonophysiscs, 77:233-256.

Yamazaki, F. and Ooida, T., 1985. Configuration of subducted Philippine Sea plate beneath the Chubu district, central

Japan. Zisin, 38:193-201 (in Japanese).

FIGURE CAPTIONS

Fig.1. Index map of the investigated region, central Japan. In the inset, EUR, PAC and PHS represent the Eurasian, Pacific and Philippine Sea plates, respectively, and the broken line shows the volcanic front.

Fig.2. Distribution of the seismic stations and block configuration of upper modeling space.

Fig.3. Distribution of the earthquakes used in this study. Different symbols indicate the ranges of focal depths (L-2 means Layer-2, and so on).

Figs.4(a)-(e). The obtained velocity perturbations in per mill for each layer from Layers 1-5 (upper) and the distribution of earthquakes located in the corresponding layer by the ISC during the period from 1964 to 1975 (lower). In the lower figures, the contours of velocity perturbations are also drawn at every 1.5 % interval where thick lines indicate high velocity anomalies and broken ones low velocity anomalies, and the regions enclosed by lines indicate the blocks where the diagonal elements of the resolution matrix are greater than 0.5.

Fig.5. Distribution of active volcanoes in this region and locations of three profiles. Closed triangles and circles indicate the volcanoes with and without histrical records of eruption, respectively (J.M.A.,1975).

Figs. 6(a)-(c). The velocity perturbations and hypocenters shown in Figs.4 projected onto the vertical cross-sections along the profiles A-A', B-B' and C-C' with no vertical exaggeration.

Contours are drawn in the same way in Fig.4. The upper figures show the enlarged maps including each profile in Fig.5.

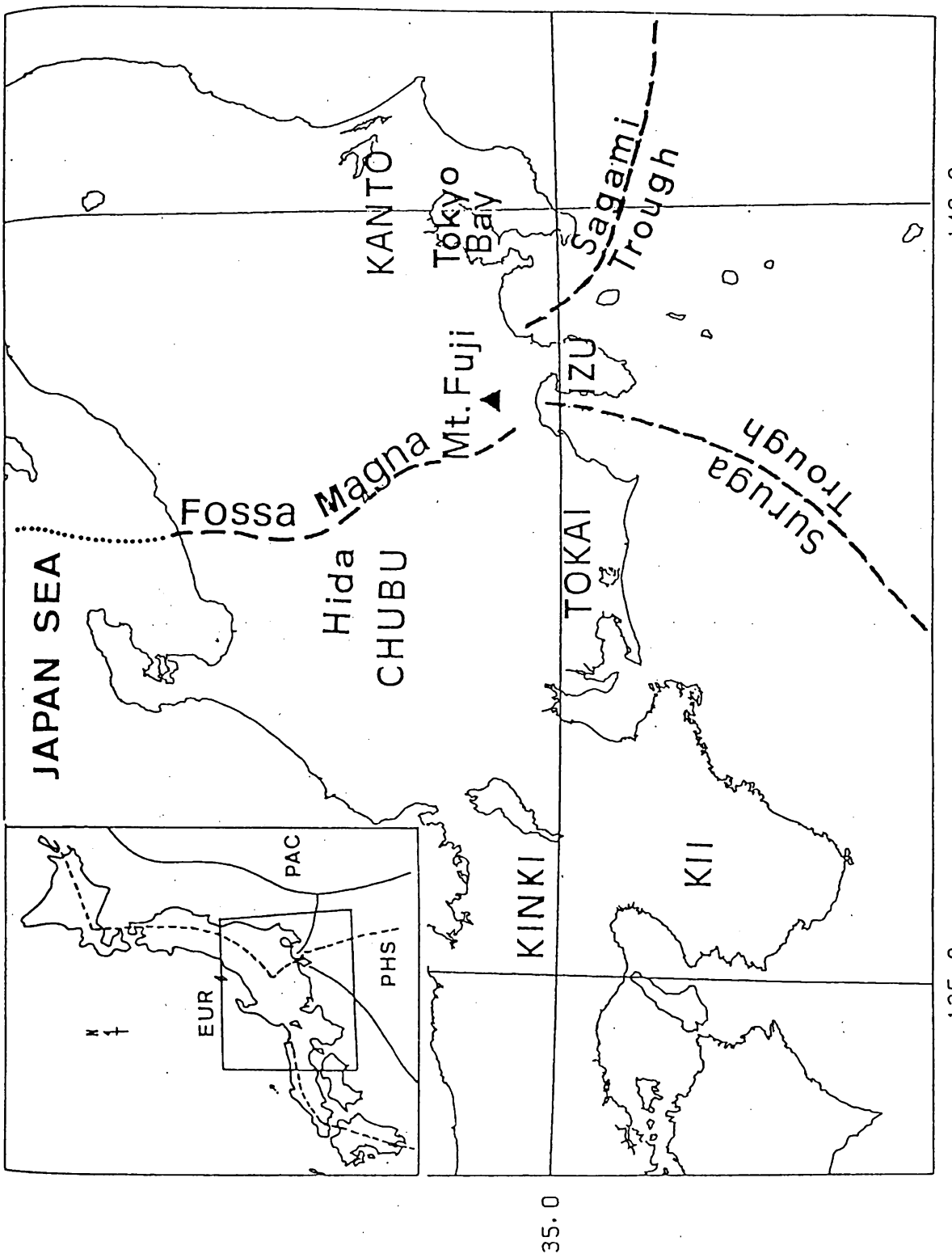
JAPAN SEA
Fossa Magna
Hida
CHUBU
Mt. Fuji
KANTO
Tokyo Bay
Sagami Trough
IZU
Suruga Trough
TOKAI
KINKI
KII
PAC
PHS
EUR
N
140.0
135.0
35.0

Fig. 1

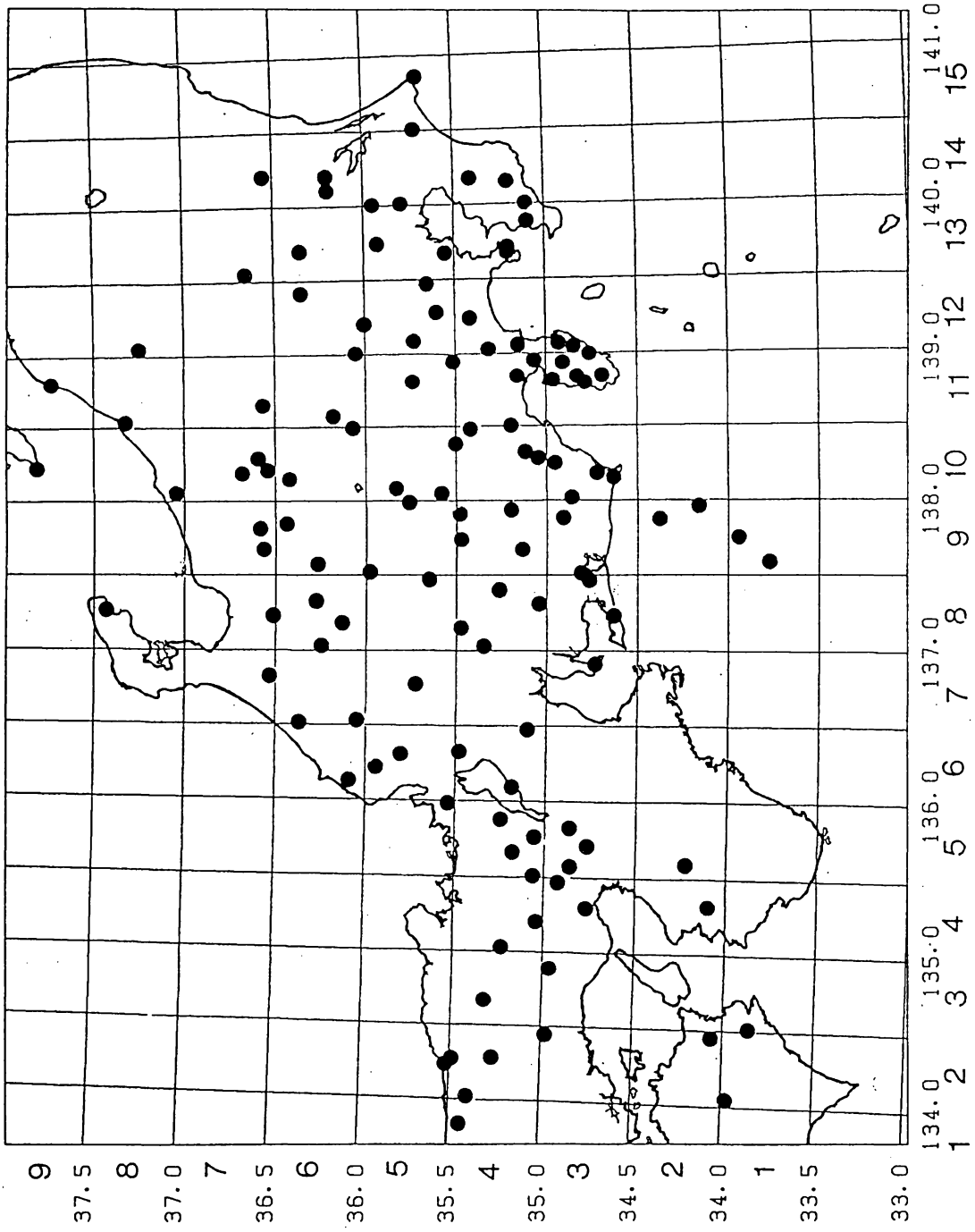
134.0
135.0
136.0
137.0
138.0
139.0
140.0
141.0
1
2
3
4
5
6
7
8
9
10
11
12
13
14
15
37.5
37.0
36.5
36.0
35.5
35.0
34.5
34.0
33.5
33.0
9
8
7
6
5
4
3
2
1

Fig. 2

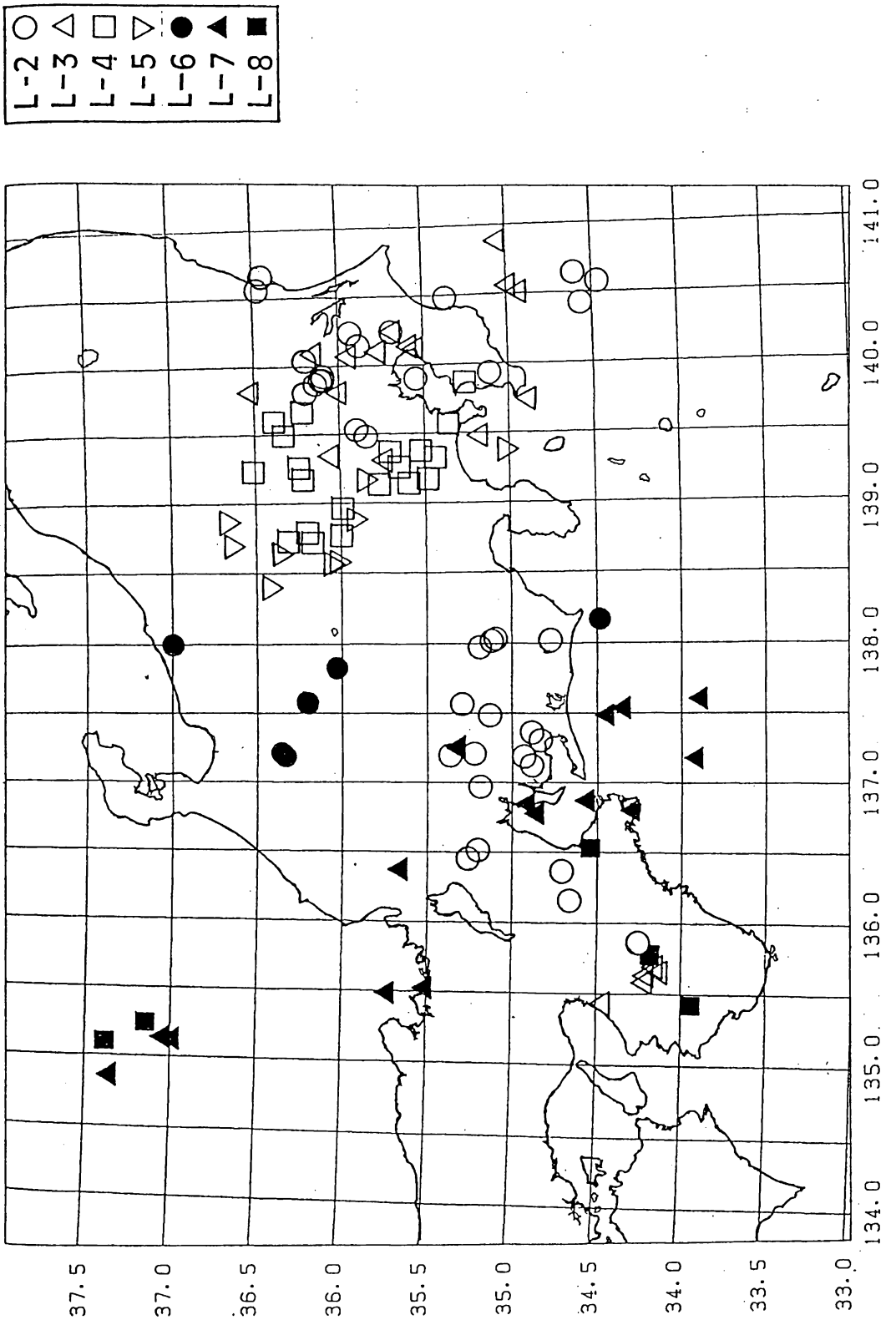
L-2
L-3
L-4
L-5
L-6
L-7
L-8
37.5
37.0
36.5
36.0
35.5
35.0
34.5
34.0
33.5
33.0
134.0
135.0
136.0
137.0
138.0
139.0
140.0
141.0

Fig. 3

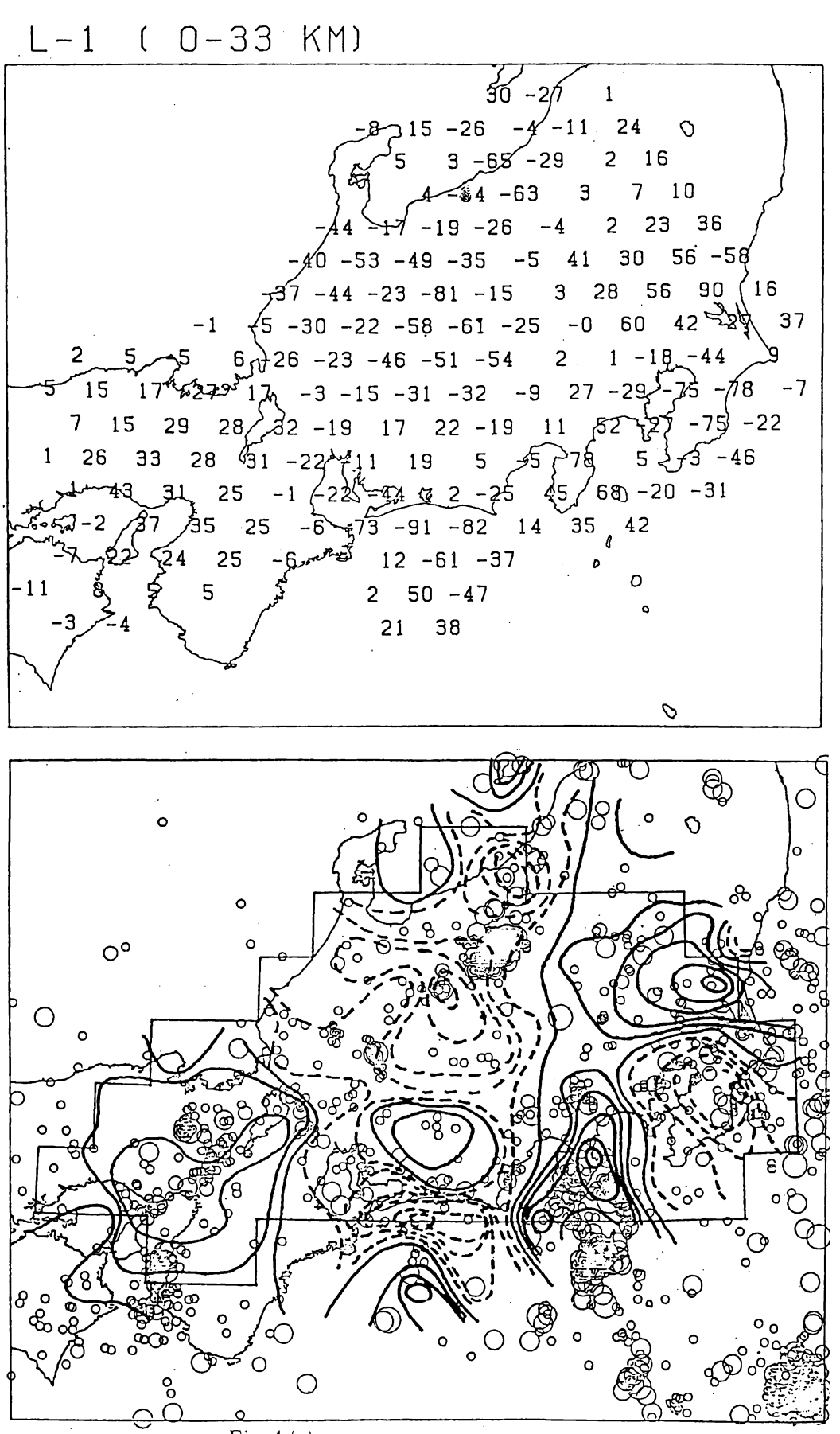
L-1 (0-33 KM)
30 -27 1
-8 15 -26 -4 -11 24 0
5 3 -65 -29 2 16
4 -64 -63 3 7 10
-44 -17 -19 -26 -4 2 23 36
-40 -53 -49 -35 -5 41 30 56 -58
-37 -44 -23 -81 -15 3 28 56 90 16
-1 -5 -30 -22 -58 -61 -25 -0 60 42 37
2 5 5 6 -26 -23 -46 -51 -54 2 1 -18 -44 9
5 15 17 27 17 -3 -15 -31 -32 -9 27 -29 -75 -78 -7
7 15 29 28 32 -19 17 22 -19 11 52 -75 -22
1 26 33 28 31 -22 11 19 5 -5 78 5 -3 -46
1 43 31 25 -1 -22 -44 2 -25 45 68 -20 -31
-2 37 35 25 -6 -73 -91 -82 14 35 42
-7 22 24 25 -6 12 -61 -37
-11 8 5 5 2 50 -47
-3 -4 21 38

Fig. 4 (a)

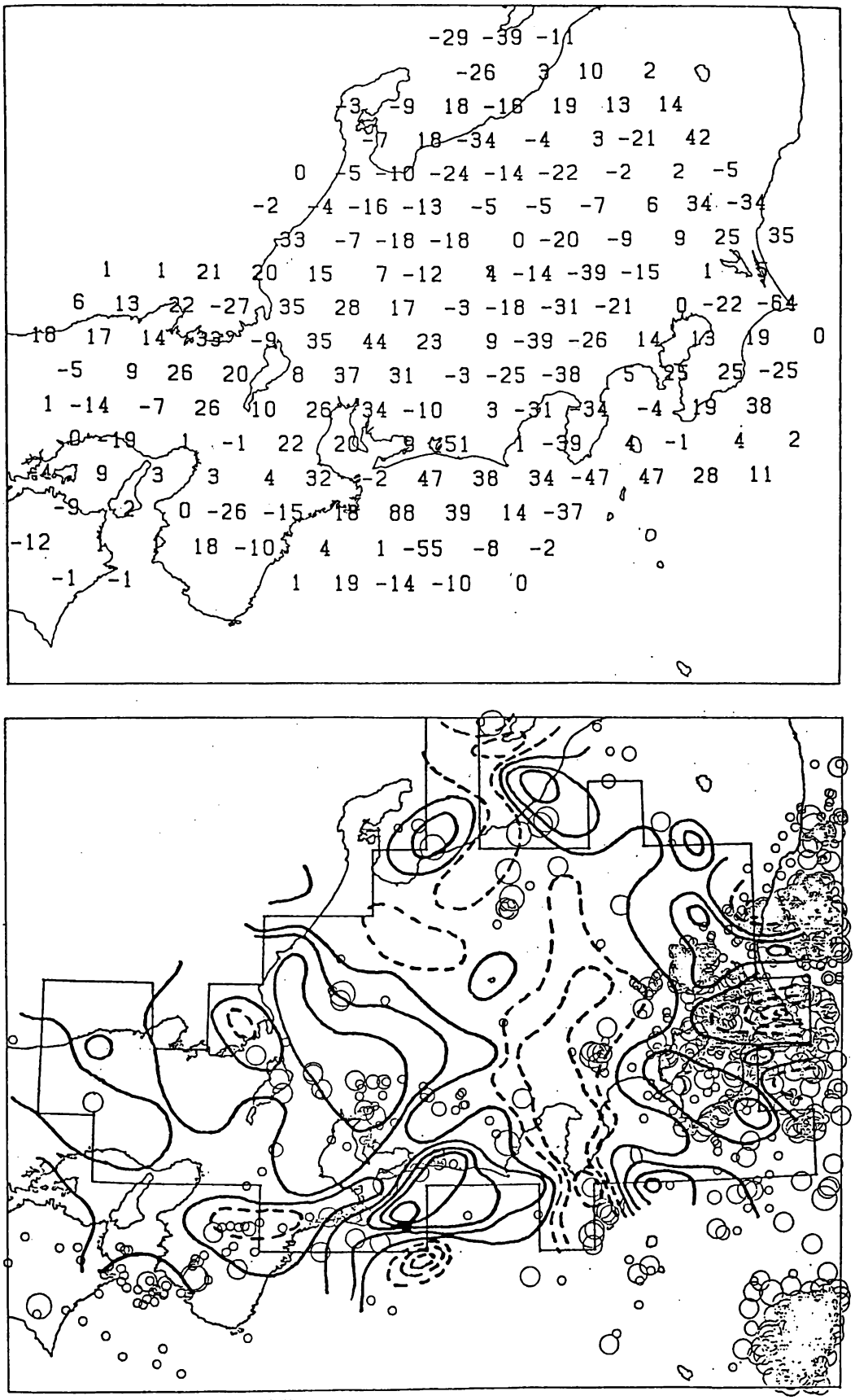
L-2 (33-66 KM)
-29 -39 -11
-26 3 10 2 0
-3 -9 18 -16 19 13 14
-7 18 -34 -4 3 -21 42
0 -5 -10 -24 -14 -22 -2 2 -5
-2 -4 -16 -13 -5 -5 -7 6 34 -34
33 -7 -18 -18 0 -20 -9 9 25 35
1 1 21 20 15 7 -12 4 -14 -39 -15 1 5
6 13 22 -27 35 28 17 -3 -18 -31 -21 0 -22 -64
18 17 14 33 -9 35 44 23 9 -39 -26 14 13 19 0
-5 9 26 20 8 37 31 -3 -25 -38 5 25 25 -25
1 -14 -7 26 10 26 34 -10 3 -31 -34 -4 19 38
0 -19 1 -1 22 20 9 51 1 -39 4 -1 4 2
4 9 3 3 4 32 -2 47 38 34 -47 47 28 11
-9 2 0 -26 -15 18 88 39 14 -37
-12 18 -10 4 1 -55 -8 -2
-1 -1 1 19 -14 -10 0

Fig. 4 (b)

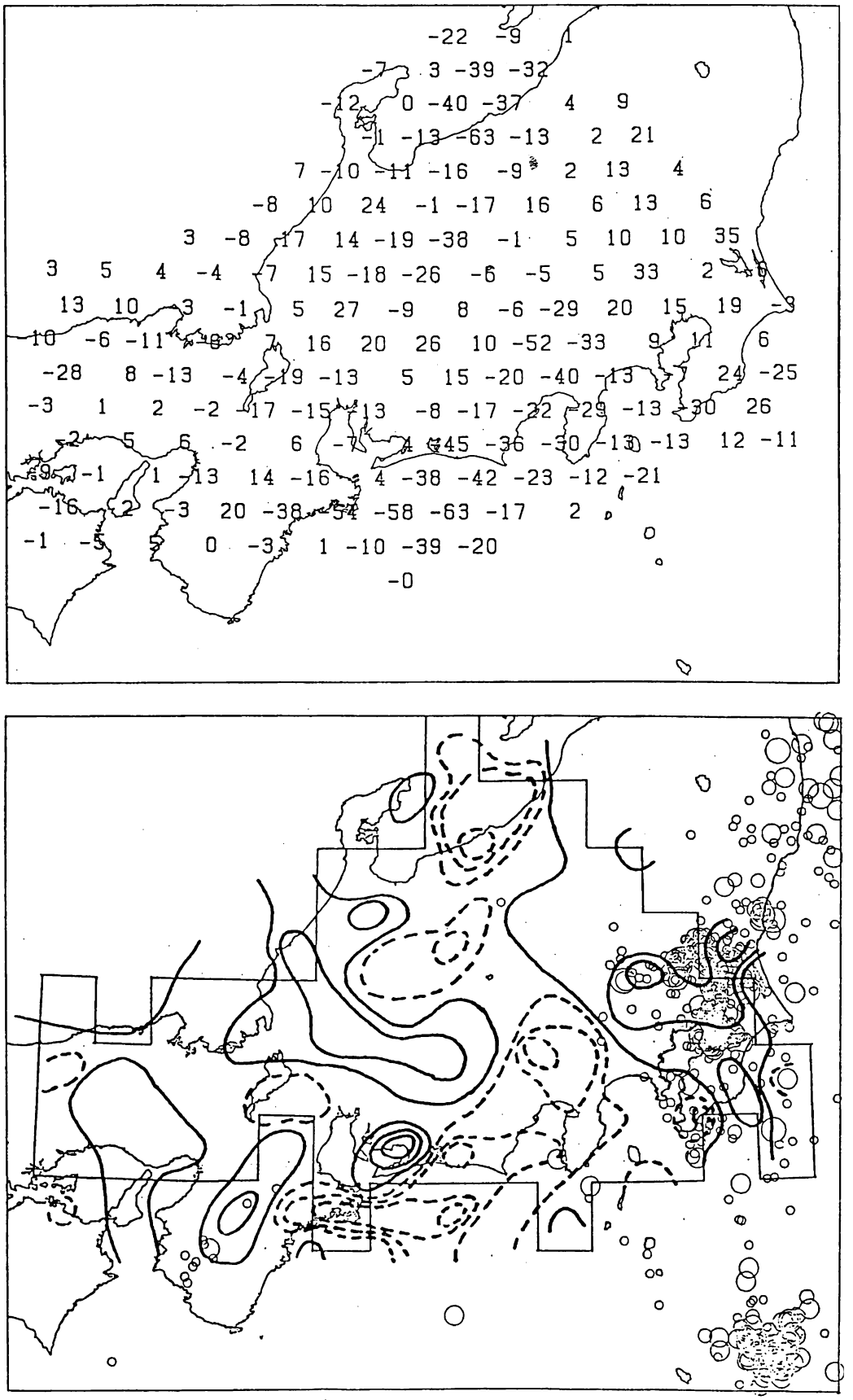
L-3 (66-100 KM)
-22 -9 1
-7 3 -39 -32
-12 0 -40 -37 4 9
-1 -13 -63 -13 2 21
7 -10 -11 -16 -9 2 13 4
-8 10 24 -1 -17 16 6 13 6
3 -8 17 14 -19 -38 -1 5 10 10 35
3 5 4 -4 -7 15 -18 -26 -6 -5 5 33 2
13 10 3 -1 5 27 -9 8 -6 -29 20 15 19
10 -6 -11 7 16 20 26 10 -52 -33 9 11 6
-28 8 -13 -4 -19 -13 5 15 -20 -40 -13 24 -25
-3 1 2 -2 -17 -15 13 -8 -17 -22 -29 -13 -30 26
-2 5 6 -2 6 -7 4 45 -36 -30 -13 -13 12 -11
-1 1 -13 14 -16 4 -38 -42 -23 -12 -21
-16 2 -3 20 -38 54 -58 -63 -17 2
-1 -5 5 0 -3 1 -10 -39 -20
-0

Fig. 4 (c)

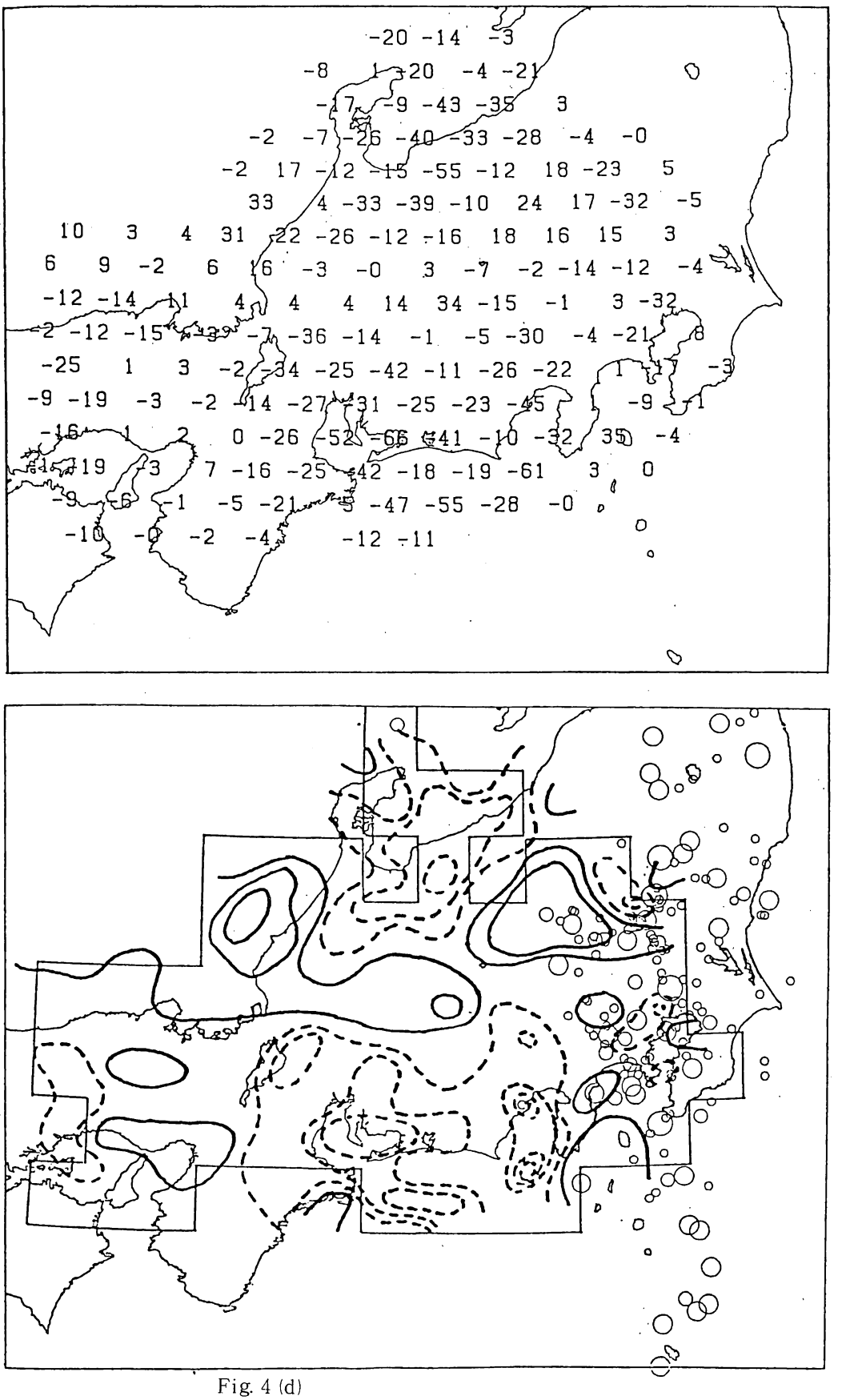
L-4 (100-150 KM)
-20 -14 -3
-8 1 -20 -4 -21
-17 -9 -43 -35 3
-2 -7 -26 -40 -33 -28 -4 -0
-2 17 -12 -15 -55 -12 18 -23 5
33 4 -33 -39 -10 24 17 -32 -5
10 3 4 31 -22 -26 -12 -16 18 16 15 3
6 9 -2 6 16 -3 -0 3 -7 -2 -14 -12 -4
-12 -14 11 4 4 4 14 34 -15 -1 3 -32
-2 -12 -15 -3 -7 -36 -14 -1 -5 -30 -4 -21 8
-25 1 3 -2 -34 -25 -42 -11 -26 -22 1 -3
-9 -19 -3 -2 -14 -27 -31 -25 -23 -45 -9 -1
-16 1 2 0 -26 -52 -66 -41 -10 -32 35 -4
-19 3 7 -16 -25 -42 -18 -19 -61 3 0
-9 -6 -1 -5 -21 -5 -47 -55 -28 -0
-10 -0 -2 -4 -12 -11

Fig. 4 (d)

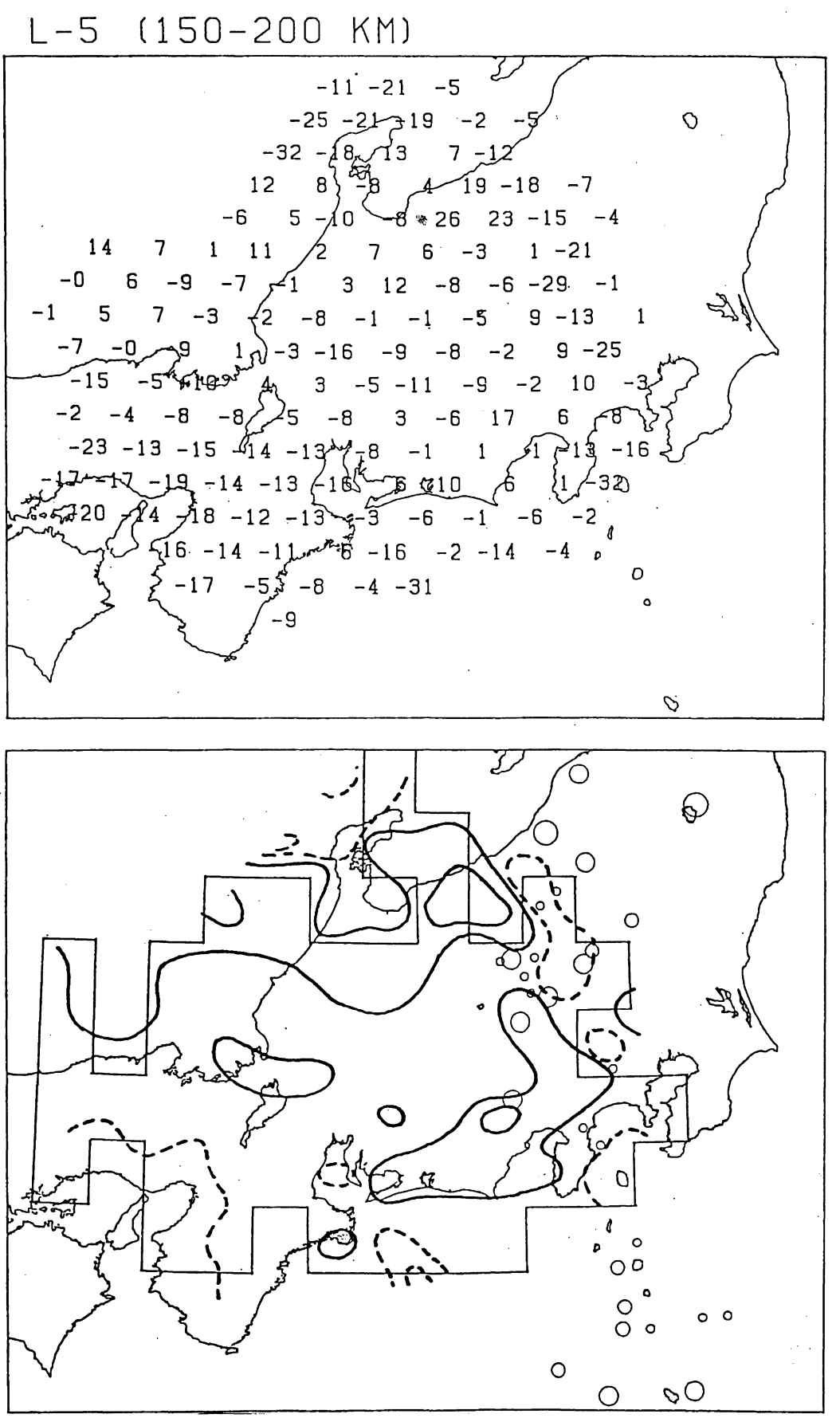
L-5 (150-200 KM)
-11 -21 -5
-25 -21 -19 -2 -5
-32 -18 13 7 -12
12 8 -8 4 19 -18 -7
-6 5 -10 -8 26 23 -15 -4
14 7 1 11 2 7 6 -3 1 -21
-0 6 -9 -7 -1 3 12 -8 -6 -29 -1
-1 5 7 -3 -2 -8 -1 -1 -5 9 -13 1
-7 -0 9 1 -3 -16 -9 -8 -2 9 -25
-15 -5 10 4 3 -5 -11 -9 -2 10 -3
-2 -4 -8 -8 5 -8 3 -6 17 6 -8
-23 -13 -15 -14 -13 -8 -1 1 -1 -13 -16
-17 -17 -19 -14 -13 -16 -6 10 6 1 -32
-20 -14 -18 -12 -13 -3 -6 -1 -6 -2
-16 -14 -11 -6 -16 -2 -14 -4
-17 -5 -8 -4 -31
-9

Fig. 4 (e)

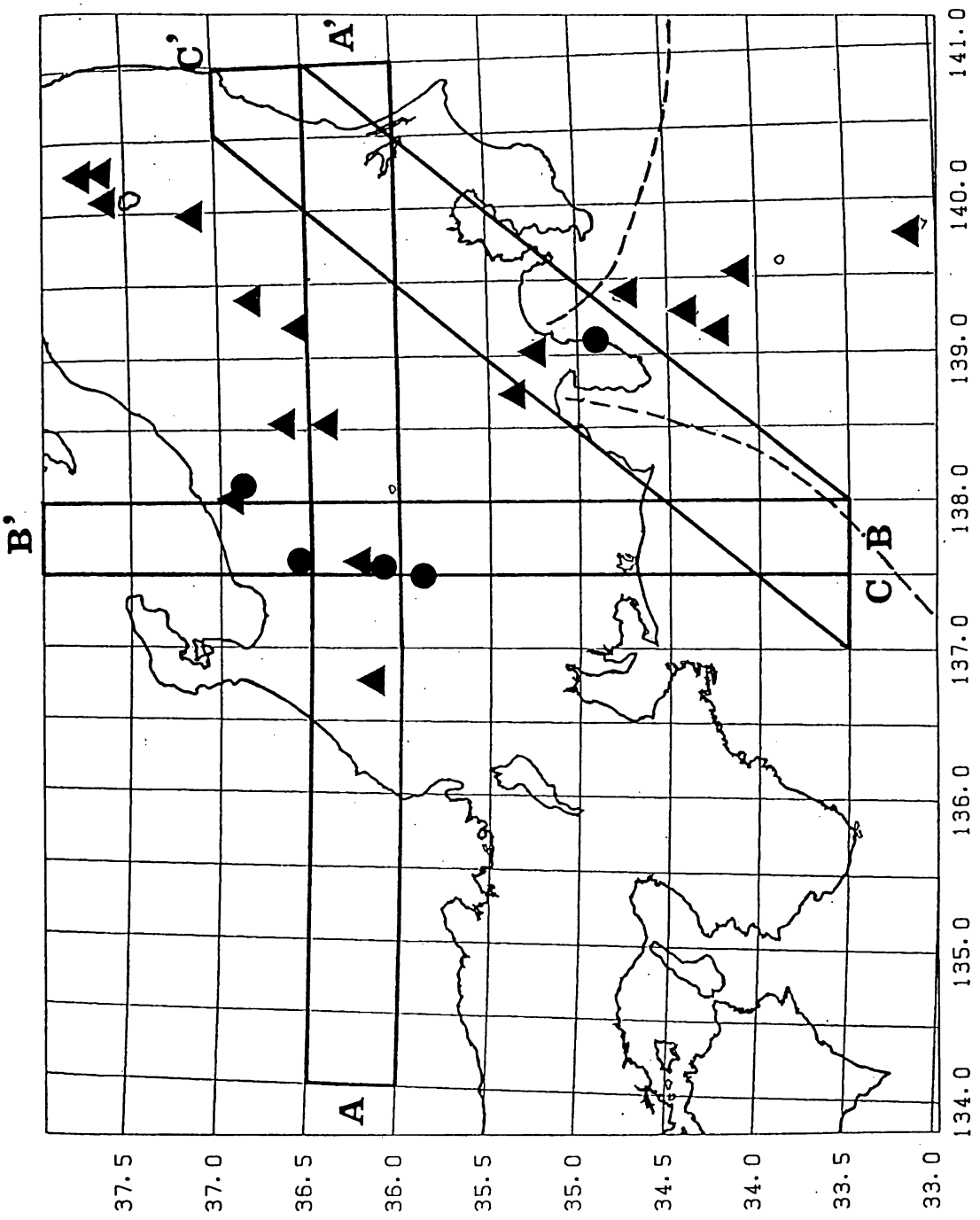
A
A'
B
B'
C
C'
134.0
135.0
136.0
137.0
138.0
139.0
140.0
141.0
33.0
33.5
34.0
34.5
35.0
35.5
36.0
36.5
37.0
37.5

Fig. 5

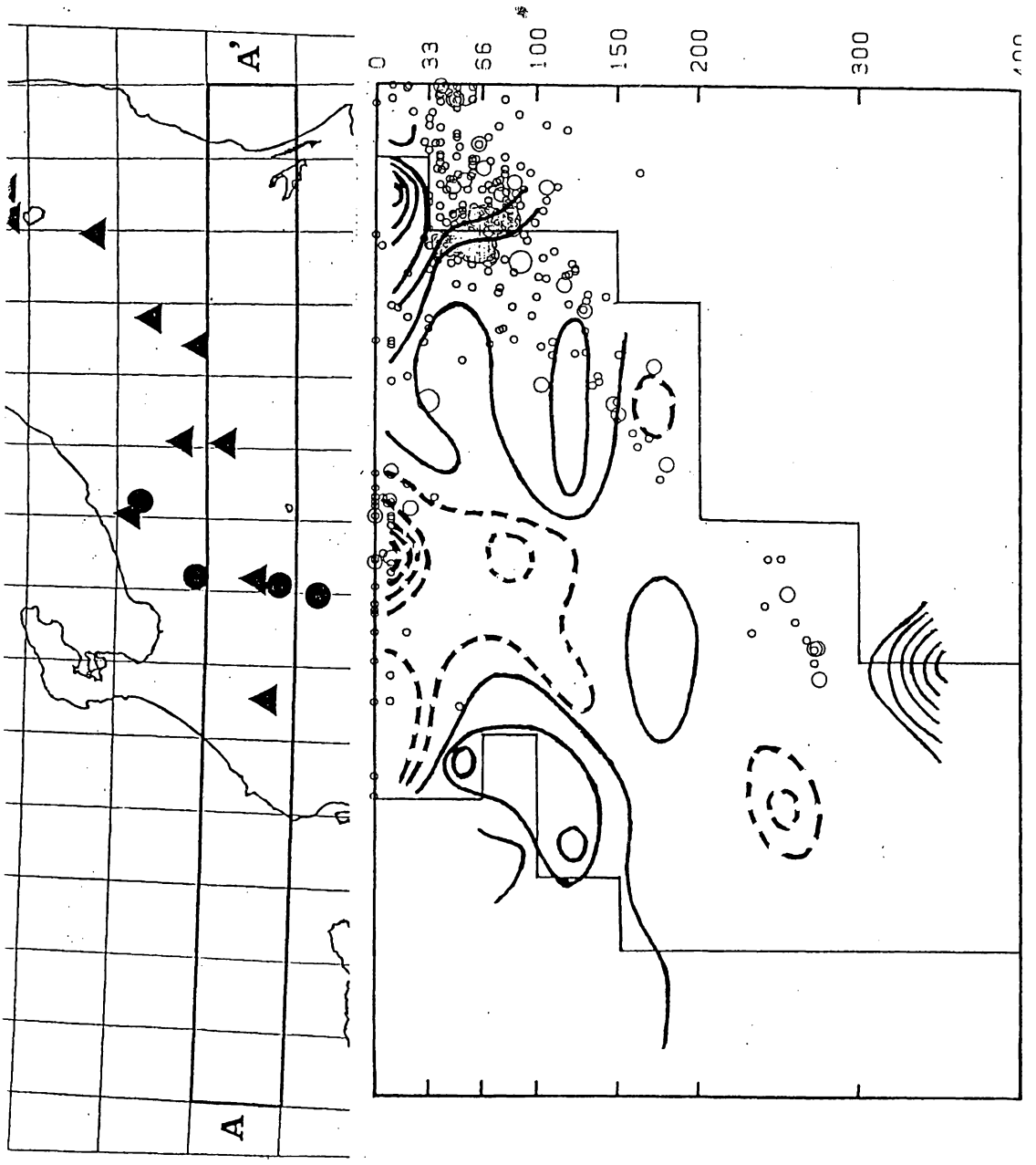

Fig. 6 (a)

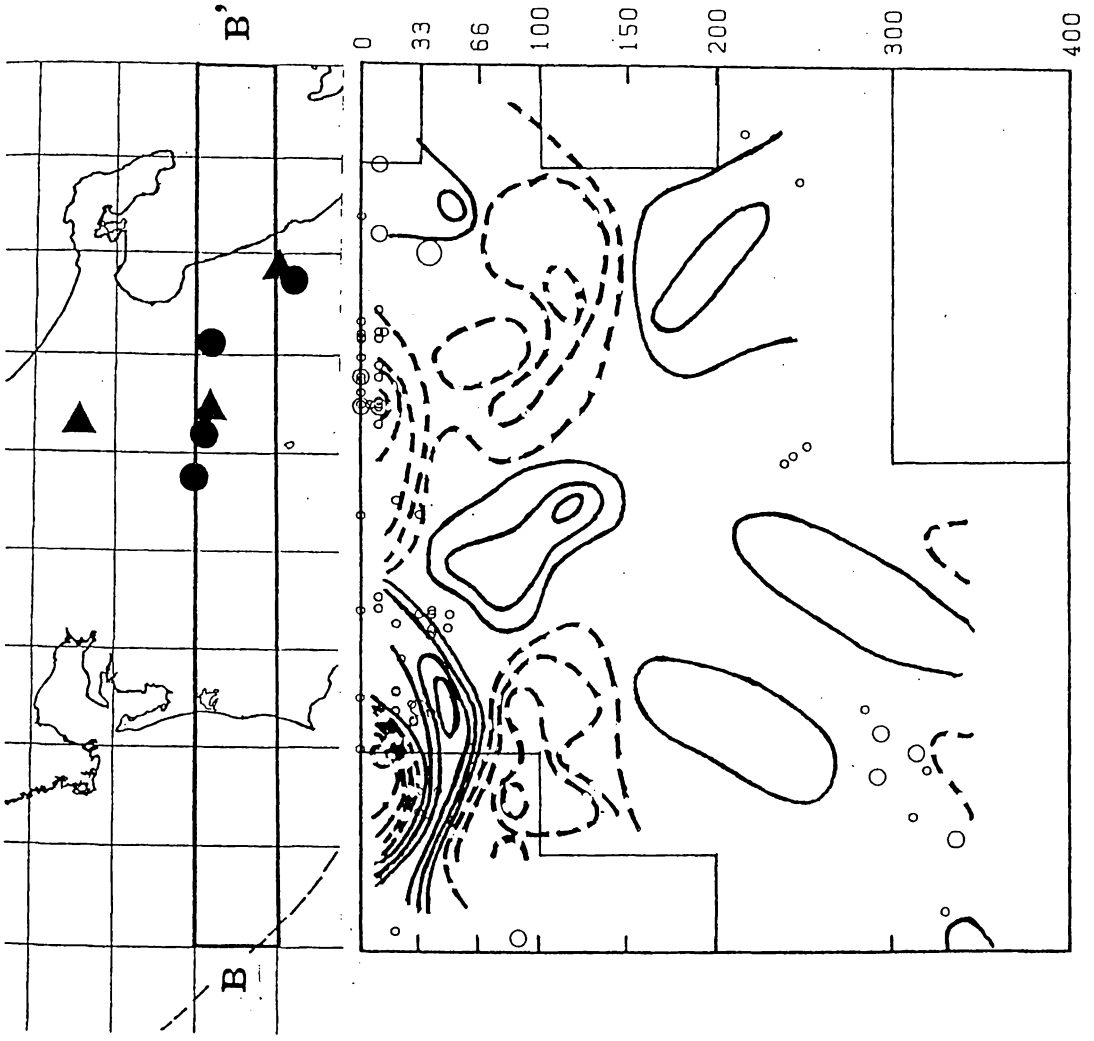

Fig. 6 (b)

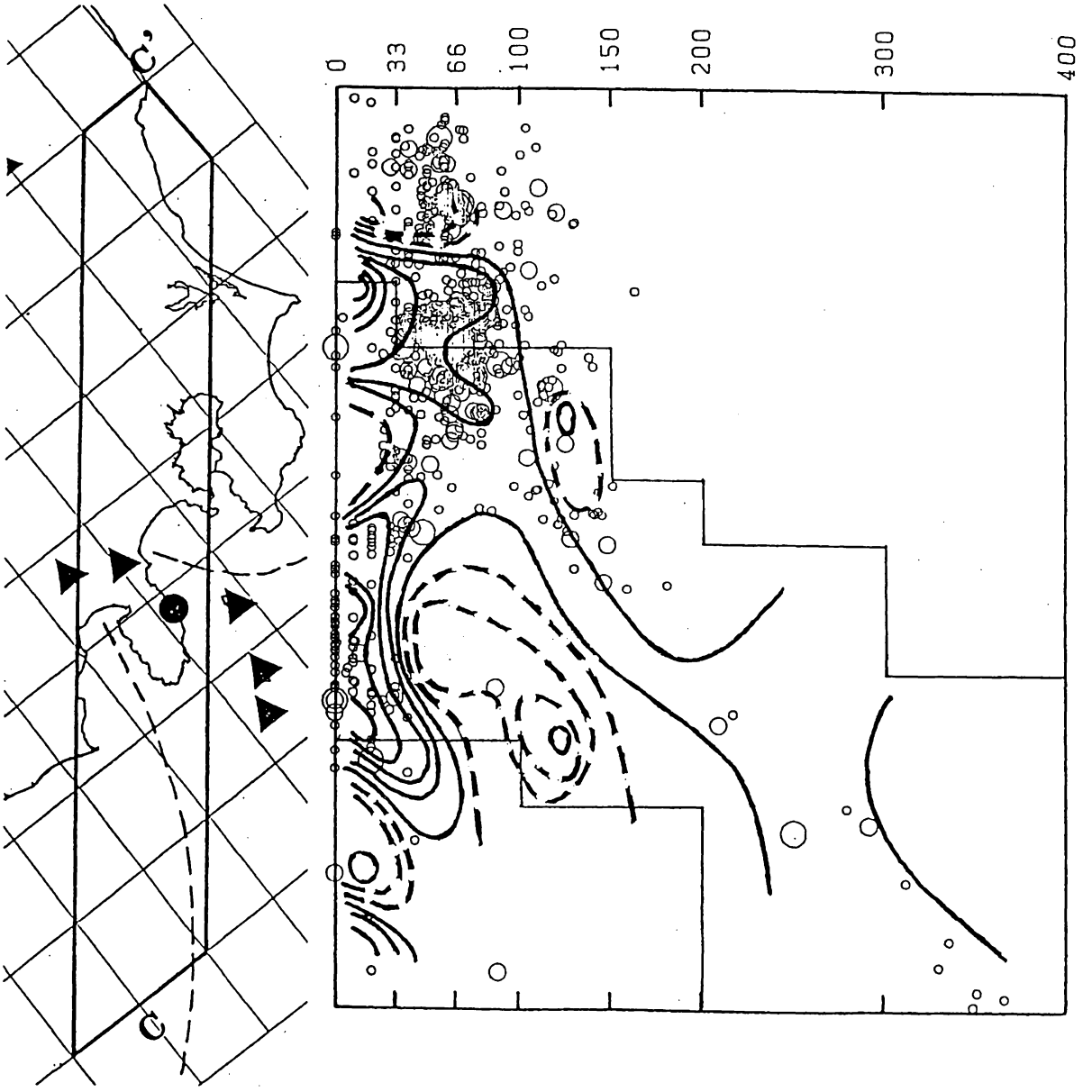

Fig. 6 (c)

Third Version

SEISMOTECTONICS OF THE HIDA REGION, CENTRAL HONSHU, JAPAN.

Takeshi MIKUMO [1], Hiroo WADA [2] and Makoto KOIZUMI [1]

[1] Disaster Prevention Research Institute, Kyoto University, Uji, Kyoto 611, Japan

[2] Kamitakara Geophysical Observatory, Disaster Prevention Research Institute, Kyoto University, Hongo, Gifu 506-13, Japan

Submitted to Tectonophysics, July, 1986

Revised May 10, 1987

Accepted June 22,1987

ABSTRACT

Seismotectonic features of the northern Hida region, central Honshu, Japan have been investigated in some detail, mainly on the basis of the latest six years' observations of seismicity and focal mechanism of a large number of earthquakes, with reference to the geological and tectonic setting and evidence of a large past earthquake.

It was found that high seismicity is concentrated with a remarkably clear lineation, but with a relatively lower activity in the central section, along the Atotsugawa fault extending for about 70 km, which is one of major Quaternary faults in this region. The high seismicity with spatially non-uniform distribution may be related to post-seismic stress concentration after the 1858 Hida earthquake (M=7.0), and to heterogeneous fault strength. Seismicity is also high with belt-like extension beneath the Hida mountain range which is the highest mountain system in the Japan Islands.

The depth distribution of seismicity is clearly bounded at 15 km below the Atotsugawa fault and 8 km beneath the Hida mountains. The local variations can be interpreted as the difference in the brittle/ductile transition depth, which suggests higher temperature beneath the mountains involving active volcanoes.

The focal mechanism solutions indicate that the maximum compressive stress is oriented in the ESE-WNW direction, which is more consistent with the direction of motion of the Pacific plate relative to the Eurasian plate rather than suggested relative motion between the North America and Eurasian plates. The magnitude of the shear stress working in this region is estimated to be less than 700 bars.

INTRODUCTION

The Hida region, which is characterized by a high mountain plateau, is located at the northwestern part of the Chubu district, central Honshu, Japan, (Figure 1). The highland region is bounded on the east by the Hida mountain range which is the highest mountain system in Japan, and on the west by the Ryohaku mountains (Figure 2). The northern and southern rims of the region are bounded by the Toyama plain and the Mino mountain belt. A number of conjugate sets of Quaternary faults are distributed in the Hida region, and thus the region may now be recognized as one of the most active Quaternary tectonic provinces in the Japan Islands. The existence of the conjugate sets of Quaternary faults suggests that the region has been subjected to strong compressive stress during the Quaternary period. There have been several large historical earthquakes in and around the region. One of the largest earthquakes was the 1858 Ansei Hida earthquake with a magnitude around 7.0, which is believed to have occurred due to the movement of the Atotsugawa fault. Recent seismic observations made by a dense network of seismograph stations have revealed clear lineation of seismic activity along the fault, as well as high seismicity beneath the Hida mountain range.

The main purpose of the present paper is to discuss what is the driving stress to generate Quaternary faults and high seismic activity in this region, and why the activity is concentrated along the Atotsugawa fault and beneath the Hida mountain range. For this purpose, we describe, in some detail, the geological and tectonic setting in the Hida region, some evidence for past large

earthquakes, and present seismic activity over the northern Hida region. We also discuss a possible relation between the faulting process of the 1858 earthquake and the present seismicity, and some tectonic implications of the depths of a seismogenic layer in this region.

GEOLOGICAL AND TECTONIC SETTING

(1) The Hida region is composed mainly of Paleozoic to Mesozoic formations, and partly of Tertiary to Quaternary volcanic rocks. The central part of the region is covered by Hida metamorphic complex and granitic complex (early Mesozoic) and Tetori Group (early Cretaceous), and the Hida mountain range located in its eastern part is composed of older granitic rocks (Paleozoic) and Triassic formations. The western and southern parts are covered by Nohi rhyolite (latest Paleogene to Cretaceous), while the northern part consists of Tertiary volcanic rocks and sediments (Geological Survey, Japan. 1978). The Hida mountain range with elevations higher than 2000 m involves four active volcanoes located from north to south; Mt. Tateyama (strato-volcano with post-caldera lava flows), Mt.Yakedake (lava dome), Mt.Norikura (group of strato volcanoes), and Mt.Ontake (group of strato volcanoes), as shown in Figure 2. Two active volcanoes are also situated west of the Hida region; Mt. Hakusan (two strato volcanoes) and Mt. Dainichi.

(2) The most remarkable tectonic feature of the Hida region is the existence of many conjugate sets of active Quaternary faults, which have been identified from interpretation of aerial

photographs, including those from artificial satellites (LANDSATS), together with topographical and geological field surveys (e.g. Research Group for Active Faults of Japan, 1980 a,b; Huzita, 1980). The degree of fault activity estimated from long-term average slip rates is classified into A (10-1 m/1000yr), B (1-0.1m/1000yr) and C (0.1-0.01m/1000yr) (Matsuda, 1975; Research Group for Active Faults of Japan, 1980 a,b). The Hida fault system consists of two sets; one is right-lateral strike-slip faults trending in the ENE-WSW to NE-SW directions and the other is left-lateral faults trending in the NNW-SSE to NW-SE directions. The first group in the central part includes the Atotsugawa, Ushikubi, Mozumi, and other minor faults, and the second group consists of the Atera, Miboro, and other minor faults. In the northern part west of the Toyama plain, there are minor faults such as the Isurugi, Horinji and Takashozu faults. The locations of the above major faults and active volcanoes are shown in Figure 2. No major active faults have been identified in the Hida mountain range.

(3) The Atotsugawa fault was first identified in 1912, but its overall pictures have been revealed from detailed topographical and geological surveys made recently by Matsuda(1966), Takemura and Fujii(1984) and others. The fault is located between two volcanoes, Mt.Tateyama-caldera and Mt.Hakusan extending for about 70 km in the ENE-WSW direction, running through Magawa, Arimine, Otawa, Atotsugawa, Takahara River, Miya River, Odori River, Amo Pass, and Shirakawa (Matsuda, 1966) (See Figure.3). The fault trace has an average strike of about N60^{o}E, and the fault plane

near the ground surface is almost vertical (Matsuda, 1966). The topographical offsets along the fault, which may be the displacements accumulated over the last 1-2 million yrs, amount to 2.7-3.5 km over a distance of 40 km between the Amo-Pass and Takahara River (as evidenced clearly by a right-lateral stream offset of 3 km in the central section) and to about 1.6 km over 25 km east of Arimine (in the eastern section of the fault). (Matsuda, 1966). The long-term average slip rates are of the order of 1.0-5.7 m/1000yrs and 1-4m/1000yrs in the horizontal and vertical components, respectively (class A) (Matsuda,1966; Takemura and Fujii, 1984).

(4) The Ushikubi fault runs almost parallel to and about 6 km north of the Atotsugawa fault, extending for about 85 km with a few parallel subfaults from the Kurobe valley to Shirakawa crossing several streams (Fujii and Takemura 1978; Takemura and Fujii, 1984). The horizontal topographical offsets across these streams are 0.9-2.5 km from which the average rate of horizontal displacement is estimated as 0.8-1.5 m/1000 yrs (class A)(Takemura and Fujii, 1984). The Mozumi fault obliquely connects the eastern section of the Atotsugawa fault near the Tateyama-caldera and the western section of the Ushikubi fault, and extends for 45 km with a strike of N80°E (Fujii and Takemura, 1979; Takemura and Fujii, 1984). The estimated average rate of horizontal displacements is more than 0.6 m/1000 yrs (class B) (Takemura and Fujii, 1984).

(5) Two major faults run in the NNW-SSE direction almost perpendicularly to the foregoing faults. One is the Miboro fault which starts in the northwestern part of the Hida region,

intersects the western ends of the Ushikubi and Atotsugawa faults, and extends further south of the Miboro Dam for about 60 km (Research Group for Active Faults of Japan, 1980). The topographical offsets in some places along the fault are about 1 km, from which the average slip rate may be larger than 0.4 m/1000yrs (class B) (Takemura and Fujii, 1984). The Atera fault, which is a more pronounced left-lateral fault, can be traced from topographical offsets from north of Hida-Hagiwara, Tukechi, Sakashita, Magome for about 80 km (Sugimura and Matsuda, 1966). The average rate of horizontal slip has been estimated as 2-4 m/1000 yrs, which can be ranked as class A. The horizontal displacements are about five times larger than the vertical displacements (Sugimura and Matsuda, 1966). A number of minor faults are located parallel to each other and perpendicularly to this major fault particularly in the central to southern sections.

EVIDENCE ON PAST EARTHQUAKES IN THE HIDA REGION AND ALONG THE ATOTSUGAWA FAULT

The topographical offsets along the above active faults may be regarded as accumulated seismic displacements at past large earthquakes that occurred during the Quaternary period, if we assume that there have been no substantial creep displacements. The horizontal offset of 3 km seen in the central section of the Atotsugawa fault would suggest the recurrence of large earthquakes over 1000 times if we assume that a possible seismic displacement during an earthquake was less than 3 m, and their recurrence interval would be of the order of 1000-2000 yrs.

(1) There is some evidence which has come from a recent paleo-seismic trenching survey into the fault. The trenching survey was made in July, 1982 across a fault scarp on the river-terrace of the Miya River, at Nokubi near the central section of the Atotsugawa fault (Research Group for Excavation of the Atotsugawa fault, 1983). Figure 4 shows the exposed geological profiles across the fault, provided by the courtesy of the Research Group. A clear-cut northward dipping fault plane with upward bend of sedimentary layers can be seen on both the east and west side walls, along which thrust faulting with the north side upthrown appears to have taken place. The deformation of minor subsidiary faults, the change of thickness of humic soil layers away from the fault plane, and the lack of a part of layers on the upthrown side, suggest that there have been more than four events along the fault. ^{14}C dating for humic soils has allowed dating of three of these events at < 820 yrs B.P., 5200 ± 200 yrs B.P. and 8600 ± 400 yrs B.P.(Research Group for Excavation of the Atotsugawa fault, 1983; Tsukuda, 1985). The latest event probably corresponds to the 1858 Ansei Hida earthquake. It was also suggested on the basis of detailed inspection that there could be another event between the latest and the second latest events. If there was indeed an intervening event, the recurrence interval of large earthquakes along the central to western section of the fault in pre-historic ages would be 1100-2500 yrs.

(2) Evidence of historical earthquakes in the Hida region and along the Atotsugawa fault can be traced back to 400 years ago (Ministry of Education, 1940; Yamazawa, 1929,1930; Usami, 1980).

One of the historical records (Yamazawa, 1929) indicate that about 210 strong felt-shocks took place in the Hida region during 80 years from 1777 to 1857. The seismicity during the period appears to have been more active as compared with that in recent ten years from 1977 to 1986. To be noted among these shocks are three major earthquakes on August 28, 1826 (M=6.2), March 18, 1855 (M=6.7), and April 9, 1858(M=7.0). It is not clear, however, whether the first two earthquakes were associated with the Atotsugawa fault or not.

(3) The largest and best documented earthquake is the April 9, 1858 Ansei Hida earthquake (M= 7.0). The great earthquake was followed only 2 hours later by another large earthquake (M=6.9). The reported damage during the first earthquake in 70 villages in the central part of the Hida region includes: 203 people dead, 45 injured, 323 houses collapsed and 377 damaged (Usami, 1980). It has been noticed that the "meizoseismal area" with heavy damage is concentrated along a zone trending in the ENE-WSW direction between Mt.Tateyama and Mt.Hakusan. It was inferred (e.g. Matsuda, 1966) that this earthquake might have been associated with the Atotsugawa fault. The second earthquake, however, might have been triggered by rapid stress propagation to some active faults located west of the Hida region, since similar damage was reported far west of the region..

(4) Closer investigations (Usami et al., 1979) into a number of previously undiscovered historical records have disclosed local distribution of the earthquake damage around the fault zone. Figure 5 shows the distribution of percentages of damaged houses, which have been estimated from the number of totally collapsed

houses and half of the number of heavily damaged houses. Different symbols indicate their damage in percentage plotted at the location of each village. The percentages higher than 50 % appear concentrated within 1.5 km of the fault zone, and several villages near the western section of the fault were subjected to the heaviest damage higher than 80 %. There is no plot of damage east of Otawa in the eastern section of the fault because no houses were there at that time, but heavy landslides were recorded near Mt.Tateyama caldera. The damage decays rapidly with distance from the fault trace in the southeastern side, but remains at 50% in the northwestern side and around the western end of the fault. The asymmetric distribution of the damage may be attributed either to the difference in ground conditions between the both sides or to possible oblique faulting motion along the fault plane dipping slightly northwestwards. Since the topography around the fault suggests long-term northwest-side upthrown movements with right-lateral offsets, possibly the 1858 earthquake was also accompanied by this type of oblique faulting along a northwestward dipping plane. The above evidence strongly suggests that the 1858 Ansei Hida earthquake was caused by faulting motion of the Atotsugawa fault.

(5) The inference is also supported by some other geological evidence in addition to the results of the trenching survey. One is fresh fissures northeast of Otawa detected on the fault outcrop in the Tetori Group located in the eastern section of the fault (Matsuda, 1966). The second is the results of ^{14}C dating for pieces of woods buried in a gravel layer at Magawa in the

eastern section of the fault. It gave the date of 490±170 yrs B.P. (Takemura and Fujii, 1984) suggesting faulting after the date. The third evidence comes from paleomagnetic dating of fault activity, which made use of the direction of re-magnetization of fault zone sediments liquified by earthquake fault motions. The dating was made at two different locations; at Nokubi, the trenching site in the western section and at Magawa in the eastern section of the fault. It yielded the date of 1880± 60 yrs A.D. (Sakai and Hirooka, 1983; Takeuchi and Sakai, 1985). All the above geological evidence, particularly the third one, indicates that the fault rupture took place both in the eastern and western sections of the Atotsugawa fault in 1858.

SEISMICITY AND MECHANISM OF EARTHQUAKES OVER THE NORTHERN HIDA REGION

Observation and Data Analysis

(1) It is only recently that seismicity over the northern Hida region has been revealed by high-sensitivity seismic observations. Preliminary observations made in 1971-1973 with three temporary seismograph stations by the Kamitakara Geophysical Observatory, Kyoto University, indicated rather high rates of microearthquakes around the Atotsugawa fault (Wada and Kishimoto, 1974; Wada, 1975), while routine JMA (Japan Meteorological Agency) observations had located only several minor shocks in the area during 15 years from 1958 to 1972.

(2) In 1977 and 1980, a telemetering observation system was introduced to the Observatory, which had 4 network stations, Kamitakara(KTJ), Nirehara(NRJ), Amo(AMJ), and Fukumitsu(FMJ) and

was also linked with 3 stations of Nagoya University, Takayama(TAN), Yakedake(YKE) and Takane(TKN) (See Fig.7). Most of these stations are equipped with 3 component short-period, high-sensitivity seismographs. Seismic signals recorded are converted at a sampling rate of 100 Hz through an A/D converter, telemetered in real time through special telephone lines at a speed of 4800 or 9600 bits/sec to the Observatory, D/A converted, and then recorded on triggered analogue data recorders and pen-recorders. The overall frequency characteristics have a flat response to ground velocity over frequencies of 1-30 Hz, and the highest sensitivity reaches 1 mm/3μkine at stations under favourable conditions with low noise level. Time resolution of the first arrival of P-waves is of the order of 1/100 sec. The detection capability of microearthquakes from this observation network covers the entire Hida region including the Hida mountain range, the Toyama plain and the southern part of the Toyama Bay and Noto Peninsula. The results from early observations for May, 1977 - December, 1978 and during the first five years' period up to June, 1982 have been reported elsewhere (Wada, Mikumo and Koizumi, 1979; Mikumo and Wada, 1983; Mikumo, Koizumi and Wada, 1985). In the present paper, more recent seismicity will be described, mainly on the basis of the latest six years' observations up to June, 1986.

(3) The crustal structure in the Hida region, which is used for hypocenter location, has been taken from three sources. The upper part of the structure is based on seismic observations of Tetori quarry blasts (Wada et al., 1979), which give a P-wave velocity

of 5.5 km/sec for the uppermost 3 km overlying a 6.15 km/sec-layer. The underlying structure has been estimated from a combined analysis of seismic explosion observations, dispersion of surface waves and gravity anomalies (Mikumo, 1966), and also from the results from the Noto-Atsumi explosion observations (Aoki et al. 1972). The velocity profiles obtained are shown in Figure 6, where a smoothing has been applied and the resultant solid curve is used. The method of hypocenter location employed here is a sort of iterative non-linear least squares, in which the square sum of the difference between the observed arrival times (Toj) of P-waves at recording stations and the corresponding travel times (Ttj) calculated from the adopted structure is minimized. The precision of hypocenter location for each shock is roughly estimated from the average travel time residual $\sigma = \sqrt{\sum_j (Toj-Ttj)^2/N}$, together with the reading accuracy of the observed P first arrivals. It may be of the order of $\pm\bar{V}*2\sigma$, where N is the number of stations used and $\bar{V}$ is the average crustal velocity.

General Features of Seismicity

Figure 7 shows spatial distribution of the epicenters over the northern Hida region for the period from April, 1980 to June, 1986. These epicenters are denoted by five different sizes according to their magnitudes; $M \geq 4.0$, $3.0 \leq M < 4.0$, $2.0 \leq M < 3.0$, $1.0 \leq M < 2.0$, and $1.0 < M$, which are estimated from the F-P times observed at KTJ. More than 5000 earthquakes with magnitudes greater than 0.5 are included in this seismicity map. The probable errors estimated for these locations are less than 1.0

km in the horizontal direction and 2.0 km in the focal depth, within a distance of 25 km from the center of the network. The corresponding errors are estimated to be less than 1.5 km and 3 km respectively, within the distances between 25 km and 50 km. Within the square area shown at the right bottom of Figure 7, there have been swarm earthquakes since 1978 and many aftershocks of the 1984 western Nagano earthquake (M=6.8). We will not discuss these unusual activities in the present paper, but the focal mechanisms of some of these events are incorporated in later discussions. The general features of seismicity over the HIDA region are described here.

(1) High seismicity is concentrated, indicating a clear lineation, along the Atotsugawa fault, that is more active both in the eastern and western sections of the fault with an intermediate zone of lower activity. The high activity in the eastern section appears to be connected through Mt.Tateyama with that beneath the northern part of the Hida mountain range. There is also high seismicity just north of the western end of the Ushikubi fault, which included somewhat larger shocks with magnitudes around M=4.0, although no lineations have been observed along the fault. Also noticeable is the high seismicity along the Mozumi fault running obliquely from the eastern section of the Atotsugawa fault to the junction to the western section of the Ushikubi fault. There is another weak lineation of seismicity extending southwestwards from the junction of the Atotsugawa and Miboro faults, where no surface fault traces have been identified.

(2) Figure 7 also shows some belt-like concentrations of seismic activity trending almost in the N-S direction beneath the axial portion of the Hida mountain range, which extends southwards to the swarm earthquake region southeast of Mt.Ontake (Fig.2). High seismicity including earthquakes sometime with magnitudes 4-5 has also been observed west of the Hida mountain range and northeast of the northern end of the Atera fault (Takayama--Kuguno -- Hida -- Osaka -- Hagiwara regions). This activity may be related to a number of minor faults perpendicular to the Atera fault. It has been shown by early observations (e.g. Ikami et al., 1972) that seismicity along the Atera fault has been extremely low. Some concentration of minor shocks west of the fault are aftershocks of the 1969 central Gifu earthquake (M=6.6). A triangular region bounded on the northwest by the Atotsugawa fault, on the east by the Hida mountains and on the southeast by the activity just described, is a region of extremely low seismicity.

(3) Moderate seismic activity may be noticed in the west of the Toyama plain, and it appears that these shocks took place around the Isurugi, Takashozu and Horinji faults, although it is not clear whether the seismicity can be associated with these faults. The latest activity in this region was the swarm earthquakes of June 9-10, 1986 including five larger shocks with magnitudes ranging from 3.5 to 4.0, all of which have been located at the northern end of the Miboro fault. No seismicity has been observed in the midst of the Toyama plain.

Seismicity along and around the Atotsugawa fault

(1) Figure 8 shows a detailed seismicity map including 1200 shocks around the Atotsugawa, Mozumi and Ushikubi faults. The highest seismicity has been observed for 20 km between Kurobe(KR) and Arimine(AR) in the eastern section of the Atotsugawa fault and for 28 km between Sugamura(SG) and Amo(AM) in its western section, whereas seismicity in the middle section for 22 km is not very high. The seismicity in the eastern section north of Arimine(AR) appears to be a eastward continuation of the seismicity along the Mozumi fault. Seismicity near Amo(AM) at the western end of the Atotsugawa fault may be much more active than indicated here, since a number of minor shocks with S-P times shorter than 1 sec have been recorded only at the nearest station AMJ and are not plotted on the map. Possible interpretation for the non-uniform seismicity will be discussed later. Thus, seismic activity can be clearly recognized over 70 km along the fault. Close examination shows small deviations of most of these epicenters 2-3 km northwest of the fault trace on the ground surface, while quite a small number of shocks fall southeast of it. The deviations may not be attributed to possible shift of hypocenter location resulting from the difference in the upper crustal structure between the northern and southern sides of the fault, since the observed results of the Tedori quarry blasts indicated no appreciable velocity difference between the two sides. For this reason, taking into account the accuracy of epicenter location in the midst of our network, the above deviations may be real.

(2) Figure 9 shows depth distributions of these shocks projected

onto a plane perpendicular to the fault, which includes three different sections, 1) AM-SG, 2) SG-AR, and 3) AR-KR. The hypocentral distribution in the eastern section 3) dips northwestwards at about 85°, while it appears almost vertical or dipping slightly southeastwards in the western section 1). If we look more carefully at the fault traces on the ground (A,M and U), however, these hypocenters appear located around a plane almost vertical or dipping slightly northwestwards down to about 15 km, which suggests the average dip of the fault plane at depth of the Atotsugawa fault. This is consistent with the northwest side upthrown fault movement along a northwestward dipping fault plane inferred from geological and topographical evidence. The hypocenter distribution projected onto a profile parallel to the fault is illustrated in Figure 10. The pattern clearly demonstrates again that seismicity is relatively low in the central portion of the fault between Suganuma (SG) and Arimine (AR). There appears to be a well-defined lowest depth of seismicity. The depth appears to change along the fault from about 12 km below Amo near the western end increasing to 15 km below the central portion and again becoming shallower to about 14 km below Kurobe near the eastern end, except several deeper shocks. Although the slight change in the lowest depth might be only an apparent feature due to limited precision of focal depth estimates, it seems likely that the depth of deepest seismicity may be the bottom of the seismogenic layer.

Seismicity beneath the Hida mountain range

(1) High seismicity observed beneath the Hida mountain range is not uniform in time over a length of 150 km of the range, but characterized by intermittent swarm-like activity. The swarms include moderate-size earthquakes sometimes with magnitudes greater than 4.0, particularly beneath Mts. Tsurugi, Tateyama, Eboshi, Yari, Yake and Norikura. The larger shocks take place alternatively in the section north of Mt.Yari and in the section south of it particularly the southernmost region southeast of Mt.Ontake. The activity beneath Mt.Norikura is not concentrated but somewhat extended around the mountain area. The latest activity there was two moderate-size earthquakes with M=5.2 on March 7, 1986 and M=4.2 on April 29, 1986, which occurred in a previously aseismic area southwest of Mt. Norikura. Since Mts. Tateyama, Yake, Norikura and Ontake, are active volcanoes, one might expect that the activity would be directly related to volcanism rather than due to tectonic origins. The hypothesis has not been well established, although the swarm earthquakes southeast of Mt. Ontake might have been more or less affected by the October 28, 1979 volcanic eruption of Mt.Ontake.

(2) Figure 11 shows the depth distribution of these shocks in a cross section parallel to the mountain range. There are several concentrations of seismicity beneath Mts. Tateyama, Eboshi and Yari and also beneath north of Mt. Tsurugi and south of Mt. Norikura. The focal depths of these shocks appear bounded at 8 km in the central to southern portions, except for several deeper shocks, while in the northern portion the depth increases to about 20 km towards the north of Mt. Tsurugi. The focal depth of about 8 km is significantly shallower than that below the

Atotsugawa fault and some other parts of the region, even if some error of the focal depths was taken into account.

Focal mechanism

The focal mechanisms of moderate-size shocks with magnitudes greater than 3.0 that occurred over the northern Hida region are closely investigated here to see what type of tectonic stress causes the present seismicity. The data used here are taken from the P-wave first arrivals recorded at a number of university network stations distributed over the Chubu district, central Japan.

(1) Figure 12 provides schematic focal mechanism diagrams of larger shocks along and around the Atotsugawa fault. Ten shocks that occurred along the Atotsugawa fault and one shock along the Ushikubi fault consistently indicate strike-slip mechanisms. The strike of the nodal planes trending in the ENE-WSW direction is nearly parallel to that of the fault trace. If we take this plane as the fault plane, the slip direction is right-lateral and hence consistent with that of long-term movements of the Quaternary fault inferred from topographical and geological studies (Matsuda, 1966). Also the maximum compressive stress is oriented in the ESE-WNW direction. This evidence strongly suggests that the present shocks may have taken place under the same tectonic stress which had driven these faults during the Quaternary period. Two shocks on a westward extension of the Atotsugawa fault also indicate almost the same mechanism.

(2) In the northwest region bounded by the Ushikubi and Miboro faults, on the other hand, there are different types of

mechanism. Two shocks just north of the Ushikubi fault indicate almost a pure dip-slip mechanism, three shocks north of them show thrust-type faulting, and two shocks located further north indicate normal faulting. Both the maximum compressive stress and tensional stress here are not aligned in one direction. This suggest a complicated stress state or localized perturbations, possibly affected by right-lateral motion of the Ushikubi fault and left-lateral motion of the Miboro fault. Also in this region, which is a southwestward continuation of the Toyama plain, there are several minor faults with normal or thrust fault component (Fujii and Takemura, 1979). The above earthquakes may be associated with these minor faults rather than reflecting the general tectonic stress prevailing over the northern Hida region.
(3) Figure 13 shows the focal mechanism solutions of 17 shocks in the northern to central sections of the Hida Mountains from Mt.Tsurugi down to the south of Mt. Norikura. These shocks include those of the latest two large earthquakes in 1986. Fukao and Yamaoka (1983) have studied 7 shocks of 1979 which are included here and obtained similar solutions. The above solutions indicate that many of the shocks in the northern section have similar strike-slip mechanisms, but with some normal faulting components in two shocks. One of the nodal planes of these shocks appears almost parallel to the axial direction of the mountain range, but no major faults trending in this direction have been identified here. Since the maximum compressive stress inferred from the solutions is oriented in the ESE-WNW direction, these shocks may have been associated with latent en-echelon minor

faults within the shallow portion of the mountain range formed under the above tectonic stress. Three of the 17 shocks in the central section, May 11, 1981, March 7 and April 29, 1986, indicate, however, thrust faulting mechanisms, and a P-axis oriented in the SSE-NNW direction. The direction of the maximum tensional stress oriented almost vertically in this case suggests the possible prevalence of this type of stress rather than the compressive stress mentioned before.

(4) The solutions of 17 shocks located in the southern section are shown in Figure 14. Twelve of them belong to the swarm earthquakes that occurred southeast of Mt.Ontake since May, 1978, and the other five are the main shock (M=6.8) and 4 larger aftershocks of the 1984 western Nagano earthquake. The upper diagram includes 6 strike-slip and 6 thrust mechanisms concentrated in a limited area. Similar complexities have been pointed out (Hori et al., 1982) for a different group of swarm earthquakes which included the two shocks treated here. These complexities might be due to minor pre-existing faults with different orientations. In contrast, all of the five larger earthquakes of 1984 with magnitudes ranging from 5.0 to 6.8 indicate consistently strike-slip mechanisms (Earthquake Research Institute, 1985).

(5) Figure 15 provides the focal mechanisms of another 17 shocks located in a region west of the mountain range and northeast of the Atera fault. Almost all the solutions are consistent with strike-slip mechanisms except a shock with normal fault component and a few shocks with thrust component. The direction of one of the nodal planes is nearly parallel to that

of minor faults perpendicular to the Atera fault or that of the Atera fault itself. The maximum compressive stress lies in the ESE-WNW direction.

DISCUSSION

Possible relation between the present seismicity along the Atotsugawa fault and the faulting process of the 1858 Hida earthquake

We discuss here possible driving forces to generate the high seismicity along the Atotsugawa fault and also possible reasons as to why there is a notable difference in the seismicity along the different sections of the fault.

(1) The first to be considered is a possible stress concentration and/or the decrease of frictional strength of the fault surface after the 1858 Hida earthquake. It has been demonstrated, from the spatial distribution of earthquake damage at that time and geological evidence including trenching surveys, ^{14}C datings, and paleomagnetic dating, that the 1858 earthquake may have been caused by the fault movement of the Atotsugawa fault. If so, it is possible to consider that a part of the present high seismicity results from post-seismic stress concentration after the 1858 earthquake. The second conceivable interpretation on the high seismicity is minor brittle fractures due to creep movements of fault gouge layers in the upper crust or to the drag given by creep in a lower ductile crustal section to an upper brittle crustal section (Tsukuda,1983). Electro-optical distance measurements made along several base-lines across the Atotsugawa fault, however, have yielded no indications of creep movements to date in the uppermost part of the crust

(Kato, 1983). Triangulation surveys made during 90 yrs covering a wider area (Geographical Survey Institute, Japan, 1984) also do not suggest any possibility of creep-like fault movements in the lower crust. The third possibility which would be the simplest explanation, is failures of small pre-existing planes of weakness along major faults between crustal blocks due to an increase of regional tectonic stress. In this case, however, a number of shocks would take place concurrently along many major faults distributed in the region under consideration, and there would be no particular reason of high concentration of seismicity only along the Atotsugawa fault. There is no evidence that the fault zone along the Atotsugawa fault involves many more pre-existing weak planes as compared with that along other major fasults such as the Atera fault which has extremely low seismicity.

(2) From the above considerations, we believe that the first interpretation may be most probable. For this interpretation, however, we have to provide reasonable explanations for the prolonged seismic activity lasting for almost 130 yrs since 1858, and for the higher rate of seismicity in the eastern and western sections of the fault with intermediate lower activity in the central section. A possible explanation for the long-lasting high seismicity, which amounts to more than 200 shocks/yr, ($0.5<M<4.5$) could be strongly heterogeneous fault strength. Numerical experiments based on a three-dimensional, frictional fault model indicate that more heterogeneous distribution of the fault strength yields smaller decay constants p of aftershock activity and larger b-values for seismicity versus magnitudes (Mikumo and Miyatake, 1979). This is because it takes longer time

to complete the readjustments of the shear stress after the main faulting, and smaller aftershocks occur more frequently than larger ones.

(3) The approximate b-values for three different sections of the Atotsugawa fault are estimated from the accumulated seismicity versus magnitude diagram shown in Figure 16. These are 0.81 for the western section between Amo(AM) and Suganuma(SG), 0.50 for the central section between Suganuma(SG) and Arimine(AR), and 0.75 for the eastern section between Arimine(AR) and Kurobe(KR). These differences in b-values between the different sections of the fault suggest heterogeneous fault strength along the fault or heterogeneous stress concentration due to a non-uniform rupture mechanism of the 1858 earthquake. The geological evidence suggests that there were fault displacements at Nokubi, Otawa and Magawa through the western to eastern section of the Atotsugawa fault at the time of the 1858 earthquake, while the spatial distribution of earthquake damage indicates the strongest ground motions during the earthquake near the western section of the fault. From the above evidence, we may be allowed to raise two different interpretations for the rupture mechanism of the 1858 earthquake. One plausible explanation would be that fault motion occurred with nearly the same displacement over the entire section of the fault which had different degrees of heterogeneous strength.

(4) An alternative interpretation would be that the earthquake occurred with larger fault displacements in the central section of the fault and smaller ones in the western and eastern

sections, and hence that most of the accumulated stress was released in the central section to give low present seismic activity. The heavier earthquake damage in the western section and large-scale landslides in the eastern end of the fault may partly be attributed to high-frequency ground motions with large accelerations rather than to fault displacement itself. It has been demonstrated that strongly heterogeneous faults could easily radiate high-frequency seismic waves (Mikumo and Miyatake, 1978) and make aftershock activity continue for longer periods (Mikumo and Miyatake, 1979). The western and eastern sections of the fault appear more heterogeneous than the central section in view of the difference in the estimated b-values. Another reason may be seismic energy concentration at the two ends of the fault due to bilateral rupture propagation. The less hetrogeneous central section, would release most of the applied shear stress, allowing larger fault displacements there. Similar situations for the spatially non-uniform fault displacements and stress drops have been observed in the case of the 1891 Nobi earthquake (Mikumo and Ando, 1976).

(5) If we arbitrarily assume that coseismic displacements are nearly proportional to the topographical stream offsets integrated during the Quaternary period along the fault, the average fault displacements D can be estimated as 1.8 m, 2.6 m and 1.3 m for the western, central and eastern sections, respectively. These displacements could generate the 1858 Hida earthquake with a seismic moment of 6.7×10^{26} dyne*cm (comparable to a magnitude 7.0; Ohnaka, 1978), taking the total fault length L=70 km, the fault width W=14 km and the crustal rigidity

μ =3.5*10^{11}c.g.s.. The static stress drop at these three sections would be 25, 44 and 21 bars, respectively, suggesting that the remnant stress could still be somewhat larger in the western and eastern sections than in the central section. However, the above assumption may be too speculative, since there is no other supporting evidence for it. If this is indeed the case, however, the alternative model postulated here appears to be able to account for all the information including the present seismicity, the earthquake damage and geological evidence at the 1858 earthquake.

Implication of deepest seismicity

(1) Figures 10 and 11 show that the seismicity along the Atotsugawa fault is clearly bounded shallower than 15 km, confined within the granitic layer with a P-wave velocity of 6.1-6.2 km/sec, while the deepest seismicity beneath the central to southern parts of the Hida mountains is about 8 km which is significantly shallower than beneath the other areas in the Hida region. One plausible explanation for the difference is the difference in mineralogical compositions and geochemical constituents of rock materials between different crustal depths. No clear relationship has been found, however, between the deepest focal depth in various regions of the world and the depths to the boundary between different crustal layers. It has been recently reported, on the other hand, that the depth distribution of seismicity may be more or less related to the regional heat flow (Kobayashi, 1976; Sibson,1982,1984); deepest

seismicity is bounded above 10-12 km in high heat-flow regions with 1.5-2.5 HFU (63-105 mW/m^2), and particularly shallow in geothermal areas with 200-300 ^oC, 15-20 km in regions with 1.0-1.5 HFU (42-63 mW/m^2), and 20-40 km in regions with heat flow lower than 1.0 HFU (42 mW/m^2), although these relations are somewhat different for different tectonic regions. The above evidence suggests that the temperature distribution within the crust may have strong effects on the depth distribution of seismicity, so that rock materials including quartzite would become ductile below a certain depth, prohibiting brittle fractures.

In the present case, the depth of the seismogenic layer, appears to vary quite sharply from 15 to 8 km within a local scale. We discuss here whether the sharp variation could be explained on the basis of the prevailing brittle/ductile transition model (Brace and Kohlstehdt, 1980; Sibson, 1982,1984; Meissner and Strehlau, 1982), together with available heat flow data.

(2) Following this model, the frictional shear resistance τ to sliding on a fault plane located in the brittle regime within the upper crust may be expressed, on the basis of Byerlee's experimental law (1978), as $\tau = \tau_o + \mu \sigma_n'$, where τ_o is the resistance near the ground surface, μ is the coefficient of static friction and σ_n' is the effective normal stress. σ_n' is given by $\sigma_n' = \sigma_n - p$ and $p = \lambda \sigma_v$, where σ_n, p and σ_v are normal stress, pore pressure and vertical overburden load, λ is the ratio of the pore pressure to hydrostatic pressure, and $\sigma_v = \int_0^z \rho(z) g dz$. τ and σ_n are, in principle, related as $\tau = (\sigma_1 - \sigma_3)/2$ and

$\sigma_n=(\sigma_1+\sigma_2+\sigma_3)/3$, where σ_1, σ_2 and σ_3 are the maximum, intermediate and minimum principal stresses, respectively. For strike slip faults as in the present case, $\sigma_v=\sigma_2\cong(\sigma_1+\sigma_3)/2=\sigma_n$, since σ_1 and σ_3 lie in the horizontal plane and σ_2 is directed vertical, so that $\tau=\tau_o+\mu(1-\lambda)\int_o^z \rho(z)gdz$. This indicates that the shear resistance in this regime increases almost linearly with depth, the rate of which depends on the parameters involved.

In the ductile regime within the middle to lower section of the crust, on the other hand, quasi-plastic dislocation creep dominates, and the constitutive flow law takes the form; $\dot{\varepsilon}=A(\sigma_1-\sigma_3)^n\exp(-Q/RT)$ (e.g. Goetz, 1978), where $\dot{\varepsilon}$ is the strain rate, T is the absolute temperature, R is the gas constant, and A, n and Q are numerical constants. From this relation, the shear resistance in this regime may be estimated as, $\tau=\{\dot{\varepsilon}/A\exp(-Q/RT)\}^{1/n}/2$. The temperature distribution within the crust has been given in the form, $T(Z)=T_o+Q_o Z/K+A_o Z^2/2k$, where T_o is the surface temperature, Q_o is the surface heat flow, k is the thermal conductivity and A_o is the radioactive heat generation. The above formula indicates a rapid decrease of τ with depth.

Based on the above relations, we calculate a number of cases for the depth variations of the shear resistance, taking the following values; τ_o=100 bars, μ=0.60, λ=0.36-0.72, $\dot{\varepsilon}=10^{-12}-10^{-15}$, $A=(3-5)*10^{14}$, n=2.44-3.0, Q=0.2-0.5 MJ/mol (Koch et al.,1980), and Q_o=1.5-2.5 HFU, $A_o=2.3\mu W/m^3$ and k=2.7 W/m ^oK. These parameters have considerable uncertainty but it can be seen that the brittle-ductile transition depth becomes shallower for

larger heat flow, smaller strain rates, and for smaller λ. An example of the calculated shear resistance curves for likely parameters is shown in Figure 17, which is similar to those obtained by previous workers (Sibson, 1982,1984; Meissner and Strehlau, 1982; Doser and Kanamori,1986).

(3) Heat flow mesurements have been made at the Kamioka mine near the central section of the Atotsugawa fault, and yielded a value of 1.80 HFU (Uyeda and Horai, 1964). This value has been obtained from the measured geothermal gradient of 2.77 ^{o}C/100 m and thermal conductivity of $6.49*10^{-3}$ cal/cm.sec^{o}C. Geothermal gradients have also been measured at 12 sites within or very close to the northern section of the Hida mountain range north of Mt.Yari, which were found to be in the range of 6-10^{o}C/100 m (Hokuriku Department of Agriculture and Foresty, private communication, 1986). These values are a few times larger than the geothermal gradient measured near the Atotsugawa fault, suggesting larger heat flows beneath the Hida mountain range, although thermal conductivity at these sites has not been obtained.

(4) For a hydrostatic pore pressure of λ=0.36 and a strain rate of $\dot{\varepsilon}=10^{-14}$, the brittle/ductile transition depths at 8 km would correspond to the surface heat flow of 2.0 HFU, but the depth of 15 km would not be explained by the curves shown in Figure 17. For a strain rate of $\dot{\varepsilon}=10^{-12}$, all the curves in the ductile regime go down by about 2 km, in such a way that the depths at 15 and 8 km below the Atotsugawa fault and the Hida mountains would be approximately fitted to the shifted curves of 1 and 3 HFU, respectively. The difference in these values would

roughly correspond to the geothermal gradients measured at the two different locations. Also, the lowest depth of a seismogenic layer does not correspond exactly to the brittle/ductile transition depth but could extend slightly down into the ductile regime. For the above reasons, the local variations of the deepest seismicity may probably be attributed to the contrast in the heat flow between the two different locations. A most probable explanation of the high temperatures would be magmatic activity beneath some of the Hida mountains which involve active volcanoes, such as Mts. Tateyama, Yake, Norikura and Ontake.

(5) On the other hand, three-dimensional seismic P-wave velocity structure over central Japan has recently been investigated in some detail (Hirahara et al.,1986). The results obtained along two orthogonal vertical cross sections across the Hida mountain range ($137^{o}.5$-$138^{o}.0$E and $36^{o}.0$-$36^{o}.5$N) are reproduced in Figure 18. The results clearly indicate a low velocity zone (-3.5 - 7.5%) within the crust just beneath the Hida mountains. The low-velocity zone extends down to about 150 km in the upper mantle beneath the central to northern parts of the mountains as seen from Figure 18. Figure.18 also shows another low-velocity zone in the crust beneath Mt.Hakusan west of the Hida region. These low-velocity zones are a strong manifestation of high heat flow beneath the Hida mountains and Mt.Hakusan, and possibly of the existence of partially melt diapirs in the upper mantle, as has been suggested by Ando et al.(1983). Thus, the local shallowing of the deepest seismicity beneath the Hida mountains can also be evidenced from seismic velocity structure.

Tectonic Stress

(1) The horizontal directions of the P-axes derived from all the focal mechanism solutions of shocks with magnitudes greater than 3.0 are plotted in Figure 19. Their general trend, which may be an indication of that of the regional maximum compressive stress, appears oriented in the ESE-WNW to E-W direction. The deviations from the general trend may be attributed either to seismic faulting along pre-existing faults or to the existence of internal friction within rock materials. Several larger earthquakes with magnitudes ranging from 6 to 7 that occurred in the adjacent area southwest of the Hida region, 1934 Gujo-Hachiman (M=6.2)(Ichikawa,1971), 1961 Kita-Mino (M=7.0)(Kawasaki, 1975), 1969 central Gifu (M=6.6)(Ichikawa,1971; Mikumo,1973), and 1972 Fukui-Gifu border (M=6.0)(Yamada and Fujii,1973) earthquakes, consistently indicate nearly the same direction of P-axes. In the region east of the Hida mountain range and west of the Fossa Magna tectonic belt (Figure 1), the general trend of the P-axes also shows similar patterns, although there is a slight change in the focal mechanism across the Itoigawa-Shizuoka tectonic line which is the western periphery of the Fossa Magna (Fukao and Yamaoka,1983). Near the Japan Sea coast north of the Hida region, however, the P-axes appear to be oriented in the SE-NW direction (Yamazaki et al., 1985; Mikumo et al., 1986), which is significantly different from those in the inland region. Except in the last region, it is evident that the inland central Honshu including the Hida region is subjected to the maximum compressive tectonic stress working in the ESE-WNW direction.

(2) The conjugate sets of major Quaternary active faults distributed in the Hida region, such as the Atotsugawa, Ushikubi, Miboro and Atera faults, and of many minor faults, indicate that the region had been compressed by strong tectonic stress during the Quaternary period (Huzita, 1980). The direction of the compressive tectonic stress inferred from the existence of these faults is again oriented in the ESE-WNW direction, which is also consistent with the direction inferred from the alignment of monogenetic volcanoes located in central Honshu (Ando,1979). The average direction of the maximum principal strains in central Honshu derived from the triangulation surveys over the last 90 years (Nakane, 1973) is also found to be nearly parallel to the above direction. This stituation is particularly clear in Figure 20 indicating the principal strains for 80 yrs up to 1985 over the Hida region and the northern part of the Fossa Magna (Hashimoto and Tada, 1986). Their general pattern is remarkably consistent with that from the focal mechanism solutions shown in Figure 19. On the other hand, the direction of convergence of the Pacific plate relative to the Eurasian plate can be estimated as N70°W at a location(φ=35.0°N and λ=142.0°E) on the Japan trench, from the RM2 model of Minster and Jordan (1978). This is almost consistent with the above described directions inferred from the various observations. All the above evidence suggests that the crust in the region under consideration has been constantly subjected to the compressive stress due to the movement of the Pacific plate during the last 2 Ma.

(3) A new plate-tectonic hypothesis for the Japan Islands has

recently been presented, however, (Kobayashi,1983;Nakamura,1983) to postulate that the northeastern Honshu arc is a part of the North American plate, and that the Eurasian plate is subducting eastwards under northeastern Honshu at the eastern margin of the Japan Sea (as shown by a broken line in Figure 1). It is also assumed in this model that the northeastern Honshu arc should be subducting beneath or colliding against the southwestern Honshu towards the west across the Fossa Magna to give rise to the uplift of the Hida and other high mountains. This subduction or collision would yield west-dipping thrust-type earthquakes around the Fossa Magna and also provide strong tectonic stress to the Hida region now in consideration. Although a few moderate-size earthquakes with magnitudes 6.0-6.5 actually took place near the northern Fossa Magna, their focal mechanisms were of strike slip type rather than of thrust-type. Minor shocks located between the Fossa Magna and the Hida mountain range also indicate strike-slip mechanisms (Fukao and Yamaoka,1983). If there were actually relative motions between the North American and Eurasian plates across the Fossa Magna, the RM2-model of Minster and Jordan (1978) gives the direction of the relative motion and hence of the horizontal compressive stress at a location (φ =35°.5N, λ=138°.5E) near the central Fossa Magna to be N95°W. This appears significantly different from N70°W which is the direction of the relative motion between the Pacific and Eurasian plates. The stress directions derived from the various observations are more consistent with the N70°W.

(4) The above consistency appears to suggest that the Hida region would be subjected to only minor effects from the relative

motion between the North America and Eurasian plates, if any, but much larger effects from that between the Pacific and Eurasian plates. If this is indeed the case, northeastern Honshu should be regarded as a microplate (e.g. Seno, 1985) which acts only to transmit the tectonic stress from the Pacific plate to the southwestern Honshu arc. In the above consideration, however, the effects of the northwestward subduction of the Philippine Sea plate under the southern part of central Honshu has not been taken into account. More complete calucuations incorporating a combined effect from the relative motions between the three plates (e.g. Tada, Nakabori and Hashimoto, 1986) will give a solution to the observed stress state in this region. More recently, however, another hypothesis has been presented that an eastward movement of the Amurian plate would yield the Japan Sea convergence along its eastern margin (Tamaki and Honza, 1985). If this is the case, and if a part of the southwestern Honshu arc is involved in this plate, the Hida region would be subjected to compressive stress from the east by the Pacific plate and from the west by the Amurian plate. This is beyond the scope of the present paper but will be discussed elsewhere, incorporating the tectonic stress state on a wider regional scale..

(5) The magnitude of the tectonic compressive stress acting in the Hida region may be roughly evaluated from the relations described in the foregoing section. For this case, the maximum compressive stress σ_1 may be related to $\sigma_1 = \tau + \sigma_v$, and the stress difference $\sigma_1 - \sigma_2 = \tau$, where τ and σ_v have been estimated in such a way as given in Figure 17. The shear stress τ_o to cause

sliding on a fault would be slightly smaller than the shear resistance τ, but their estimates critically depend on the choice of λ. For a hydrostatic case (λ=0.36) and a wet crust (λ=0.72), conservative estimates of σ_0 may be of the order of 700 and 400 bars respectively at depths down to 8 km, with an average of 400-250 bars over the depths beneath the Hida mountain range. On the other hand, the magnitude of the stress difference has been estimated (Fukao and Yamaoka, 1983) to account for the uplifting of the Hida mountains, with the rate of more than 1 m/1000 yr during the Quaternary period, and also from the observed Bouguer gravity anomalies of -80 mgals (Kono et al., 1982; Yamamoto et al.,1982) which would be larger by 200 mgals than expected from an isostatic compensation. Their conclusion is that the horizontal compressive stress of tectonic origin should be at least of the order of 300 bars. This value is actually the differential stress between the maximum compressive stress σ_1 and the vertical stress σ_2, and hence may be compared with the present estimate. Our estimate of 700 and 400 bars based on the brittle/ductile transition model may be regarded as the upper bound of the horizontal differential stress, while their estimate gives its lower bound.

CONCLUSIONS

The main conclusions we have obtained here are ;

(1) High seismicity is concentrated with a remarkably clear lineation along the Atotsugawa fault extending for about 70 km with an intermediate zone of relatively lower activity in the

central section with a length of 22 km.

(2) The high seismicity along the Atotsugawa fault may be attributed to post-seismic stress concentration after the 1858 Ansei Hida earthquake. The spatially non-uniform seismicity along the fault, which is also indicated by different b-values, may be interpreted as a manifestation of more heterogeneous fault strength in the eastern and western sections, larger seismic displacements in the central section, and possibly bilateral rupture propagation towards both ends during the large earthquake.

(3) A belt-like concentration of seismicity has been observed beneath the axial portions of the Hida mountain range over a length of about 150 km. The activity is characterized by intermittent and repeated swarms which appear to migrate between the northern and southern portions.

(4) The depth distribution of seismicity is clearly confined above 15 km below the Atotsugawa fault, while it appears bounded at 8 km beneath the central to southern portion of the Hida mountains. These local variations of deepest seismicity can be interpreted as due to the difference in the brittle/ductile transition depth. The observed larger geothermal gradients suggest higher heat flow beneath the Hida mountains involving several active volcanoes. This is consistent with the seismic low velocity structures derived from the three-dimensional analysis.

(5) The focal mechanism solutions of moderate-size shocks indicate that the maximum compressive stress working in the

present region is generally oriented in the ESE-WNW direction. The direction is consistent with that inferred from the distribution of conjugate sets of Quaternary faults and from triangulation surveys. This also appears parallel to the direction of relative motion between the Pacific and Eurasian plates rather than suggested motion between the North American and Eurasian plates. There still remains uncertainty about the source of the compressive tectonic stress working in the Hida region. The magnitude of the shear-stress in the shallow crust beneath the Hida mountains may be less than 700 bars.

ACKNOWLEDGMENTS

We are grateful to the staff members of the following organizations for providing seismic data; the Regional Observation Center for Earthquake Prediction and Takayama Seismological Observatory of Nagoya University, the Hokushin Seismological Observatory of the Earthquake Research Institute, University of Tokyo, and the Hokuriku Microearthquake Observatory of the Disaster Prevention Research Institute, Kyoto University, and also to Mr. Akio Yamamoto, Hokuriku Department of Agriculture and Forestry for providing the geothermal data. Helpful comments given by Prof. S. Uyeda and Prof. M.Bath and anonymous reviewers for the improvement of the manuscript are sincerely acknowledged. We also wish to thank Satoshi Kaneshima and Yoshinobu Hoso for making preparations of the manuscript. The expense of the present study was partly supported by the Scientific Research Found (No.B-6046005) provided by the Ministry of Education, Science and Culture of Japan.

REFERENCES

Ando, M., 1979. The stress field in the Japan islands during the last half a millions years, The Earth Monthly, 7 : 541-546. (in Japanese).

Ando, M., Ishikawa, I., and Yamazaki, F., 1983. Shear wave polarization anisotropy in the upper mantle beneath Honshu, Japan, J. Geophys. Res., 88: 5850-5864.

Aoki, H., Sasaki, T., Oida, T., Muramatsu, I., Himamura, H. and Furuya, I., 1972. Crustal structure in the profile across central Japan as derived from explosion seismic observations, J. Phys. Earth, 20 : 197-223.

Brace, W.F. and Kohlstedt, D.L., 1980. Limits on lithospheric stress imposed by laboratory experiments, J. Geophys. Res., 85: 6248-6252.

Byerlee, J.D., 1978. Friction of rocks, Pure & Appl. Geophys., 116 : 615-626.

Doser, D.I. and Kanamori, H., 1986. Depth of seismicity in the Imperial Valley region (1977-1983) and its relationship to heat flow, crustal structure, and the October 15, 1979 earthquake, J. Geophys. Res., 91, 675-688.

Earthquake Research Institute, University of Tokyo, 1980. Historical Documents of Earthquakes in Japan, 1 : 138-170 (in Japanese).

Earthquake Research Institute, University of Tokyo, 1985. Aftershock observations of the September 14, 1984 Naganoken-Seibu earthquake (M6.8). Part 1, Aftershock distributions, Rep. Coord. Commit. Earthq. Pred., 33 : 63-68 (in Japanese).

Fujii, S. and Takemura, T., 1979. Active faults in the Toyama prefecture and its adjacent regions, Res. Rep. Counterplans for Earthquakes in the Toyama Prefecture, 39-72. (in Japanese).

Fukao, Y. and Yamaoka, K., 1983. Stress estimate for the highest mountain system in Japan, Tectonics, 2 : 453-471.

Geographical Survey Institute, Japan, 1984. Crustal movements in the Hokuriku district, Rep. Coord. Commit. Earthq. Pred., 31 : 412-419 (in Japanese).

Geological Survey of Japan, 1978. Geological Map of Japan, 2nd Ed.(1978).

Goetze, C., 1978. The mechanism of creep in olivine, Phil. Trans. Roy. Soc. London, Ser.A, 288 : 99-119.

Hashimoto, M. and Tada, T., 1986. Stress field in the northern Fossa Magna derived from triangulation surveys, and its tectonic implications, Abstr. Seism. Soc., Japan, 1986, No.2, A28 (in Japanese).

Hirahara, K., Ikami, A., Ishida, M. and Mikumo, T., 1986. Three-dimensional P-wave velocity structure beneath central Japan -- Low-velocity bodies in the wedge portion of the upper mantle above high velocity subducting plates --, submitted to Tectonophysics.

Hori, S., Aoki, H. and Ooida, T., 1982. Focal mechanisms of the earthquake swarm southeast of Mt. Ontake, central Honshu, Japan, ZISIN, II, 35 : 161-169 (in Japanese with English abstract).

Huzita, K., 1980. Role of the Median Tectonic Line in the Quaternary tectonics of the Japan islands, Mem. Geol. Soc., Japan, 18 : 129-153.

Ichikawa, M., 1971. Reanalyses of mechanism of earthquakes which occurred in and around Japan, and statistical studies on the nodal plane solutions obtained, 1926-1968, Geophys. Mag., 35 : 207-274.

Ikami, A., Ankyu, T. and Aoki, H., 1972. Low seismic activity associated with the Atera fault, central Japan, ZISIN, II, 25 : 232-242 (in Japanese with English abstract).

Kato, M., 1983. Electro-optical distance measurements and continuous observations of crustal movements across and around the Atotsugawa fault, The Earth Monthly, 5 : 341-345 (in Japanese).

Kawasaki, I., 1975. The focal process of the Kita-Mino earthquake of August 19, 1961, and its relationship to a Quaternary fault, the Hatogayu-Koike fault, J. Phys. Earth, 23 : 227-250.

Kobayashi, Y., 1976. A relationship between the distribution of focal depth of microearthquakes and surface heat flow in the southwestern Japan and central Japan, Proc. Symposium for Earthq. Prediction Res., 184-193 (in Japanese with English abstract).

Kobayashi, Y., 1983. Incipient subduction of a lithospheric plate under the eastern margin of the Japan Sea, The Earth Monthly, 5 : 510-514 (in Japanese).

Koch, P.S., Christie, J.M. and George, R.P., 1980. Flow law of " wet " quartzite in the α -quartz field (abstract), EOS, Trans. Am. Geophys. Union, 61 : 376.

Kono, Y., Hibi, T., Kubo, M., Michigami, O., Shibuya, K., Sunami, M., Suzuki, K. and Furuse, N., 1982. Gravity anomaly over the northern part of the central Japan (1),(2), Sci. Rep., Kanazawa Univ., 27 : 71-83, 117-146.

Matsuda, T., 1966. Strike-slip faulting along the Atotsugawa fault, Bull. Earthq. Res. Inst., 44 : 1179-1212 (in Japanese with English abstract).

Matsuda, T., 1975. Magnitude and recurrence interval of earthquakes from a fault, ZISIN II, 28 : 269-282 (in Japanese with English abstract).

Meissner, R. and Strehlau, J., 1982. Limits of stresses in continental crusts and their relation to the depth-frequency distribution of shallow earthquakes, Tectonics, 1 : 73-89.

Mikumo, T., 1966. A study on crustal structure in Japan by the use of seismic and gravity data, Bull. Earthq. Res. Inst., 44 : 965-1007.

Mikumo, T., 1973. Faulting mechanism of the Gifu earthquake of September 9, 1969, and some related problems, J. Phys. Earth, 21 : 191-212.

Mikumo, T. and Ando, M., 1976. A search into the faulting mechanism of the 1891 great Nobi earthquake, J. Phys. Earth, 24 : 63-87.

Mikumo, T. and Miyatake, T., 1978. Dynamical rupture process on a three-dimensional fault with non-uniform frictions, and near-field seismic waves, Geophys. J. Roy. Astr. Soc., 54 : 417-438.

Mikumo, T. and Miyatake, T., 1979. Earthquake sequences on a frictional fault model with non-uniform strengths and relaxation times, Geophys. J. Roy. Astr. Soc., 59 : 497-522.

Mikumo, T. and Wada, H., 1983. Seismic activity associated with the Atotsugawa fault, The Earth Monthly, 5 : 325-334 (in Japanese).

Mikumo, T., Koizumi, M. and Wada, H., 1985. Seismicity, focal mechanism and tectonics in the northern Hida region, central Japan, ZISIN II, 38 : 25-40 (in Japanese with English abstract).

Mikumo, T., Wada, H., Okamoto, T., Ishikawa, I. and Sakuma, K., 1986 . Focal mechanism of the 1985 Off-Noto Peninsula earthquake and some considerations on seismotectonic features of the Japan Sea coastal regions, Abstr. Seism. Soc., Japan, 1986, No.1, A39 (in Japanese).

Ministry of Education, Committee for Earthquake Disasters, 1940. Historical records of Japanese earthquakes, Meiho-sha (in Japanese).

Minster, J.B. and Jordan, T.H., 1978. Present day plate motions, J. Geophys. Res., 83 : 5331-5354.

Nakamura, K., 1983. Possible nascent trench along the eastern Japan Sea as the convergent boundary between Eurasian and North American plates, Bull. Earthq. Res. Inst., 58 : 711-722 (in Japanese with English abstract).

Ohnaka, M., 1978. Earthquake source parameters related to magnitude, Geophys. J. Roy. Astr. Soc., 55 : 45-66.

Research Group for Active Faults of Japan, 1980a. Active faults in Japan : Sheet maps and inventories, 363 pp., Univ. Tokyo Press (in Japanese).

Research Group for Active Faults of Japan, 1980b. Active faults in and around Japan : The distribution and the degree of activity, J. Natural Disaster Science, 2 : 61-99.

Research Group for Excavation of the Atotsugawa Fault, 1983. Trenching excavation across the Atotsugawa fault, The Earth Monthly, 5 : 335-340 (in Japanese).

Sakai, H. and Hirooka, K., 1983. Fault movements inferred from paleomagnetism and rock magnetism, The Earth Monthly, 5 : 394-398. (in Japanese).

Seno, T., 1985. Is northern Honshu arc a microplate ?, Tectonophysics, 115 : 177-186.

Sibson, R.H., 1982. Fault zone models, heat flow, and the depth distribution of earthquakes in the continental crust of the United States, Bull. Seism. Soc. Am., 72 : 151-163.

Sibson, R.H., 1984. Roughness at the base of the seismogenic zone : Contributing factors, J. Geophys. Res., 89 : 5791-5799.

Sugimura, A. and Matsuda, T., 1965. Atera fault and its displacement vectors, Geol. Soc. Am. Bull., 76 : 509-522.

Tada, T., Nakabori, Y. and Hashimoto, M., 1986. Stress field in central Honshu, calculated from relative plate motions, Abstr. Seism. Soc., Japan, 1986, No.1, A54. (in Japanese).

Tamaki, K. and Honza, E., 1985. Incipient subduction and obduction along the eastern margin of the Japan Sea, Tectonophysics, 119 : 381-406.

Takemura, T. and Fujii, S., 1984. Active faults in the northern part of the Hida mountains, central Japan, The Quaternary Res., 22 : 297-312 (in Japanese with English abstract).

Takeuchi, A. and Sakai, H., 1985. Recent event of activity along the Atotsugawa fault, central Japan -- A paleomagnetic method for dating of fault activity --, Res. Active Faults, 1 : 67-74 (in Japanese).

Tsukuda, T., 1983. Microearthquakes around the Atotsugawa fault, The Earth Monthly, 5 : 417-425 (in Japanese).

Tsukuda, T., 1985. Long-term seismic activity and present microseismicity on active faults in Southwest Japan, Earthq. Pred. Res., 3 : 253-284.

Usami, T., 1980. General view of damaging earthquakes in Japan, Data and Descriptions, 327 pp., Univ. Tokyo Press (in Japanese).

Usami, T., Earthquake Research Institute, University of Tokyo, Histographical Institute, University of Tokyo, and Kamitakara Crustal Movement Observatory, Disaster Prevention Research Institute, Kyoto University, 1979. Hietsu earthquake of April 9, 1858 and the Atotsugawa fault, Rep. Coord. Commit. Earthq. Pred., 21 : 115-119 (in Japanese).

Uyeda, S. and Horai, K., 1964. Terrestrial heat flow in Japan, J. Geophys. Res., 69, 2121-2141.

Yamada, I. and Fujii, I., 1973. The Fukui-Gifu border earthquake of August 31, 1972, Abstr. Seism. Soc., Japan, No.1, 117 (in Japanese).

Yamamoto, A., Nozaki, K. Fukao, Y, Furumoto, M., Shichi, R. and Ezaka, T., 1982. Gravity survey in the central Ranges, Honshu, Japan, J. Phys. Earth, 30 : 201-243.

Yamazaki, K., Tamura, T. and Kawasaki, I., 1985. Seismogenic stress field of the Japan Sea as derived from shallow and small earthquakes, ZISIN II, 38 : 541-558 (in Japanese with English abstract).

Yamazawa, K., 1929. The great earthquake of Hida-Tsunogawa on February 26, Ansei 5, ZISIN, 1 : 125-128 (in Japanese).

Yamazawa, K., 1930. A compiled chronology of felt earthquakes in the Hida region, ZISIN I, 2 : 240-260 (in Japanese).

Wada, H., 1975. Microseismicity in the vicinity of the Atotsugawa fault (2), ZISIN II, 28 : 113-124 (in Japanese with English abstract).

Wada, H. and Kishimoto, Y., 1974. Microseismicity in the vicinity of the Atotsugawa fault (1), ZISIN II, 27 : 1-9 (in Japanese with English abstract).

Wada, H. Mikumo, T. and Koizumi, M., 1979. Seismicity and focal mechanism of local earthquakes along the Atotsugawa fault and in the northern Hida region, ZISIN II, 32 : 281-296 (in Japanese with English abstract).

Figure Captions

Fig. 1. Location map of the Hida region, central Japan together with the Northeastern and Southwestern Honshu arcs and plate boundaries.

Fig. 2. Distribution of active Quaternary faults (after Research Group for Active Faults of Japan, 1980a) and of high mountains in the Hida region. Solid and open triangles indicate the locations of active volcanoes and high mountains, and thick contours indicate a 2000 m - altitude.

Fig. 3. Detailed location map around the Atotsugawa, Mozumi and Ushikubi faults.

Fig. 4. Exposed geological cross sections at Nokubi., the trenching site on the Atotsugawa fault. Upper : east wall, Lower ; west wall. (reproduced from the results obtained by the Research Group for Excavation of the Atotsugawa fault, 1983).

Fig. 5. The percentage of damaged houses along and around the Atotsugawa fault during the 1858 Ansei Hida earthquake (after Usami et al., 1979). Solid and broken curves indicate contours of 80 and 50 % damage, respectively.
Two-letter codes indicate the sites of villages mentioned in this study; US ; Ushikubi, AM ; Amo, TN ; Tsunogawa, MR ; Moriyasu, SG ; Suganuma, HU ; Higashi-Urushiyama, DO ; Do, OT ; Otawa, AR ; Arimine, KR ; Kurobe (See also Figure 8).

Fig. 6. P-wave velocity structure around the Hida region. Thin solid and broken lines are taken from Mikumo (1966) and Aoki et al. (1972), respectively, and the smoothed solid curve was used for hypocenter location in this study.

Fig. 7. Seismicity in the northern Hida and its adjacent regions during the period from April, 1980 to June, 1986. Epicenters are classified by open circles with different sizes according to their magnitudes ; $M \geq 4.0$, $3.0 \leq M < 4.0$, $2.0 \leq M < 3.0$, $1.0 \leq M < 2.0$ and $M < 1.0$. Solid squares and triangles qith three-letter code indicate the locations of seismograph stations, and thin solid curves indicate major Quaternary faults.
Seismicity in the region enclosed by a square includes a great number of swarm earthquakes up to 1984 and aftershocks of the Western Nagano earthquake of September 14, 1984, and has been omitted from the plot.

Fig. 8. Seismicity along and around the Atotsugawa, Mozumi and Ushikubi faults.

Fig. 9. Depth distribution of the shocks located in three sections, which are projected onto a plane perpendicular to the Atotsugawa fault. 1) AM-SG, 2) SG-AR, 3) AR-KR
A, M and U indicate the locations of fault traces of the Atotsugawa, Mozumi and Ushikubi faults on the ground surface.

Fig.10. Hypocenter distribution of all shocks that occurred along the Atotsugawa fault, which are projected onto a plane parallel to the fault.

Fig.11. Hypocenter distribution of all shocks that occurred beneath the Hida mountain range, which are projected onto a plane trending in the N-S direction.

Fig.12. Schematic focal mechanism diagrams of moderate-size shocks with magnitudes greater than 3.0 along and around the Atotsugawa, Mozumi, Miboro faults. The diagrams are projected onto the lower hemisphere of the Wulff's net.

Fig.13. Schematic focal mechanism diagrams of moderate-size shocks with magnitudes greater than 3.0 located in the northern to central section of the Hida mountain range.

Fig.14. Schematic focal mechanism diagrams of moderate-size shocks located in the southern section of the Hida mountain range.
Upper ; swarm earthquakes that occurred before 1984.
Lower ; large aftershocks that occurred in an early stage after the September 14, 1984 Western Nagano earthquake (after Earthquake Research Institute, 1985).

Fig.15. Schematic focal mechanism diagrams of moderate-size shocks located in a region west of the Hida mountain range and northeast of the Atera fault.

Fig.16. Cummulative magnitude--frequency diagrams of all shocks that occurred in three sections of the Atotsugawa fault during the period from May, 1977 to June, 1986. E, C and W indicate the eastern, central and western sections, respectively.

Fig.17. Possible depth (z) variations of the shear resistance (τ) in brittle and ductile regimes within the upper to middle sections of the crust. Surface heat flow (unit in HFU) and the ratio (λ) of pore pressure to hydrostatic pressure are taken as variables for a fixed strain rate of $\dot{\varepsilon} = 10^{-14}\ \mathrm{sec}^{-1}$.

Fig.18. Three-dimensional P-wave velocity anomalies along two vertical cross sections across the Hida mountain range (after Hirahara et al., 1986). Solid and broken curves indicate contours of high and low velocity anomalies given in every 1.5 %. Solid circles indicate the locations of active volcanoes.

Fig.19. Directions of the maximum compressive stress (P-axes) derived from the focal mechanism solutions.

Fig.20. Stress field in the northern Hida and northern Fossa Magna regions derived from triangulation surveys over 80 years (after Hashimoto and Tada, 1986). Triangles indicate the bases of the surveys, and thick broken lines indicate major Quaternary faults and tectonic belt lines.

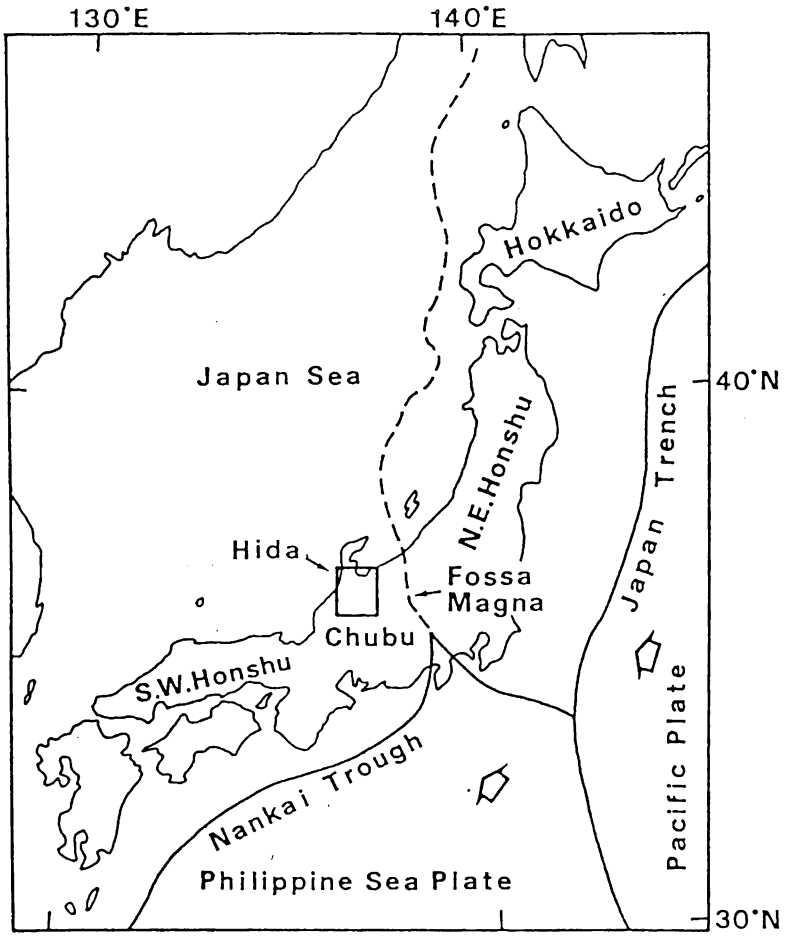
130°E
140°E
Hokkaido
Japan Sea
40°N
N.E.Honshu
Japan Trench
Hida
Fossa
Magna
Chubu
S.W.Honshu
Nankai Trough
Philippine Sea Plate
Pacific Plate
30°N

Fig. 1

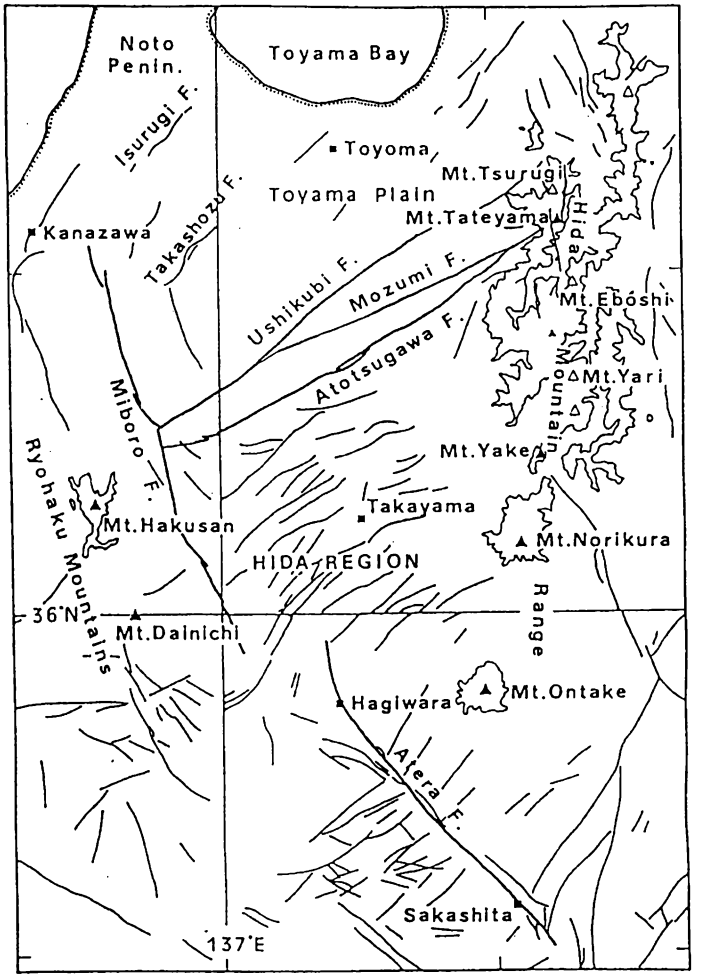
Noto
Penin.
Toyama Bay
Isurugi F.
Toyoma
Mt.Tsurugi
Toyama Plain
Mt.Tateyama
Takashozu F.
Kanazawa
Ushikubi F.
Mozumi F.
Hida Mountains
Mt.Eboshi
Atotsugawa F.
Mt.Yari
Miboro F.
Mt.Yakeyama
Ryohaku Mountains
Takayama
Mt.Hakusan
Mt.Norikura
HIDA-REGION
36°N
Mt.Dainichi
Range
Hagiwara
Mt.Ontake
Atera F.
Sakashita
137°E

Fig. 2

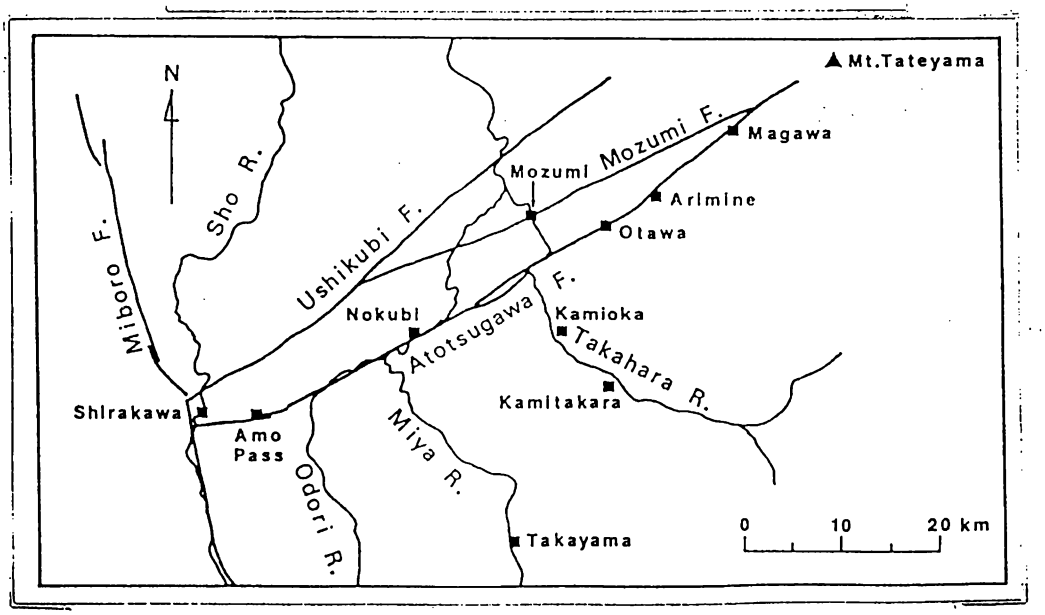
N
Mt.Tateyama
Sho R.
Mozumi Mozumi F.
Magawa
Miboro F.
Ushikubi F.
Arimine
Otawa
Nokubi
Atotsugawa F.
Kamioka
Takahara R.
Shirakawa
Amo Pass
Kamitakara
Miya R.
Odori R.
Takayama
0 10 20 km

Fig. 3

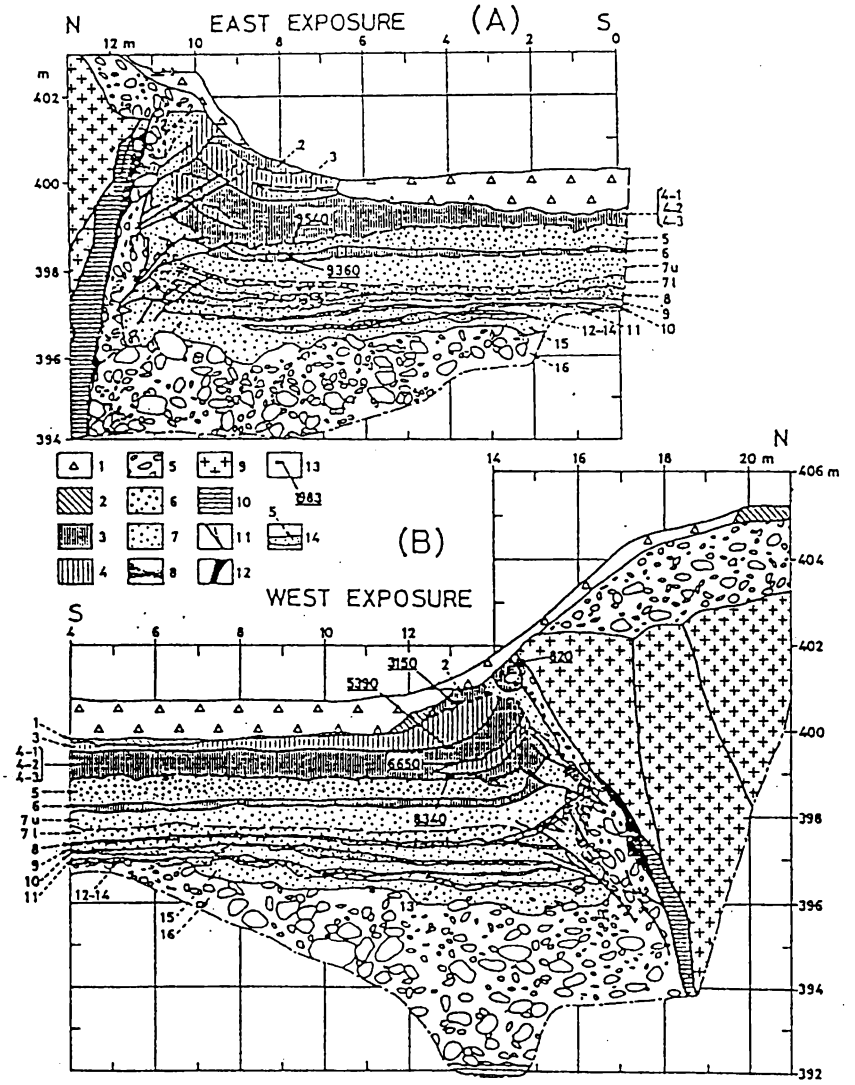

Geologic section of the east and west walls of the trench, the Atotsugawa fault. The position in the section is given by horizontal distance measured from a reference point at the southern end of the trench and height above sea level. 1: artificial deposit, 2: cultivated soil, 3: humic soil, 4: weak humic soil, 5: gravel, 6: coarse sand, 7: medium sand, 8: fine sand or silt, 9: granite, 10: crystalline limestone, 11: fault, 12: fault clay, 13: sampling position for ^{14}C dating and date in yrs B.P., 14: layer number.

Fig. 4

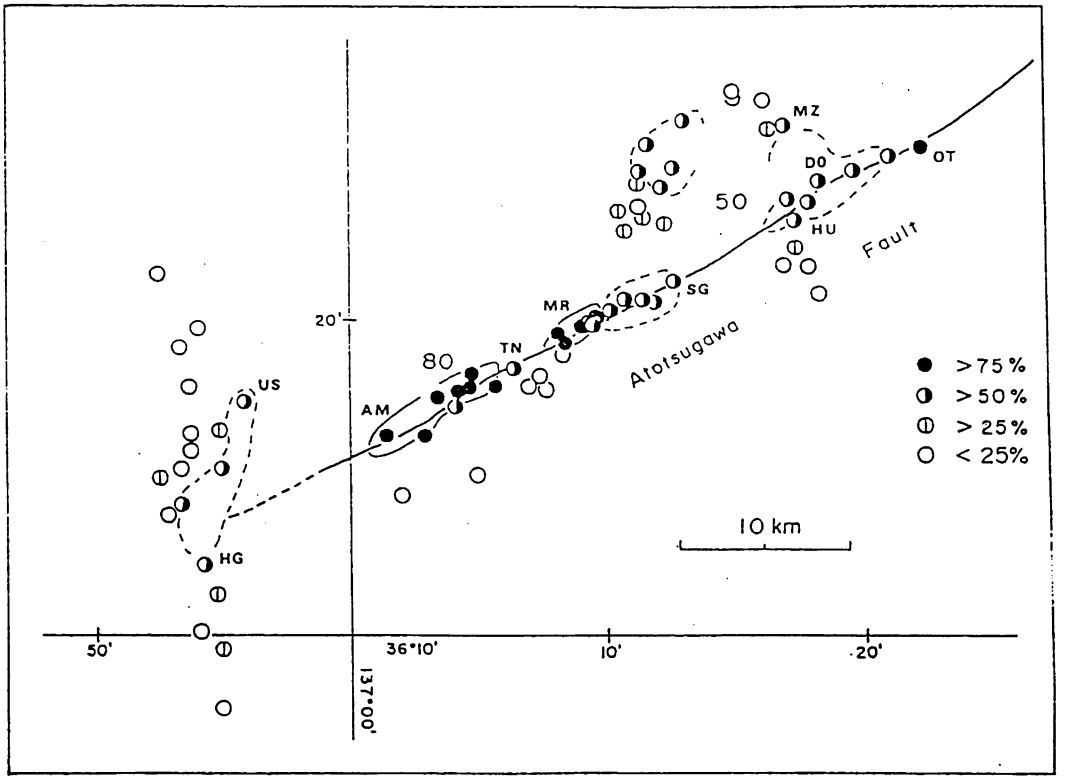
MZ
OT
DO
HU
Fault
SG
MR
TN
Atotsugawa
AM
US
HG
80
50
20'
> 75 %
> 50 %
> 25 %
< 25%
10 km
50'
36°10'
10'
20'
137°00'

Fig. 5

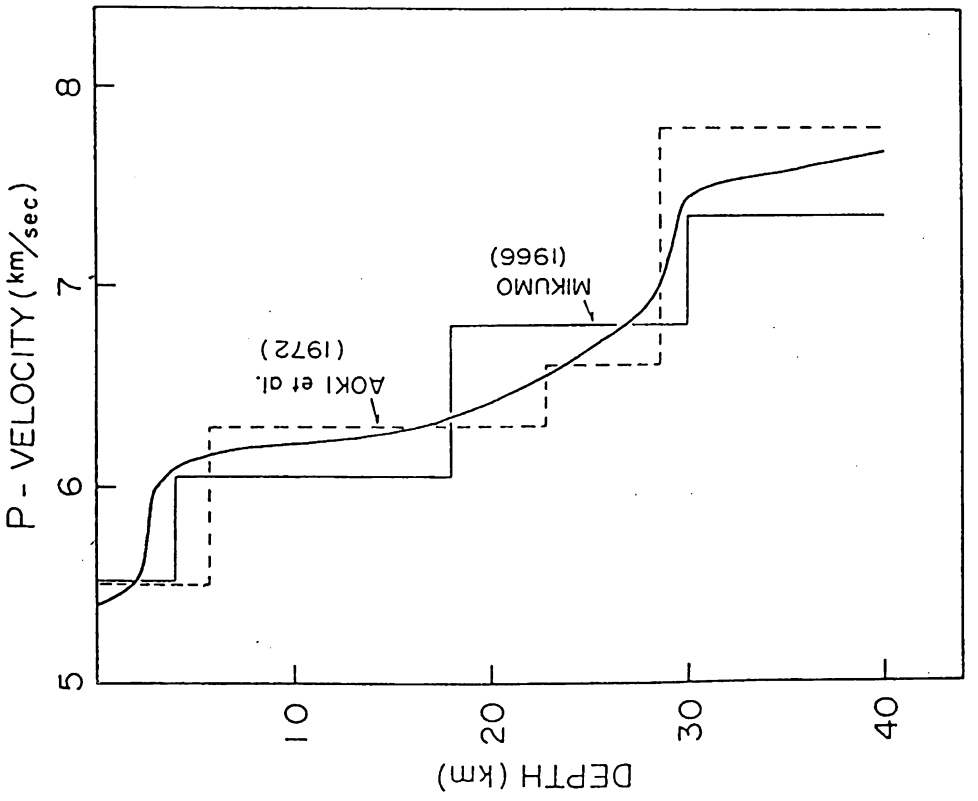
P - VELOCITY (km/sec)
DEPTH (km)
MIKUMO (1966)
AOKI et al. (1972)
5
6
7
8
10
20
30
40

Fig. 6

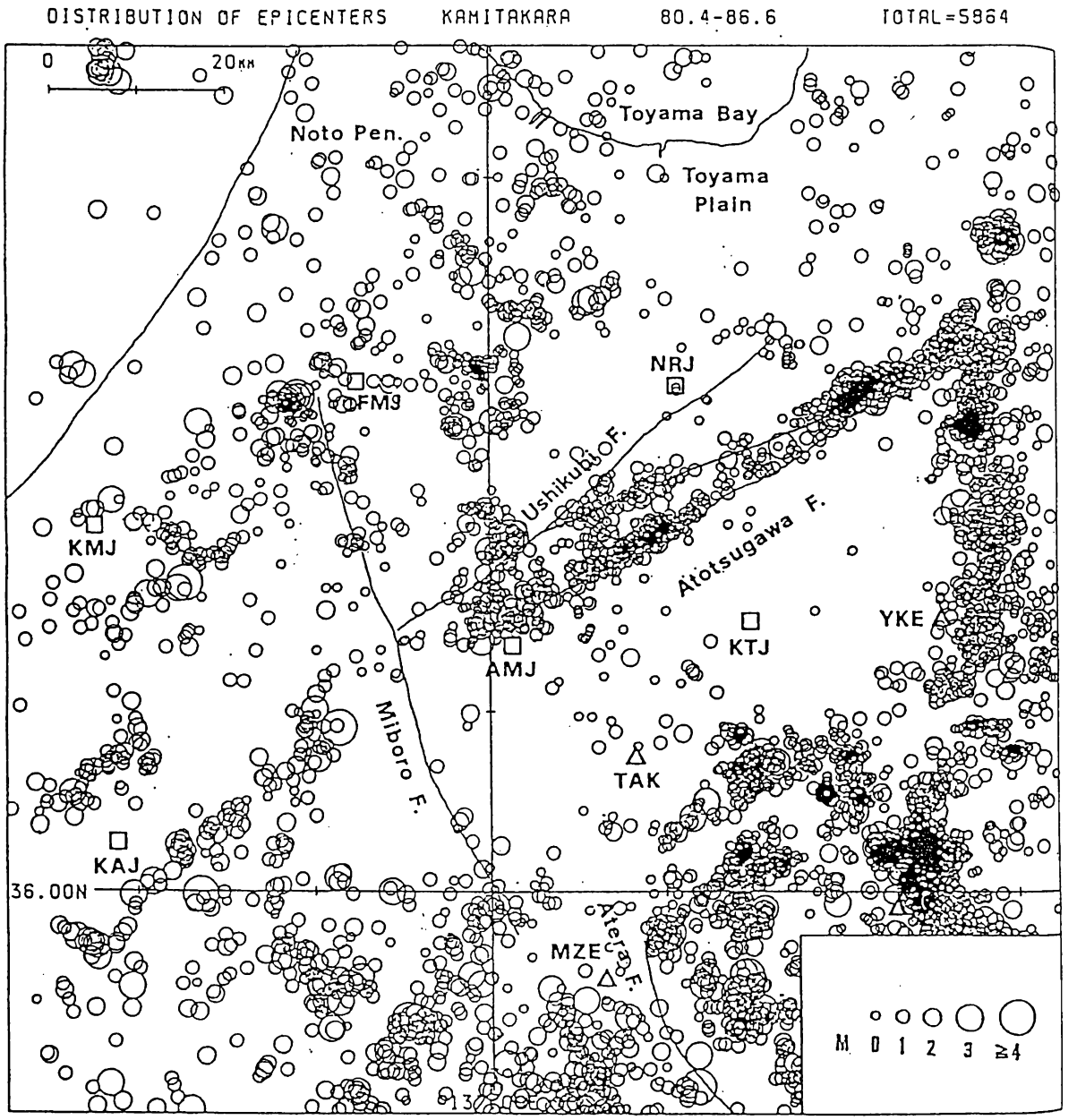
DISTRIBUTION OF EPICENTERS KAMITAKARA 80.4-86.6 TOTAL=5864
0 20KM
Noto Pen.
Toyama Bay
Toyama Plain
NRJ
FMG
Ushikubi F.
Atotsugawa F.
KMJ
KTJ
YKE
AMJ
Mibora F.
TAK
KAJ
36.00N
MZE
Ateraji F.
M 0 1 2 3 ≧4

Fig. 7

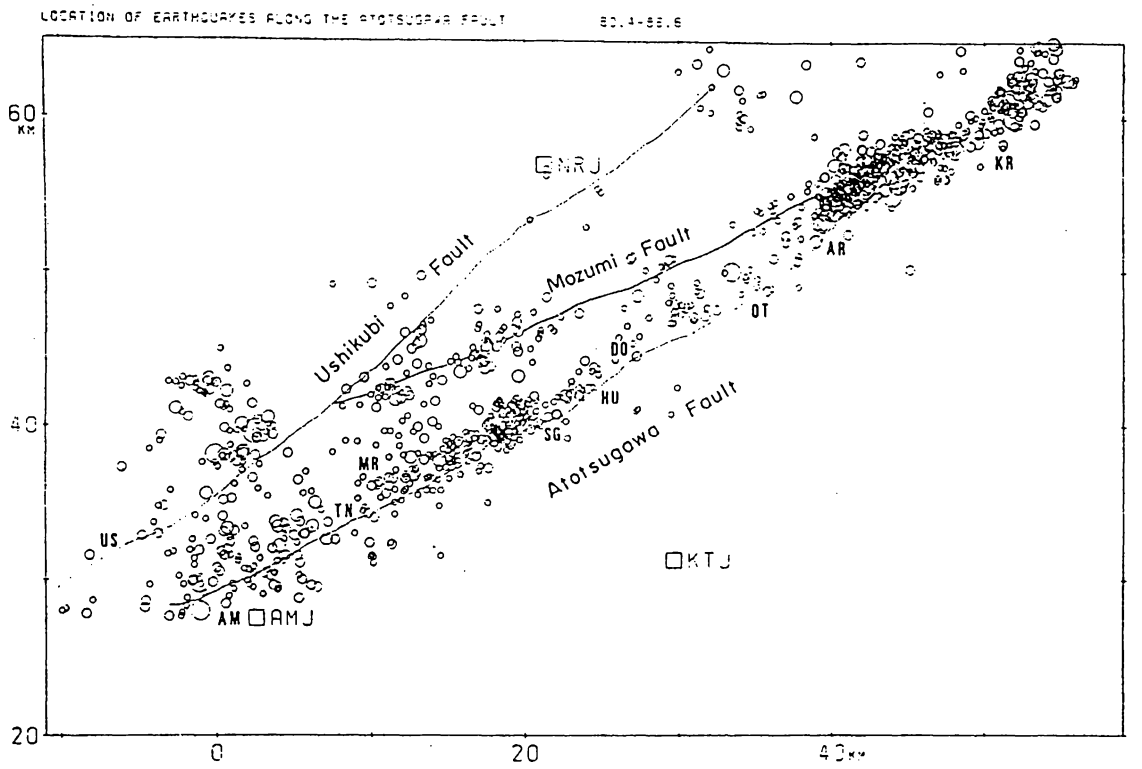
LOCATION OF EARTHQUAKES ALONG THE ATOTSUGAWA FAULT
80.4-86.6
60
KM
40
20
0
20
40KM
NRJ
Ushikubi Fault
Mozumi Fault
Atotsugawa Fault
KR
AR
OT
DO
HU
SG
MR
TN
US
AM
AMJ
KTJ

Fig. 8

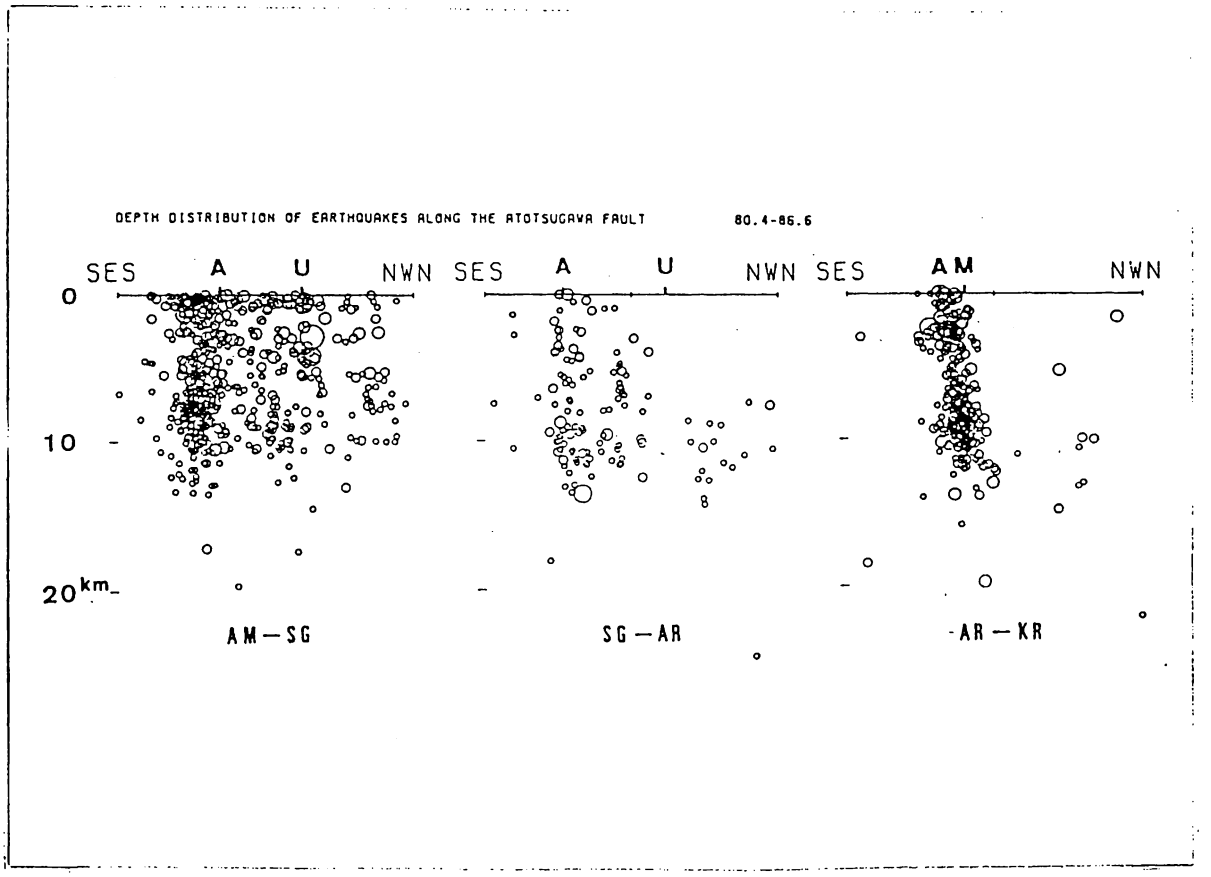
DEPTH DISTRIBUTION OF EARTHQUAKES ALONG THE ATOTSUGAWA FAULT
80.4-86.6
SES
A
U
NWN
SES
A
U
NWN
SES
AM
NWN
0
10
20km
AM—SG
SG—AR
AR—KR

Fig. 9

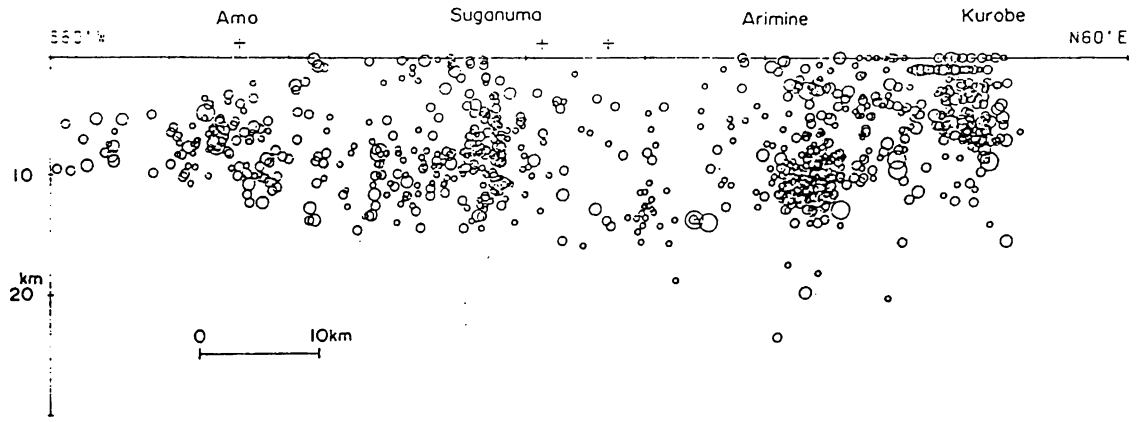
Amo
Suganuma
Arimine
Kurobe
N60°E
10
km
20
0
10km

Fig.10

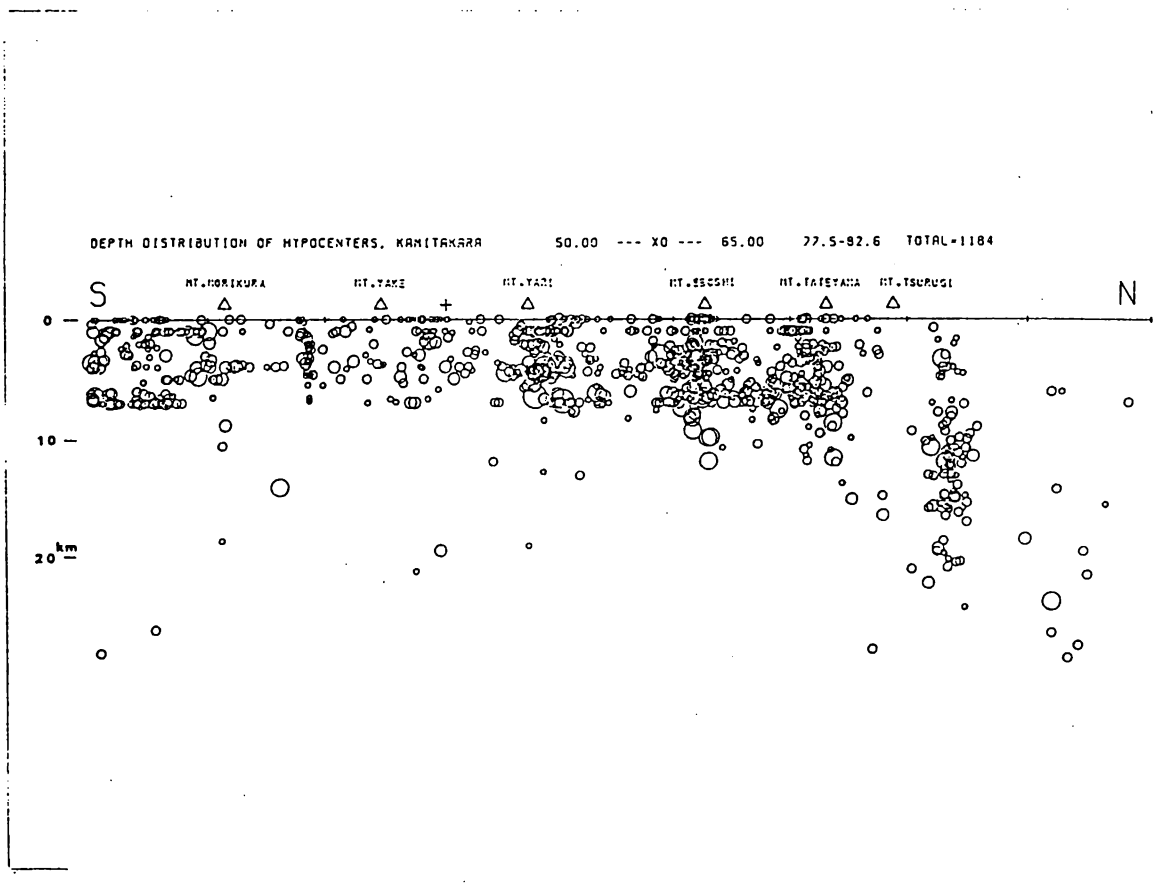
DEPTH DISTRIBUTION OF HYPOCENTERS, KAMITAKARA
50.00 --- X0 --- 65.00
77.5-82.6
TOTAL=1184
S
N
0
10
20
km

Fig.11

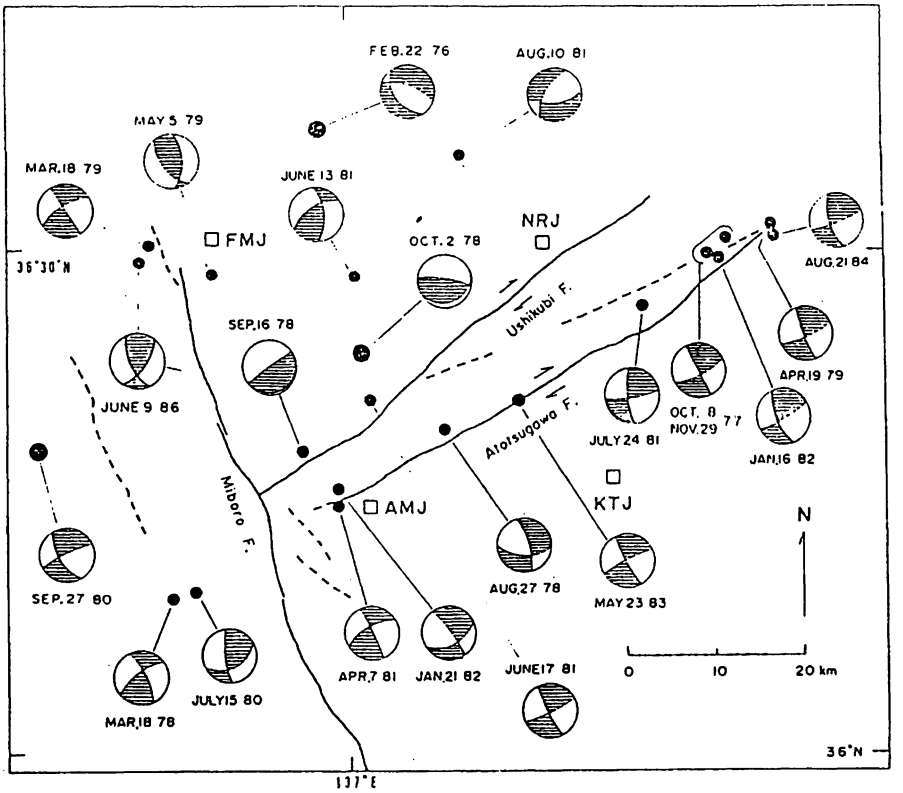
FEB.22 76
AUG.10 81
MAY 5 79
MAR.18 79
JUNE 13 81
FMJ
NRJ
OCT. 2 78
36°30'N
AUG.21 84
Ushikubi F.
SEP.16 78
JUNE 9 86
APR.19 79
Atotsugawa F.
OCT. 8
NOV.29 77
JULY 24 81
JAN.16 82
Mitoro F.
AMJ
KTJ
N
SEP.27 80
AUG.27 78
MAY 23 83
APR.7 81
JAN.21 82
JUNE17 81
0 10 20 km
JULY15 80
MAR.18 78
36°N
137°E

Fig.12

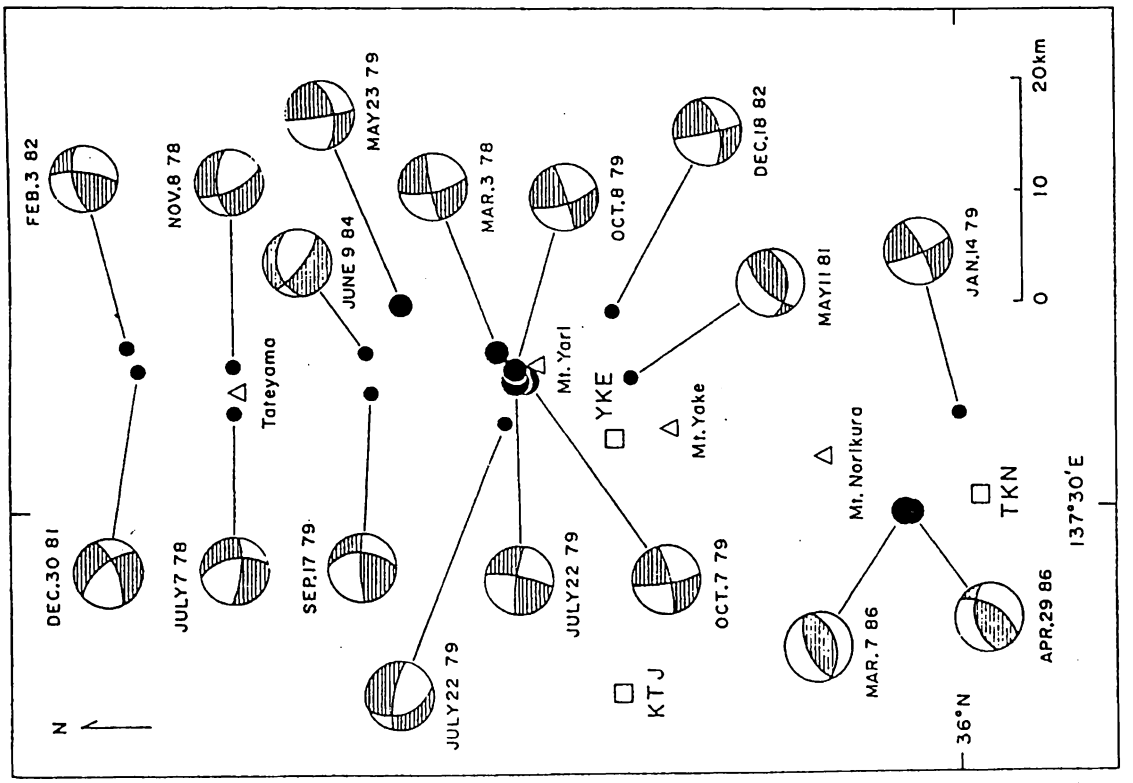
FEB.3 82
NOV.8 78
MAY23 79
MAR.3 78
OCT.8 79
DEC.18 82
JUNE 9 84
MAY11 81
JAN.14 79
Mt. Yari
YKE
Tateyama
Mt. Yake
0 10 20km
DEC.30 81
JULY7 78
SEP.17 79
JULY22 79
JULY22 79
OCT.7 79
Mt. Norikura
TKN
KTJ
MAR.7 86
APR.29 86
N
36°N
137°30'E

Fig.13

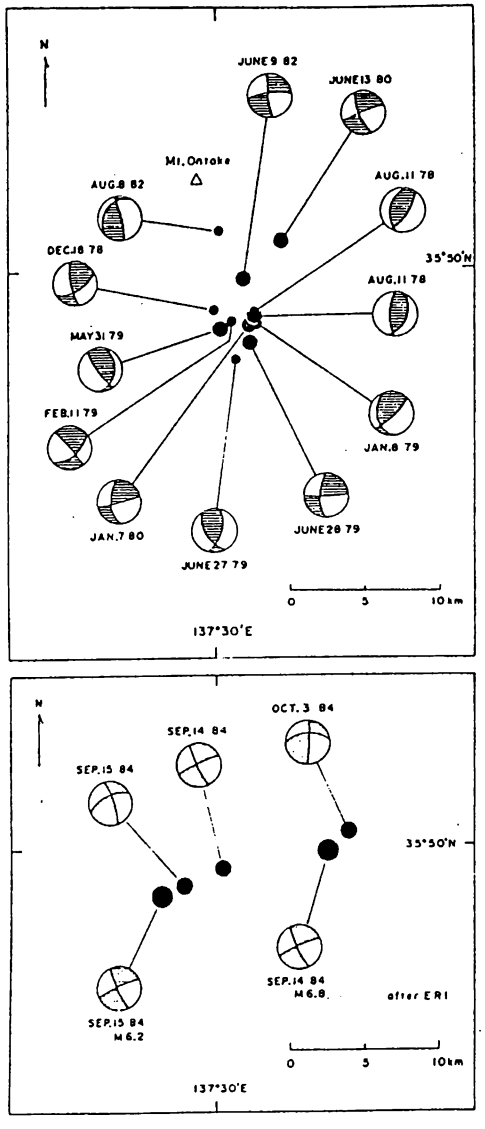
N
JUNE9 82
JUNE13 80
Mt. Ontake
AUG.8 82
AUG.11 78
DEC.18 78
35°50'N
AUG.11 78
MAY31 79
FEB.11 79
JAN.8 79
JAN.7 80
JUNE28 79
JUNE27 79
0 5 10km
137°30'E
N
OCT. 3 84
SEP.14 84
SEP.15 84
35°50'N
SEP.14 84
M6.8
after ERI
SEP.15 84
M6.2
0 5 10km
137°30'E

Fig.14

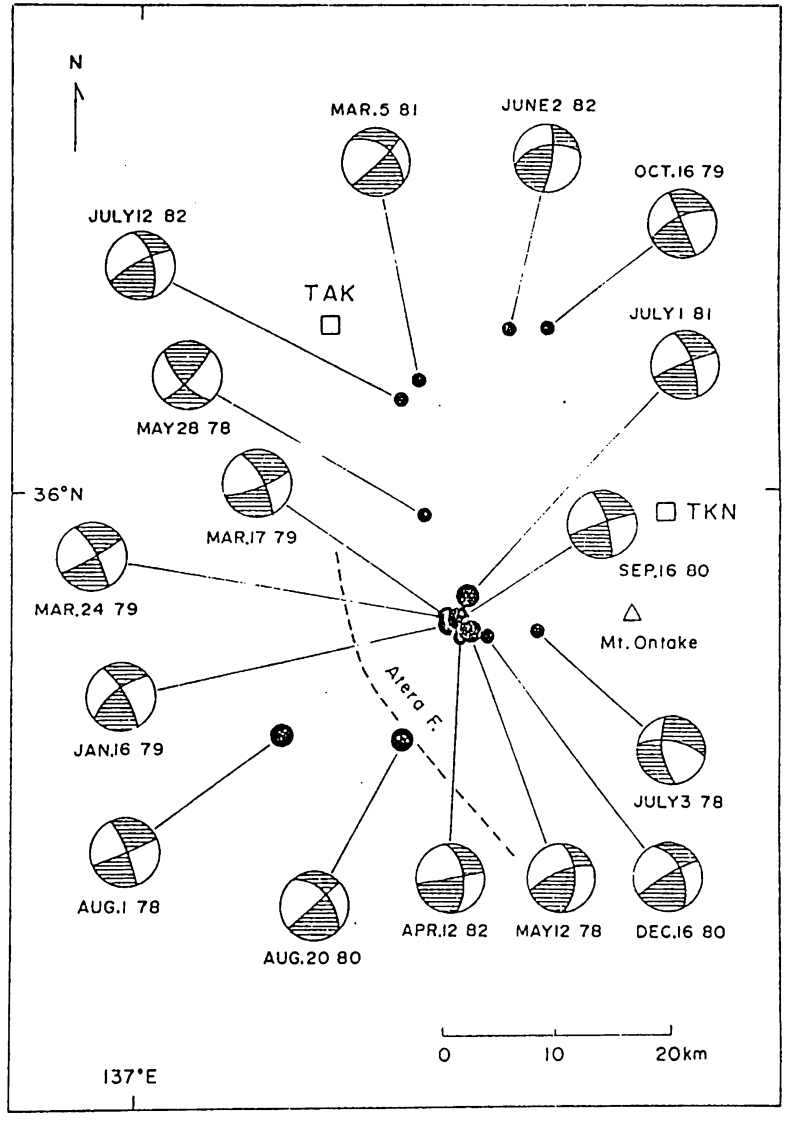
N
MAR.5 81
JUNE2 82
OCT.16 79
JULY12 82
TAK
JULY1 81
MAY28 78
36°N
TKN
MAR.17 79
SEP.16 80
MAR.24 79
Mt. Ontake
Atera F.
JAN.16 79
JULY3 78
AUG.1 78
APR.12 82
MAY12 78
DEC.16 80
AUG.20 80
0 10 20km
137°E

Fig.15

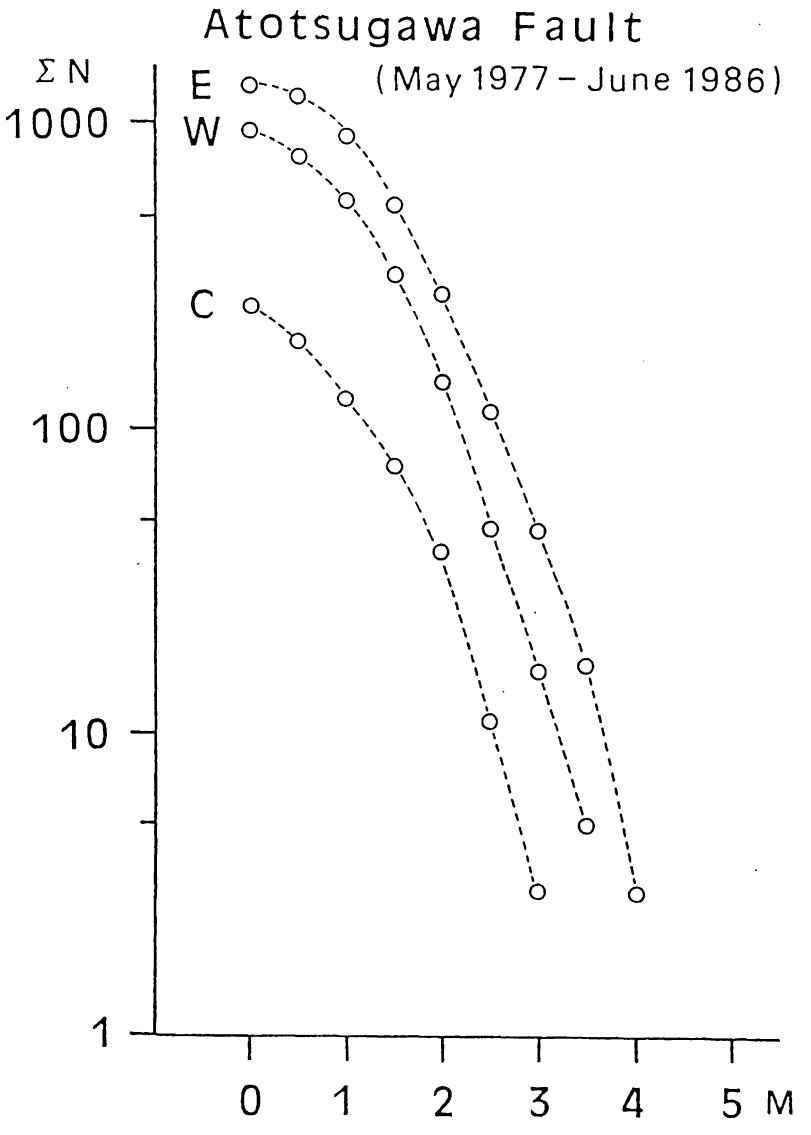
Atotsugawa Fault
(May 1977 – June 1986)
Σ N
1000
100
10
1
E
W
C
0
1
2
3
4
5 M

Fig.16

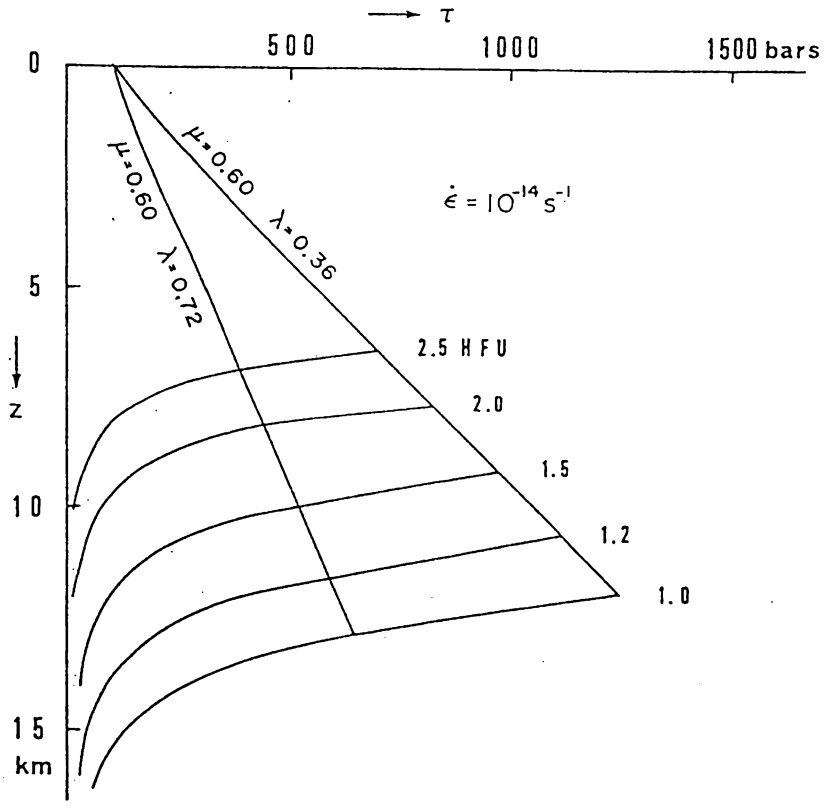
τ
500
1000
1500 bars
0
5
10
15
km
z
μ=0.60 λ=0.36
μ=0.60 λ=0.72
ε̇ = 10⁻¹⁴ s⁻¹
2.5 HFU
2.0
1.5
1.2
1.0

Fig.17

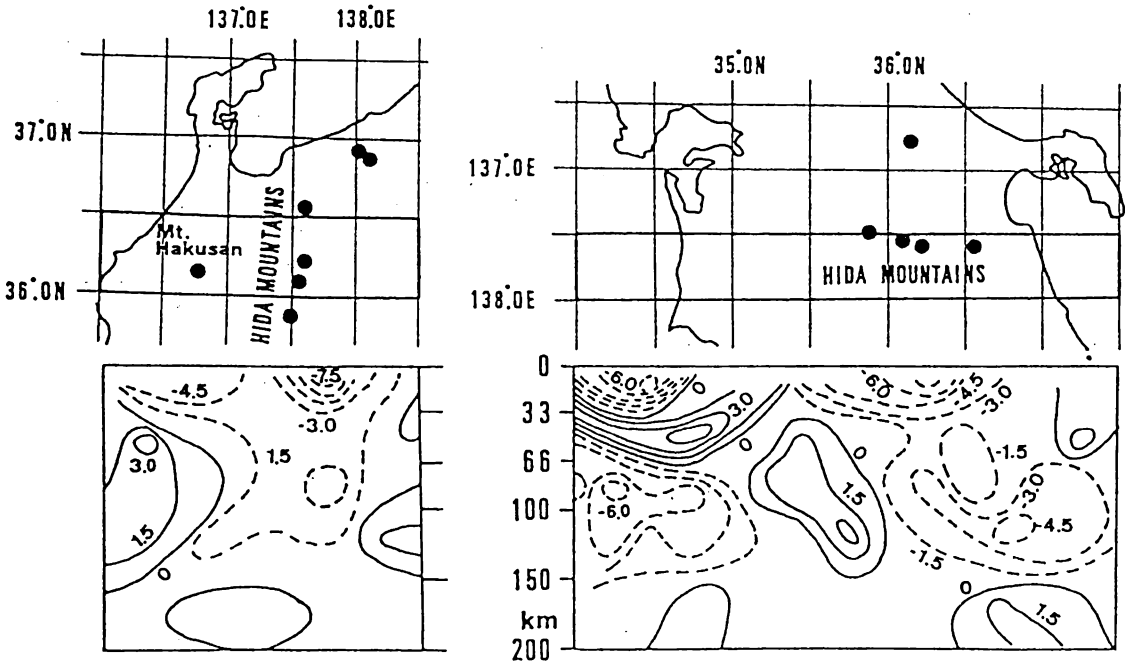
137.0E
138.0E
37.0N
36.0N
Mt. Hakusan
HIDA MOUNTAINS
35.0N
36.0N
137.0E
138.0E
HIDA MOUNTAINS
0
33
66
100
150
km
200
-4.5
-3.0
3.0
1.5
0
-6.0
-1.5

Fig.18

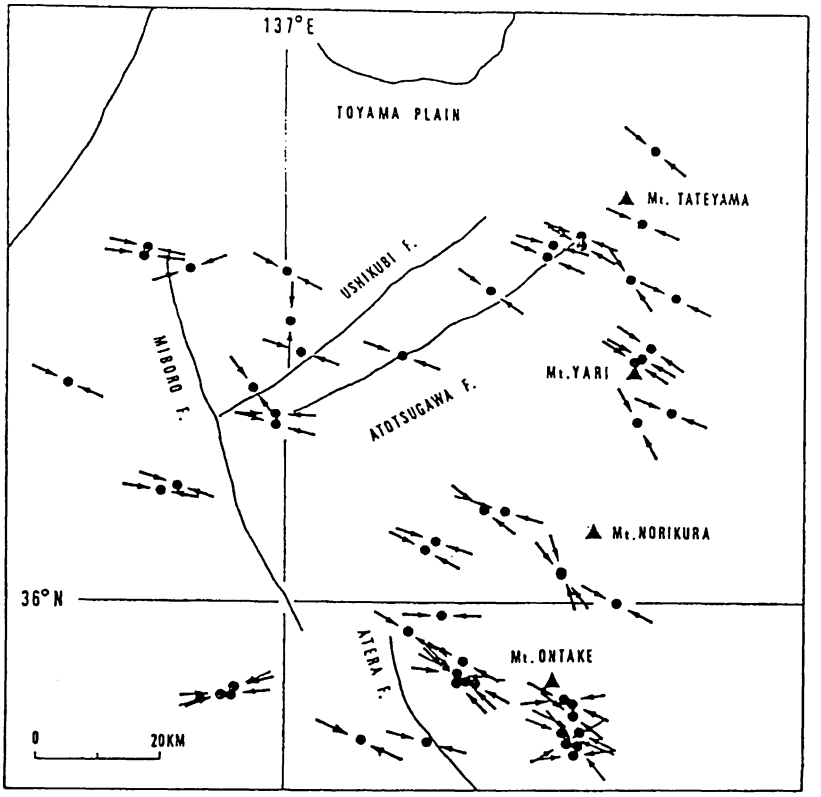
137°E
TOYAMA PLAIN
Mt. TATEYAMA
USHIKUBI F.
NIBORO F.
ATOTSUGAWA F.
Mt.YARI
Mt.NORIKURA
36°N
ATERA F.
Mt.ONTAKE
0
20KM

Fig.19

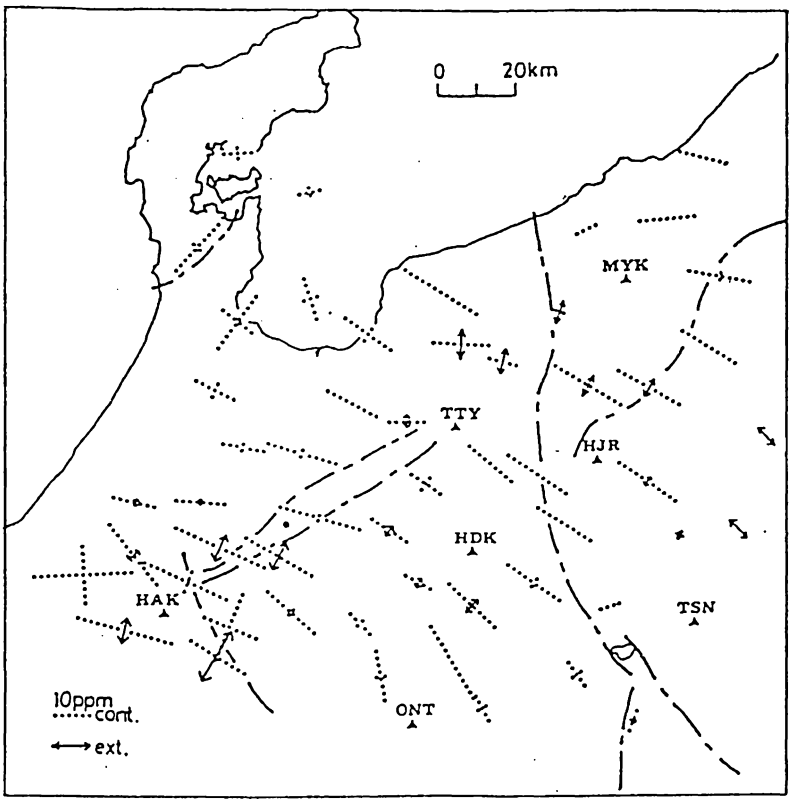
0
20km
MYK
TTY
HJR
HDK
HAK
TSN
ONT
10ppm
cont.
ext.

Fig.20

飛騨地方の３次元上部地殻構造と活断層及び地震活動

京大防災研　三雲　健、平原和朗、竹内文朗、　京大防災研・上宝　和田博夫
東大地震研　佃　為成、名大理・高山　藤井　厳、京大防災研・北陸　西上欽也

１．まえがき

本研究は、中部地方北西部のうち特に飛騨地方を中心とする地域の地殻上部の３次元構造を地震波観測データから推定し、活断層分布や地震活動がこの構造とどのような関係にあるかを論ずることを目的とするものである。

飛騨地方は、東側はわが国最高の山脈である飛騨山脈、西側は両白山脈で境され、北側は富山平野、南側は美濃山地で囲まれる高地地帯である。この地方の表層部は地質学的には主として古成層と中生層、一部は第三紀より第四紀の火山岩より成る。中央部は飛騨変成岩、花崗岩類、及び手取層群、飛騨山脈は古花崗岩層と三畳紀層群、西南部は濃飛流紋岩、北部は第三紀火山岩と堆積層に覆われる。飛騨山脈中には北より立山、焼岳、乗鞍岳、御岳の四つの活火山が含まれ、両白山脈中には白山、大日岳の両活火山が存在する。

飛騨地方の最大の特徴は、共役な第四紀活断層が多数分布することである。飛騨断層系と呼ばれるこれらの断層の主なものは、ENE-WSWないしNE-SW方向に伸びる跡津川、牛首、茂住断層などの右横ずれ断層、NNW-SSEないしNW-SE方向に走る阿寺、御母衣断層等の左横ずれ断層であり、この他、これらに平行する多数の小断層群が存在する。これらの活断層の分布はこの地域が第四紀において強い圧縮応力を受け、地殻上層部の破砕度が大きいことを示唆するものである。この地域の活断層の分布を、山脈、活火山とともにFig.1に示した。

２．地震活動

この地方に多くの活断層が存在することは、過去200万年以後の第四紀に多数の地震が発生したことを意味する。記録に残る主要な地震としては、1586年天正飛騨地震（M＝7.9）、1858年安政飛騨地震（M＝7.0）の大地震のほか、1826年（M=6.2）、1855年（M=6.7）の中規模地震が挙げられる。このうち1858年の地震は当時の被害分布や最近のトレンチ発掘調査等の結果から、跡津川断層の動きによって発生した地震と考えられている。（Mikumo et al.,1987）.

この地方の現在の地震活動は、1977年以来主として京大防災研究所・上宝地殻変動観測所のほか、同北陸微小地震観測所、名古屋大学高山地震観測所、東大地震研究所信越地震観測所の地震観測網による観測によって詳細に調べられている。Fig.2は1980年4月より1986年6月迄の約6年間に上宝観測所によって求められたM≧0.5の地震約5,800個の震央分布を示したものである（Mikumo et al.,1987）。これらの地震の震源決定には各種のデータから求められている１次元水平地殻構造にもとずき、iterative non-linear least squares の方法によった。震央の大きさはマグニチュード別を示す。

震源決定の精度は観測網中心から約25kmの範囲内では水平方向で±1km以内、深さ方向で±2km以内であるが、25～50kmの範囲ではそれぞれ±1.5km以内±3km程度である。

Fig.2より明らかなように跡津川断層に沿い長さ約70kmにわたって顕著な地震活動がみられる。この活動は断層東部～西部で活発であり、中央部ではやや低い。また飛騨山脈直下では北から南へ伸びる比較的活発な地震活動がある。このほか、富山平野西部から御母衣断層北端付近、阿寺断層北東端東側の高山東方より飛騨小坂一萩原付近にもかなりの地震活動がみられる。

3．観測データ

この地方の3次元上部地殻構造を推定するに際して用いた地震は、前節に述べた1980年4月より1986年12月迄のFig.2の地震及び1987年1-8月迄に観測された地震のうちM≧3の地震237個である。これらの地震の位置はこの地域及び周辺に広く分布するように選んだ。観測データは、京大防災研究所上宝観測網の6点、上宝KTJ、天生AMJ、楡原NRJ、福光FMJ、七尾NNJ、朝日AHJ、臨時観測点2点、上が洞KHJ、加子母KSJ；北陸微小地震観測網2点、小松KMJ、勝山KAJ；名大高山観測網4点、高山TAK、焼岳YKE、高根TKN、馬瀬MZE；東大震研信越地震観測網2点、松川MTU、長野朝日ASIの合計16観測点で上の地震の際に観測された2577個のP波初動走時である。なお、この他、補助的データとして1978年5月-8月に行われた手取川発破群（λ＝136° 38′ 51.″ 1、φ＝36° 15′ 25.″ 2、h＝350m）の際、15＜Δ＜70kmの範囲の33観測点で観測された走時（Watanabe et al.,1979）も参考として用いた。

これらの観測点の間隔は定常観測網の場合、平均約25～30km、臨時観測点の場合10km以内である。観測された走時の分解能は1/100secである。観測値に対してテレメータ・システムによる伝送遅れ（0.02-0.08sec）を補正した。最終的なP波走時の精度は、読取精度も考慮すれば5/100秒以内と考えられる。

4．解析

ここでは Thurber(1983) の方法を適用し、上の観測データを用いて damped least squares により3次元速度構造を計算した。この方法は速度構造と震源位置の両者を parameter separation をしつつ iteration 法を用いて同時に inversionすることが可能である。この結果、速度構造は媒質中に設定した3次元grid points での各速度の値として得られる。

構造の starting model としては、上宝観測所が震源決定に用いている1次元水平成層構造（和田ほか,1979）を採用した。この構造のP波速度は深さ3km以浅で5.4～5.7km/sec,深さ3～15km迄で6.0～6.3km/secで次第に増加する。

対象とした地域はFig.3-6に示す150km×150km の範囲で、深さは12kmまでである。実際の計算は（137.° 0E, 36.° 0N）を原点とする2通りのgrid pointの配置、A）X=-60～80km,Y=-30～110km, B）X=-50～90km,Y=-40～100kmに対して行い、水平方向のgrid points の間隔は20km毎に、深さは z= 0,3,7,12,18,25km に取っ

た。したがって grid points の総数は model space の両端を除けば 8x8x6=384 個 であり、これらの各点での速度及び各地震の震源位置と origin time が未知数として解くべき値である。各深さに対する速度構造はA）、B）両方の grid 配置に対して得られた速度値を平滑して求めた。

Thurberの方法は屈折波に対して circular ray（すなわち、直線的に速度が増加する構造）を仮定しているために、屈折波が到着するcritical distance以上の距離に対しては近似の程度が強い。このため、震央距離 Δ≧50km以上で観測された走時に対しては小さいweightを与え、Δ≧90kmの観測走時は用いないこととした。

damped least squares 法の適用の際に取るべきdamping factor の値は得られる結果の resolution matrixを考慮して経験的に選ぶべきものであるが、今の場合は 0.2, 0.5, 1.0, 2.0, 5.0 の場合について計算し最終的には0.5の場合を選んだ。 data varianceは2.0以下の場合に安定し、殆ど変わらない。

計算は4～6回のiterationによって良く収束し、得られたdiagonal resolution としては、対象地域の周辺部を除き、大部分の点に対して0.45～0.99の値が得られた。最終的な３次元構造を推定する際には、resolution が0.50以下の速度値は採用しないことにした。これらの場合の速度の標準偏差は0.01～0.06km/sec程度であった。最終的な解のdata variance improvement は 74%(0.040→ 0.011sec)、total RMS は0.071secであった。

5．結果及び考察

３次元速度構造が得られた範囲は、東は飛騨山脈東縁（松本盆地西側）から西は両白山脈西縁（金沢平野東側）、北は富山、砺波平野南部から南は飛騨山地南部迄を占める。得られた速度構造は深さ毎にFig.3-6に示した。またそれぞれに対応する深さ 0≦Z＜3, 3≦Z＜7, 7≦Z＜12, Z＞12km での地震の震央分布をこれとともにプロットした。実線と破線はＰ波速度6.0km/sec以上の速い速度と、それ以下のやや遅い速度のコンターを示す。

この図から明らかなように、飛騨地方の構造は中央部の高速度帯と東部、西部及び南部の大部分の低速度帯によって特徴ずけられるようである。

１）先ず中央部の跡津川断層と飛騨山脈西側で囲まれる三角帯地域には地殻最上部から12kmの深さまで,6.0～6.2km/sec 高速度層が存在する。この東縁は極めて浅い部分では飛騨山脈西側の一部まで伸びているようであるが、やや深くなる（Z=3～7km）につれてこの限界は西へ後退しているように見える。この地域は飛騨変成岩と濃飛流紋岩より成るが、 ここが高速度層であることは小断層群を含まずあまり破砕度の高くない固い地殻であることを示すものであろう。この地域で地震活動が低いことと一見調和的である。しかしこの三角地帯北西部の跡津川・茂住・牛首断層の西半部の上部地殻でも、6.2km/sec程度の高速度層が深さ7km程度まで貫入しているようであり、ここでは逆に地震活動が高い。ここでの活発な地

震活動はこの高速度層中の大きい断層の破壊（1858安政飛騨地震）に関係したものと思われる。

２）飛騨山脈の東側の地殻最上部には、速度 5.4～5.8km/secの低速度層が存在する。しかしその下の3～7kmでは通常の6km/sec程度の速度層が存在することから、最上部層は堆積層によるものであろう。一方飛騨山脈中軸部では5.4～5.8km/secのかなりの速度の遅い層が相当の深さまで連続して存在することが注目される。この低速度層は最上部から3km迄の深さまでは、北西方の活火山の立山及び跡津川断層東部迄拡がり、南西方には活火山の乗鞍岳、御岳及び阿寺断層東北端の東側まで拡がっている。南西方面でさらに速度が遅いのは、これに加えてこの地域がこれらの活火山に関係する第三紀ー第四紀火山岩で覆われているか、あるいは阿寺断層と共役な多数の小断層が存在するためではなかろうか。山脈中軸部の低速度層が7km以深ではかなり西方へ拡がりを持つように見えることも興味深い。これらの低速度層は活火山を含む飛騨山脈下火成活動による高い地熱に関係するものかも知れない。山脈下の地震活動は他地域に比べてかなり活発であるが、深さ8km程度より浅い場所に限られる（Mikumo et al.,1988）。これより深くでは低速度層がさらに約150kmの深さまで存在する（Hirahara et al.,1986）ことが見出されている。

３）飛騨地方北西部の礪波平野から御母衣断層北部周辺にかけては地殻最上部から3km程度迄は5.0～5.6km/secの低速度層が広範囲に拡がっている。深さ7km以下では、飛騨中央部と同程度のやや高速度の6.2～6.4km/sec層が見られるので、上部のこの低速度層はこの方面の堆積層を示すものと思われる。しかしこの地域で測定された地温勾配は、飛騨山脈周辺と同様、他地域に比べてやや高いので、いくらかはこれに関係する可能性も否定できない。

４）一方、飛騨地方南西部では、最西端の地殻最上部迄、やや高速度の6.0～6.2km/sec層が存在しているのが見られるが、この地域は両白山地南西の固い地殻と思われる。

しかし御母衣断層の西側から両白山地の中部には3kmの深さ迄5.6～5.8km/sec層がかなり広範囲に拡がっている。この低速度層は活火山の白山付近では深さ12km迄も伸びているのが見られる。この地殻中部まで存在する低速度層は白山の火成活動による高地熱帯を示唆するものと考えられる。このような地殻内の速度分布とこの周辺の地震活動分布との間に特に顕著な関係はみられない。

飛騨地方の３次元速度構造の深さ分布は、以上述べた結果をもとに、いくつかの断面について求めることが出来るが、現在さらに詳しく検討中である。

次に、これらの速度構造の分布とこの地方の重力のブーゲー異常の分布（e.g. Kono et al.,1982）とを比較した。

飛騨地方中央部は-10～-40mgal程度の大きさで他地域に比べて比較的大きく、こ

の地方の高速度層に対応する。特に跡津川断層西部の-6mgal程度の大きさは、地殻最上部まで存在する6.2km/sec層と良い一致を示す。また飛騨山脈中軸部では-60～-80mgalの負のブーゲー異常が存在するが、これはここで低速度層がかなり深くまで存在することと符合する。さらに、南方の御岳周辺から西方の白山付近へ伸びる低速度層の存在は、負のブーゲー異常（-40～-60mgal）のパターンと調和的である。しかし跡津川断層北西では、深さ3km迄かなりの低速度層が分布するにもかかわらず、この地域のブーゲー異常は0～15mgal 程度の正の異常であり、むしろ深さ7～12kmの高速度層のパターンに対応するように見え、ここでは必ずしも調和的ではない。

地震波走時から求められた３次元速度構造と重力異常分布の関係は、今後定量的な計算によって、さらに詳しく議論する予定である。

参　考　文　献

Hirahara,K.,Ikami,A.,Ishida,M. and Mikumo,t.,1986, Three-dimensional P wave velocity structure beneath central Japan -Low velocity bodies in the wedge portion of the upper mantle above high-velocity subducting plates-, submitted to Tectonophysics.

Kono,Y.et al.,1982, Gravity anomaly over the northern part of the central Japan (1), Sci.Rep. Kanazawa Univ., 27, 71-83.

Mikumo,T., Wada,H.and Koizumi,M.,1988, Seismotectonics of the Hida region,central Honshu,Japan, Tectonophysics 145 (in press).

Thurber,C.H.,1983, Erthquake locations and three-dimensional crustal structure in the Coyote Lake area, central California, J.Geophys.Res.88,8226-8236.

和田博夫、三雲　健、小泉 誠、1979、飛騨地方北部特に跡津川断層付近の地震活動と発震機構、地震II、32,281-296.

Watanabe,et al.,1980, Upper crustal structure in the northwestern Chubu district,Japan,as deriverd from the Tedori-River quarry blasts, Bull.Disast.Prev.Res.Inst.,Kyoto Univ.,30,31-52.

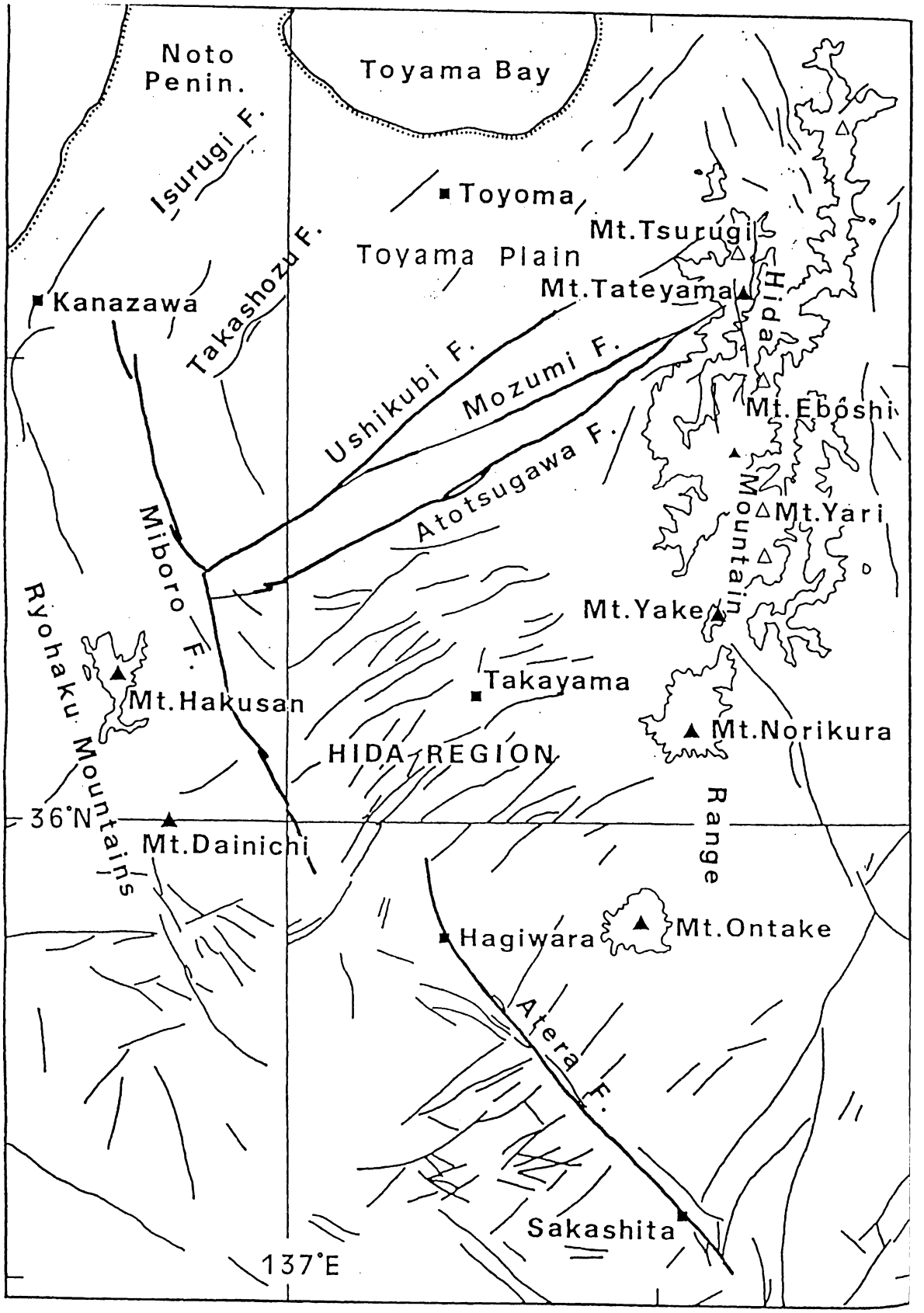
Noto
Penin.
Toyama Bay
Isurugi F.
Toyoma
Mt.Tsurugi
Toyama Plain
Takashozu F.
Kanazawa
Mt.Tateyama
Hida
Mountain
Ushikubi F.
Mozumi F.
Mt.Eboshi
Atotsugawa F.
Mt.Yari
Mibora F.
Mt.Yake
Ryohaku Mountains
Takayama
Mt.Hakusan
Mt.Norikura
HIDA REGION
36°N
Mt.Dainichi
Range
Hagiwara
Mt.Ontake
Atera F.
Sakashita
137°E

Fig. 1

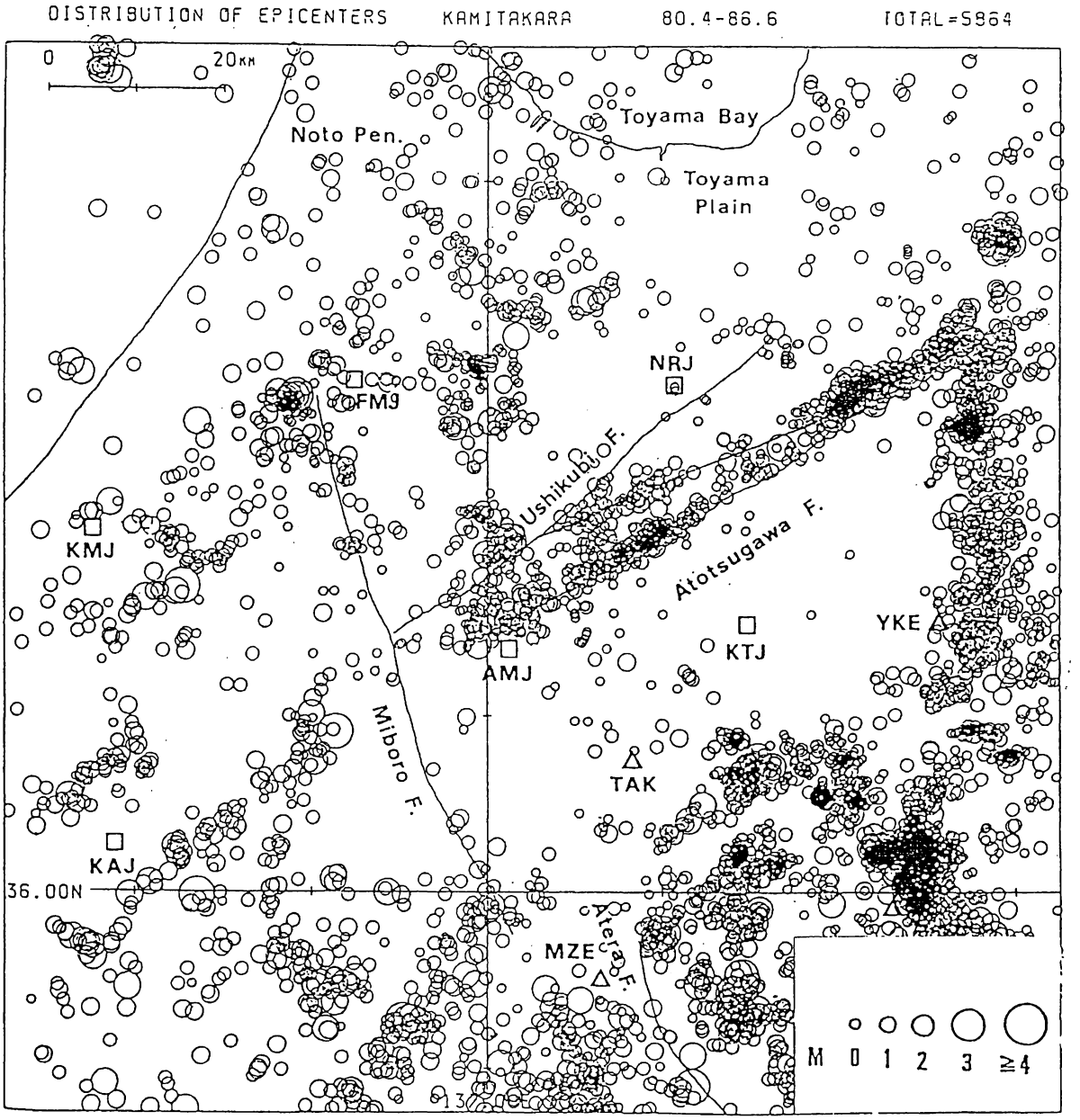
DISTRIBUTION OF EPICENTERS KAMITAKARA 80.4-86.6 TOTAL=5864
0 20KM
Noto Pen.
Toyama Bay
Toyama Plain
NRJ
FMJ
Ushikubi F.
Atotsugawa F.
KMJ
AMJ
KTJ
YKE
Mibora F.
TAK
KAJ
36.00N
MZE
Ateria F.
M 0 1 2 3 ≧4

Fig. 2

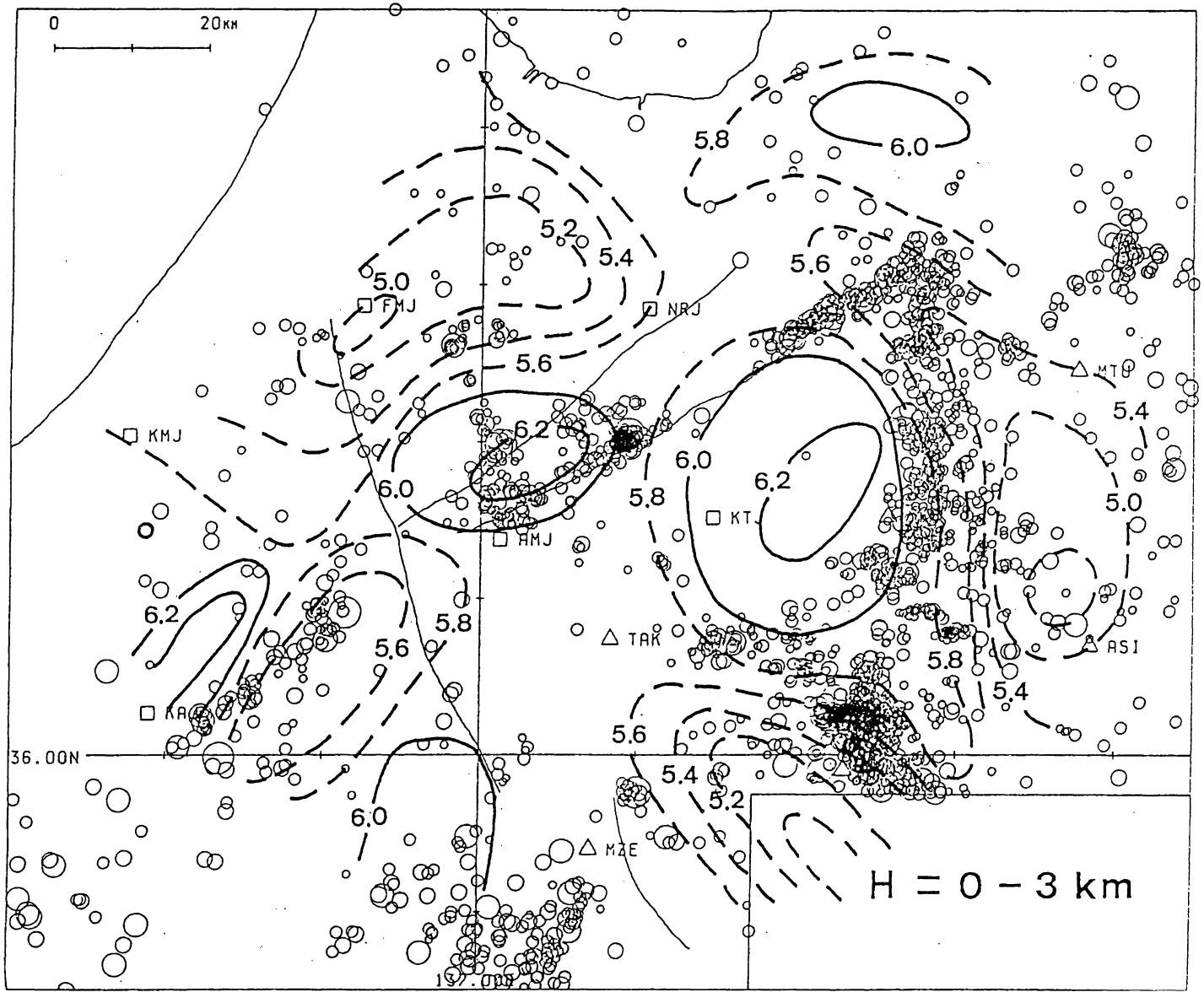
0
20KM
5.8
6.0
5.2
5.4
5.0
FMJ
NRJ
5.6
MTO
KMJ
6.2
6.0
5.4
6.0
5.8
6.2
KTJ
5.0
AMJ
6.2
5.8
TAK
ASI
5.6
5.8
5.4
KAM
5.6
36.00N
5.4
5.2
6.0
MZE
H = 0 - 3 km

Fig. 3

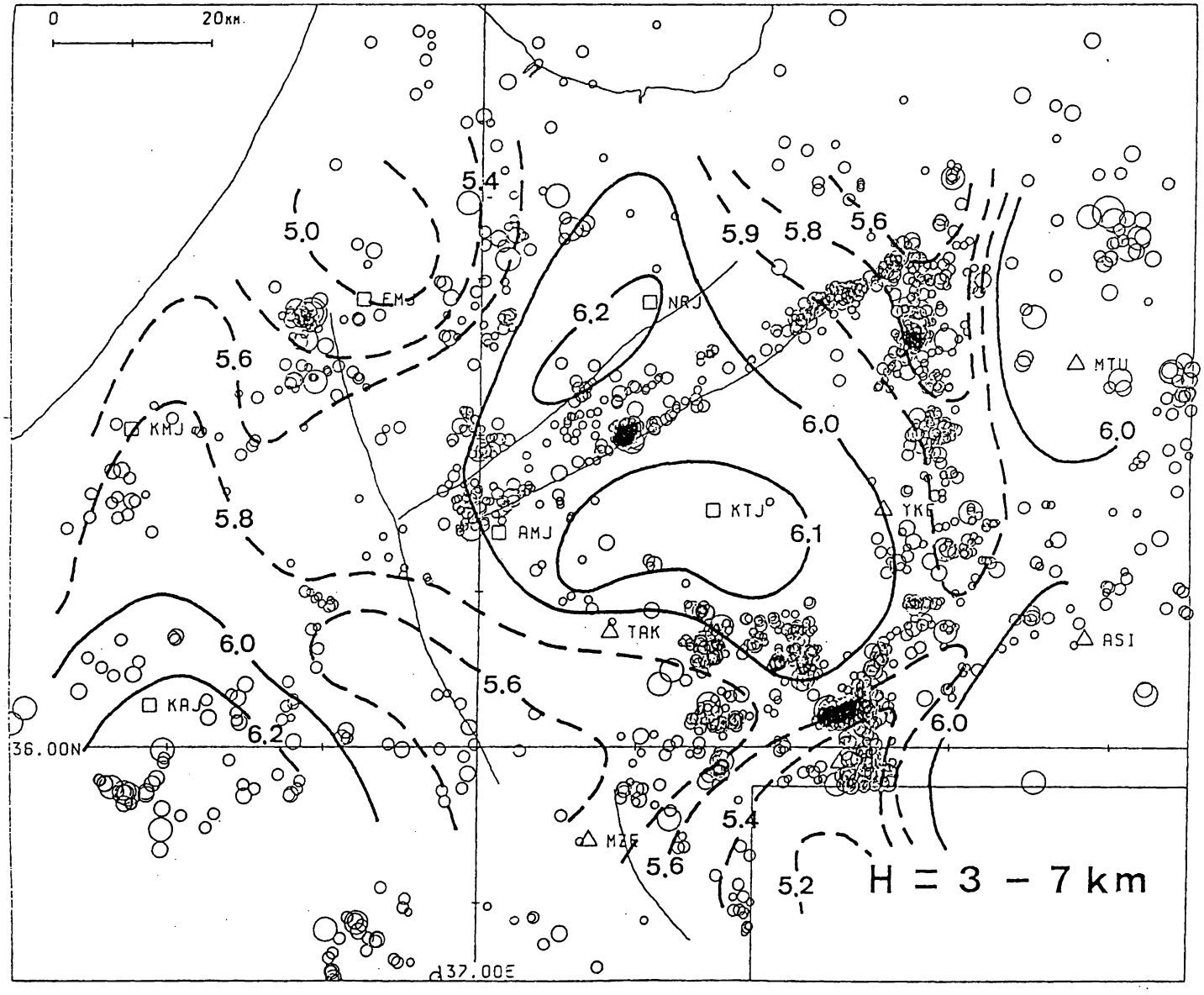
0
20KM.
5.4
5.0
5.9
5.8
5.6
EMJ
NRJ
6.2
5.6
MTU
6.0
6.0
KMJ
5.8
KTJ
YKG
AMJ
6.1
TAK
ASI
6.0
5.6
KAJ
6.2
6.0
36.00N
5.4
MZF
5.6
5.2
H = 3 - 7 km
137.00E

Fig. 4

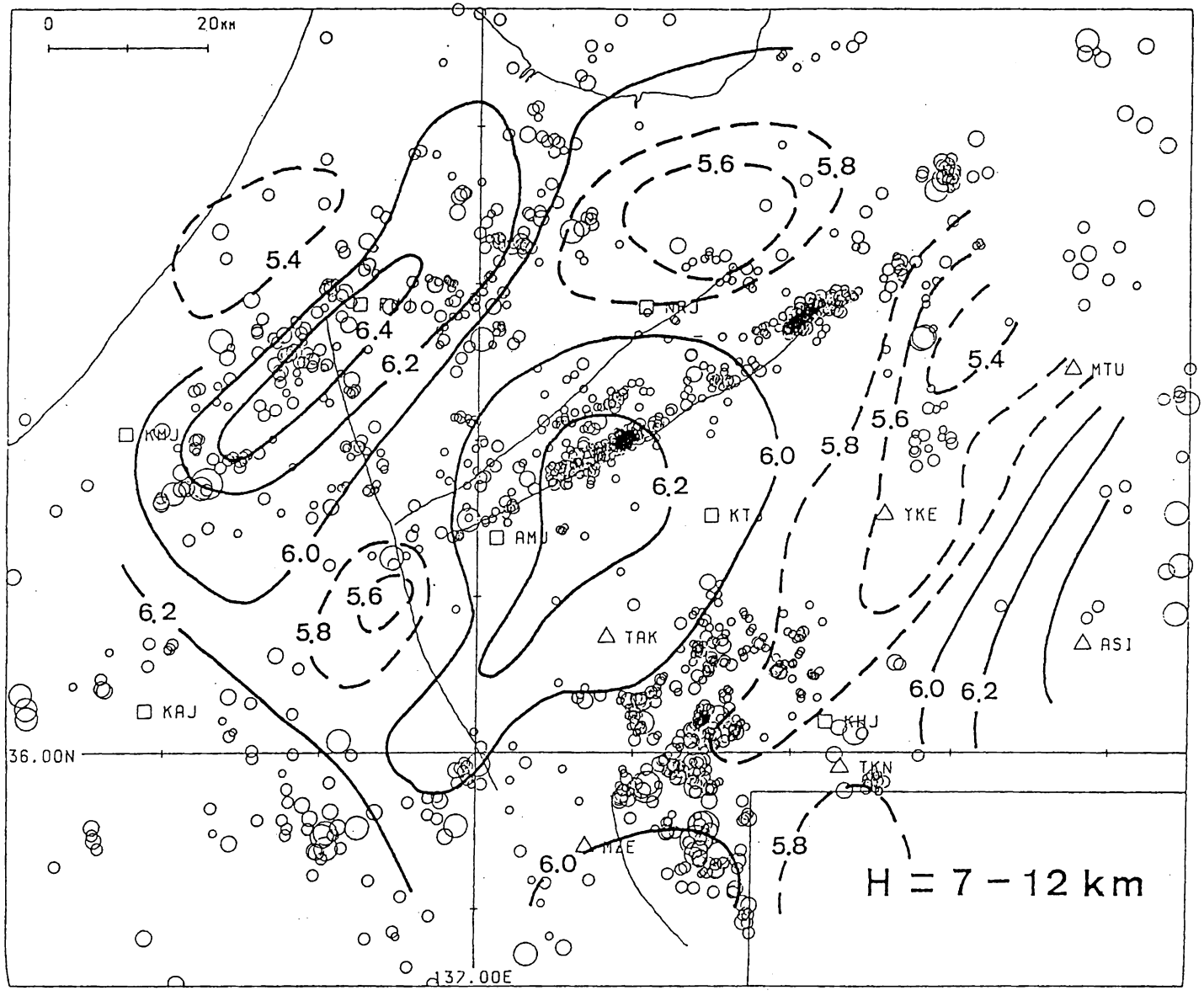
0
20KM
5.4
5.6
5.8
6.4
6.2
6.0
6.2
5.6
5.8
6.2
6.0
5.8
5.4
5.6
6.0
6.2
6.0
5.8
KMJ
KRJ
KT
AMJ
TAK
KAJ
KHJ
MAE
MTU
YKE
ASJ
TKN
36.00N
137.00E
H = 7 − 12 km

Fig. 5

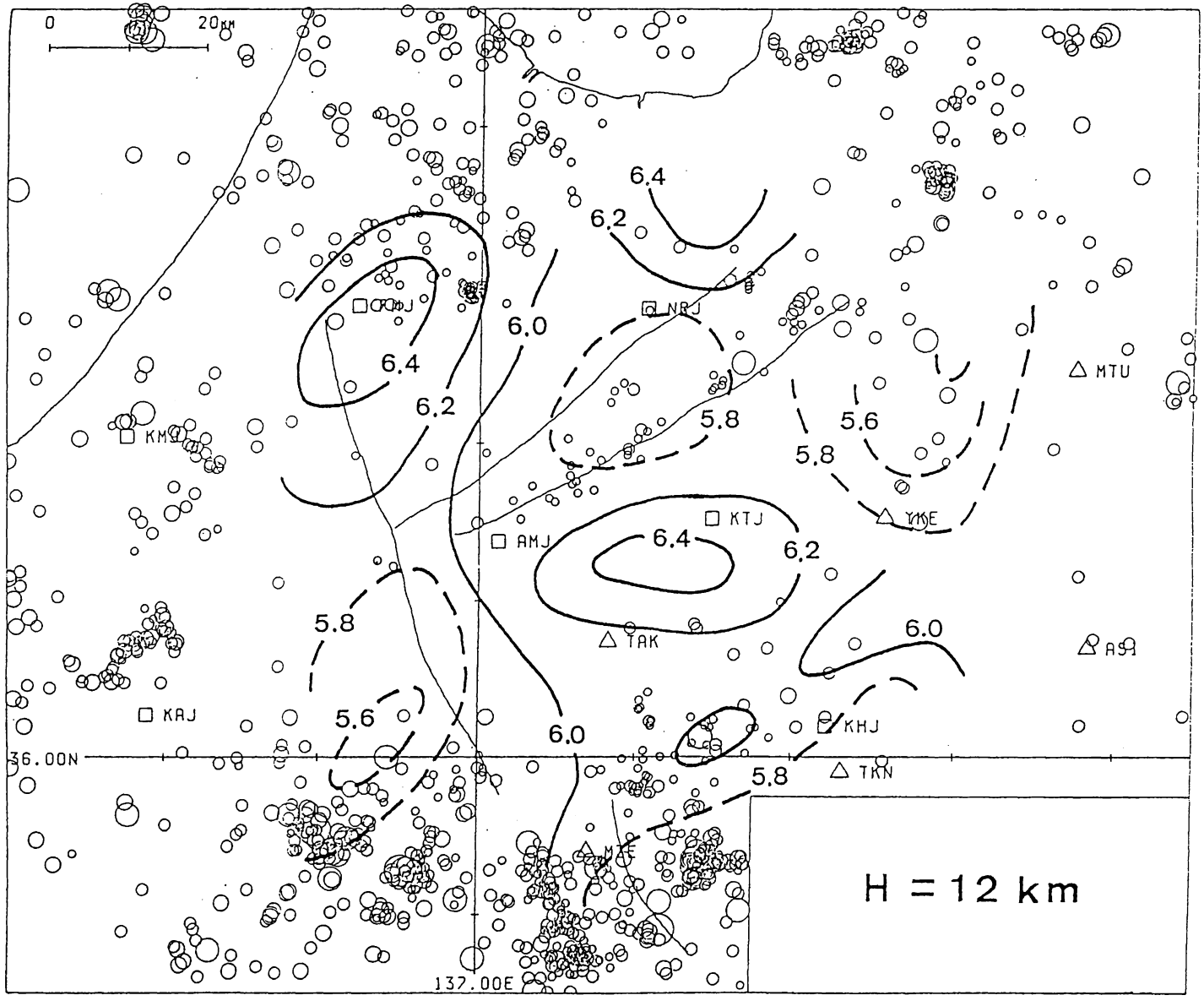
0
20KM
6.4
6.2
6.0
5.8
5.6
NRJ
MTU
KMJ
KTJ
AMJ
YKE
TAK
ASA
KAJ
KHJ
TKN
MIE
36.00N
137.00E
H = 12 km

Fig. 6